Technische Universität München

Fakultät für Chemie

Institut für Wasserchemie und Chemische Balneologie

Lehrstuhl für Analytische Chemie und Wasserchemie

Rapid methods for the analysis of pathogens, antibiotic resistance genes, and microplastic-associated bacteria in water samples

Lisa Katharina Morgane Göpfert

Vollständiger Abdruck der von der Fakultät für Chemie der Technischen Universität München zu Erlangung des akademischen Grades eines

Doktors der Naturwissenschaften (Dr. rer. nat.)

genehmigten Dissertation.

Vorsitzender:	Prof. Dr. Martin Elsner
Prüfer der Dissertation:	1. Priv.-Doz. Dr. Michael Seidel
	2. TUM Junior Fellow Dr. Christian Wurzbacher

Die Dissertation wurde am 29.03.2021 bei der Technischen Universität München eingereicht und durch die Fakultät für Chemie am 05.05.2021 angenommen.

It’s the little things that count

DANKSAGUNG

An erster Stelle danke ich besonders meinem Doktorvater, Herrn Prof. Dr. Martin Elsner, für die Möglichkeit meine Doktorarbeit am IWC anfertigen zu können. Ich konnte mich immer auf deinen Rückhalt und deine Unterstützung verlassen, auch wenn du durch den Umzug ans IWC sehr eingespannt warst. Die vielen hilfreichen Diskussionen haben erheblich zum erfolgreichen Abschluss der Doktorarbeit und dem Veröffentlichen der Paper beigetragen.

Meinem Gruppenleiter und Mentor PD Dr. Michael Seidel danke ich ganz herzlich für die spannenden und abwechslungsreichen Projekte, die ich während meiner Zeit am IWC bearbeiten durfte. Die vielen wissenschaftlichen Gespräche und Diskussionen mit dir haben meine Promotionszeit bereichert und zum Erfolg der gemeinsamen Veröffentlichungen beigetragen.

Außerdem möchte ich mich sehr bei Dr. Natalia Ivleva für die Zusammenarbeit am Mikroplastik Projekt bedanken und die Unterstützung für die virtuelle Konferenz. Dr. Rani Bakkour danke ich für die Hilfe und Unterstützung über die letzten Jahre und die vielen Diskussionen, die Lösungen für Probleme klarer erscheinen ließen.

Liebe Katy, vielen Dank für die schöne Zeit am IWC, die viele Unterstützung und das „Immer ein offenes Ohr haben“ bei Problemen in- und außerhalb des Labors. Durch die intensive Zeit, die wir erlebt haben, ist eine tiefe Freundschaft entstanden, die ich nicht missen möchte. Auch wenn wir nie Laborpartnerinnen waren, hätte ich die Promotionsjahre ohne dich nicht so gut überstanden.

Liebe Julia, vielen Dank für deine jahrelange Laborpartnerschaft von deiner Masterarbeit bis zum Ende meiner Laborzeit. Mit dir war das Hoffen und Bangen um geglückte Messungen nur halb so lang und ich konnte mich immer auf deine Unterstützung verlassen.

Liebe Julia, ich hätte mir keine bessere Studentin über all die Jahre wünschen können und da du deine Promotion am IWC angefangen hast, muss irgendwas richtig gelaufen sein. Danke für das gemeinsame Paper und die vielen Stunden gemeinsam mit „unseren“ unkooperativen Viechern.

Liebe ehemalige Biopritschler*innen – danke, dass ihr mir den Start in die Promotion so angenehm gemacht habt und, besonders Cathi, Jonas und Verena, für die Hilfe bei den mir neuen Geräten und dem Zurechtfinden im Kosmos „IWC“. Danke auch an die aktuellen Biopritschler*innen, die für jeden Spaß zu haben sind und mir so die Promotionszeit deutlich einfacher gemacht haben. Meinen Studenten, Sabrina, Rilette, Michael, Constance, Benedikt, Rosalie und Charlotte, euch danke ich für die wunderbare Arbeit,

die ihr geleistet habt, ohne die vieles in meiner Promotion nicht so gut funktioniert hätte. Danke, für die vielen Stunden im Labor, die hoffentlich nicht nur mir Spaß gemacht hat.

Lieber Philipp, danke für deine herzliche Art, die mir nicht nur den Anfang meiner Promotionszeit erleichtert und bereichert hat und die Einführung in die Geheimnisse der Ramans. Liebe Eli, vielen Dank für geniale gemeinsame Projekte, Konferenzausflüge und viele „Team Procrast“ Meetings. Deine offene und motivierende Art macht die Zusammenarbeit mit dir auch bei anstrengenden Projekten sehr angenehm. Die Freundschaft zu euch hat die letzten Jahre sehr vieles leichter gemacht. Liebe Ramans, besonders aber Christian als unverzichtbarer Teil des Crossover-Projektes, danke für die Aufnahme als Ehrenmitglied und die schöne Zeit bei Unternehmungen für und mit der Wissenschaft.

Liebe Jessi, danke für deine Hilfe bei allen ELISA-Fragen, deine Connection nach unten und deine immer positive Art, denn auch Pessimisten brauchen ein Regenbogeneinhorn. Liebe Karin, danke für deinen hilfreichen Input zu so vielen Fragen und Projekten und die hoffentlich nicht zu aufwändigen Korrekturen. Lieber David, danke für deine unkomplizierte Hilfe, wenn kurzfristig was von unten gebraucht wurde und die Unterstützung bei bio-lastigen Projekten.

Lieber David, danke für deine optimistische Art, auch dann, wenn im Labor nicht immer alles glatt ging und die angenehmen Gespräche in Labor und Büro, an denen auch der Umzug nach Garching nichts ändern konnte.

Liebe Doktoranden-Truppe, danke für die schöne Zeit am und mit dem IWC. Die Konferenz- und sonstigen Ausflüge waren immer Highlights und die Kaffeeduschen- und Draußen-Pausen nie zu kurz. Ich habe diesen Teil der Promotion zu Beginn der Coronazeit bereits sehr vermisst und dieser wichtige Teil darf nie zu kurz kommen.

Liebe Susi, liebe Christine, lieber Roland und lieber Sebastian, vielen Dank für eure Unterstützung bei meinen Projekten. Ohne euch hätte vieles deutlich länger gedauert und es wäre nur halb so gut geworden. Liebe Conny, liebe Christine, vielen Dank für die Behebung vieler Probleme abseits des Labors und die gute Atmosphäre am IWC.

Ich möchte mich auch bei meinen Freunden, besonders Kerstin für Chemikerwissen und viele gemeinsame Mittagessen, und bei meiner Familie bedanken, die mich durch die letzten Jahre in der Promotion immer unterstützt und begleitet haben und so maßgeblich zum Erfolg meiner Doktorarbeit beigetragen haben. Ohne euch wäre ich nie so weit gekommen!

PUBLICATIONS

Parts of this work have been published previously in peer-reviewed journals:

Lisa Göpfert[1], Julia Klüpfel[1], Charlotte Heinritz, Martin Elsner, Michael Seidel, *Macroporous epoxy-based monoliths for rapid quantification of* Pseudomonas aeruginosa *by adsorption elution method optimized for qPCR*, Analytical and Bioanalytical Chemistry, (412) **2020**, 8185-8196, DOI: 10.1007/s00216-020-02956-3

Lisa Göpfert, Martin Elsner, Michael Seidel, *Isothermal haRPA detection of* $bla_{CTX\text{-}M}$ *in bacterial isolates from water samples and comparison with qPCR*, Analytical Methods, (13) **2021**, 552-557, DOI: 10.1039/d0ay02000a

And as a contribution in:

FAO & IAEA, Antimicrobial movement from agricultural areas to the environment - The missing link. A role for nuclear techniques. Rome, FAO, ISBN: 978-92-5-131648-1

[1] shared first authorship

CONFERENCE CONTRIBUTIONS

Oral presentations at research conferences:

Lisa Göpfert, Elisabeth von der Esch, Christian Schwaferts, Rosalie Koros, Martin Elsner, Natalia P. Ivleva, Michael Seidel; Characterization of chemical and morphological changes in microplastics during bacterial degradation at environmentally relevant conditions, **SETAC SciCon**, **2020**, 03.–07.05.2020, digitale Konferenz.

Lisa Göpfert, Martin Elsner, Michael Seidel; Culture Independent Detection of Antibiotic Resistant Bacterial Pathogens with DNA Microarrays, **HRWM 2019**, **2019**, 15.–20.09.2019, Wien, Österreich.

Lisa Göpfert, Martin Elsner, Michael Seidel; Kulturunabhängige Detektion von Antibiotikaresistenz-genen und bakteriellen Pathogenen aus Oberflächenwasser, **Tagung Wasser**, **2019**, 27.–29.05.2019, Erfurt, Deutschland.

Lisa Göpfert, Martin Elsner, Michael Seidel; DNA Microarrays for the Culture-Independent Detection of Extended Spectrum beta-Lactamase Genes and Bacterial Pathogens, **16th Medical Biodefense Conference**, **2018**, 28.–31.10.2018, München, Deutschland.

Poster presentations at research conferences:

Lisa Göpfert, Martin Elsner, Michael Seidel; DNA microarrays for the detection of antibiotic resistance genes and bacterial pathogens, **ANAKON 2019**, **2019**, 25.–28.03.2019, Münster, Deutschland.

Lisa Göpfert, Diana Calomfirescu, Christiane Höller, Martin Elsner, Michael Seidel; Detection of CTX-M Extended Spectrum beta Lactamase (ESBL) in Pathogenic Bacteria from Surface Waters using the Heterogeneous Asymmetric Recombinase Polymerase Amplification (haRPA), **Tagung Wasser**, **2018**, 7.–9.5.2018, Papenburg, Deutschland.

Lisa Göpfert, Diana Calomfirescu, Christiane Höller, Martin Elsner, Michael Seidel; Comparison of DNA Microarrays with PCR for the Detection of Extended Spectrum beta-Lactamase gene CTX-M, **Analytica Conference, 2018**, 10.–12.4.2018, München, Deutschland.

STUDENT RESEARCH SUPERVISED DURING THIS WORK

The following student reports contain data which has contributed to the research presented in this dissertation. All internships and theses have been supervised by me.

Master's thesis:

Julia Klüpfel (2019), Quantification of *Pseudomonas aeruginosa* in Tap Water Samples after Concentration by Monolithic Adsorption Filtration.

Bachelor's theses:

Sabrina Schönberger (2017), Enrichment of sulfonamides in water samples.

Rilette Cirlem Tierra Bautista (2018), Concentration and analysis of sulfonamide antibiotics from water samples.

Michael Sandholzer (2018), Quantification of *Pseudomonas aeruginosa* and CTX-M genes by heterogeneous asymmetric recombinase polymerase amplification.

Constance Ong (2019), Monitoring of total bacteria count in a sandfilter surface water model.

Charlotte Heinritz (2020), Characterization of pH dependence for concentration of *Pseudomonas aeruginosa* with monolithic adsorption filtration.

Research internships:

Julia Klüpfel (2018), Detection of Extended Spectrum *β*-Lactamase Gene CTX-M cluster 9 using Recombinase Polymerase Amplification.

Benedict Horn (2019), Development and basic evaluation of a first prototypic manual microarray analysis setup for field measurements and testing of a manual spotter.

Rosalie Koros (2019), Characterization of chemical and morphological changes in microplastic during bacterial degradation at environmentally relevant conditions.

SUMMARY

Bacteria as pathogens from various aqueous sources can cause severe infections with antibiotic treatment being limited due to antibiotic resistance. Simultaneously bacteria have the potential to degrade antibiotics and help to decontaminate the environment. To analyze the interaction between pathogenic bacteria and antibiotic resistance in water differential diagnostic measurement tools are needed. Two key factors need to be addressed here: first, detection of the pathogenic bacteria and the antibiotic resistance simultaneously and second, detection in a culture-independent manner, thus reducing the time between sampling and results. To achieve the latter goal, an already established monolithic adsorption filtration was adapted, optimized, and calibrated for enrichment of the opportunistic biofilm-forming pathogen *Pseudomonas aeruginosa* from tap water samples. In combination with centrifugal ultrafiltration, an enrichment factor of 10^3 with a recovery of 67.1 ± 1.2% could be achieved (detection via quantitative polymerase chain reaction, qPCR). Optimizing the method for continuous surveillance is planned in a future project.

Monitoring of pathogenic bacteria and antibiotic resistant genes in environmental samples poses an additional challenge as the temperature cycling dependent qPCR is not suitable for in-field application. In contrast, the use of isothermal DNA amplification techniques allows the amplification of DNA at stable temperatures. The heterogeneous asymmetric recombinase polymerase amplification (haRPA) allows the combination of isothermal DNA amplification with an automatic chemiluminescence-based read-out at 39 °C. For the detection of the opportunistic pathogens *P. aeruginosa* and *Klebsiella pneumonia,* the haRPA was developed from the homogeneous RPA. For extended spectrum beta-lactamases, a group of antibiotic resistance genes, a new haRPA-assay was developed for the gene cluster $bla_{\text{CTX-M}}$ cluster 1 and its sensitivity and selectivity were compared to qPCR and PCR assays, respectively. While the selectivity was comparably high, the detection limit of the qPCR could not be reached with haRPA. The combination of several singleplex assays into one multiplex assay to analyze the resistance gene cluster and the pathogens simultaneously resulted in the qualitative identification of the individual parameters. Future projects should aim at quantification of these multiplex measurements.

Some bacteria are able to degrade and/or colonize microplastic particles and can help to reduce the contamination of the environment. To quantify this effect, microplastic analysis must be sensitive enough to detect these fine alterations. Initial experiments aimed at the investigation of the influence of bacterial degradation or colonization of bioplastic-based microplastic particles employing Raman microspectroscopy. Promising first results were achieved, however, necessitating further research in optimizing and refining experimental procedures.

KURZFASSUNG

Bakterien aus verschiedenen Wasserquellen können als Pathogene schwerwiegende Infektionen hervorrufen, wobei die Behandlung mit Antibiotika durch Antibiotikaresistenzen oftmals limitiert ist. Gleichzeitig haben Bakterien das Potential, Antibiotika abzubauen und können somit zur Dekontamination von Antibiotika in der Umwelt beitragen. Um das Zusammenspiel von pathogenen Bakterien und Antibiotikaresistenzen im Wasser analysieren zu können, bedarf es differentialdiagnostischer Messmethoden. Zwei Faktoren spielen hierbei eine große Rolle: Die gleichzeitige Detektion von Antibiotikaresistenz und Pathogenen sowie die kulturunabhängige Detektion, um die Zeit zwischen Probenahme und Ergebnis zu reduzieren. Für letzteren Faktor wurde die bereits erprobte monolithische Adsorptionsfiltration zur Anreicherung des opportunistischen biofilmbildenden Pathogens *Pseudomonas aeruginosa* aus Leitungswasserproben optimiert und kalibriert. Dabei konnte in Kombination mit zentrifugaler Ultrafiltration ein Anreicherungsfaktor von 10^3 bei einer Wiederfindung von 67,1 ± 1,2 % erreicht werden (Detektion über quantitative Polymerasekettenreaktion, qPCR). Die Optimierung der Methode für eine kontinuierliche Überwachung ist in einem zukünftigen Projekt geplant.

Für das Monitoring von Antibiotikaresistenzgenen und pathogenen Bakterien in Umweltproben wäre eine direkt vor Ort anwendbare Methode sehr erstrebenswert. Die weit verbreitete über Temperaturzyklen gesteuerte qPCR ist hierfür jedoch ungeeignet. Isotherme DNA-Amplifikationsmethoden, die DNA bei konstanter Temperatur vervielfältigen, bieten die Lösung. Die heterogene asymmetrische Rekombinase Polymerase Amplifikation (haRPA) kombiniert die isotherme DNA-Amplifikation mit einer automatischen Chemilumineszenz-basierten Detektion bei 39 °C. haRPA-Assays zur Detektion der opportunistischen Pathogene *P. aeruginosa* und *Klebsiella pneumoniae* wurden von homogenen zu heterogenen Systemen übertragen. Für die Extendend Spectrum beta-Lactamasen, eine Gruppe an Antibiotikaresistenzgenen, wurde für das Gencluster $bla_{\text{CTX-M}}$ cluster 1 ein haRPA-Assay neu entwickelt und dessen Sensitivität und Selektivität mit (q)PCR Methoden verglichen. Dabei zeigte sich eine gleich hohe Selektivität, jedoch wurde das Detektionslimit der qPCR mit der haRPA nicht erreicht. Die Kombination mehrerer Singleplex-Assays zu einem Multiplex-Assay zur Detektion des Resistenzgenclusters und der Pathogene führte zur erfolgreichen qualitativen Bestimmung der einzelnen Parameter. Dessen Quantifizierung ist für zukünftige Projekte geplant.

Einige Bakterien können Mikroplastikpartikel abbauen und/oder besiedeln und so zu einer Verringerung der Belastung der Umwelt mit Kunststoffmüll beitragen. Um diesen Effekt zu quantifizieren, muss die Mikroplastik-Analytik jedoch in der Lage sein, auch aufgrund von biologischen Prozessen leicht veränderte Partikel messen zu können. Hierzu wurden erste Versuche durchgeführt, die den Einfluss von bakteriellem Abbau oder Besiedelung von Bioplastik-basierten Mikroplastikpartikeln auf die Detektion mittels Raman Mikrospektroskopie untersuchen. Vielversprechende erste Ergebnisse wurden erzielt, jedoch ist weitere Forschung zur Verbesserung der Analysemethoden notwendig.

TABLE OF CONTENTS

1 INTRODUCTION

1.1 Pathogenic and antibiotic resistant bacteria in freshwater systems

Microorganisms and especially bacteria are present in various water sources such as surface waters like rivers, lakes, or the sea, (treated) wastewater, run-off water from agricultural fields, and many more. Although most of these bacteria are not harmful for human or animal life, the number of bacterial pathogens identified from water sources is increasing. While some have been known for decades, others have only been identified recently. Depending on the type bacteria, they are either harmful for a small group of people due to higher susceptibility or for mankind in general. In addition, the development of antibiotic resistances poses a major threat on our healthcare system. However, since removal of antibiotics from the environment is warranted, antibiotic resistant bacteria may, on the other hand, also play a potential role in their natural removal. Much interest is, therefore, directed at the detection of antibiotic resistance and pathogenicity of bacteria in environmental compartments.

1.1.1 Drinking water

Plumbing and water distribution system of buildings are common sources for pathogenic bacteria. Especially in private homes and hospitals they can cause great harm. While some of these bacteria find perfect living conditions in these systems, their presence leads to complications and health risks for humans [1]. One of the bacteria commonly associated with plumbing contamination is *Legionella* spp. [2]. These bacteria are responsible for legionellosis which include Legionnaires' disease and Pontiac fever [3,4]. Recently, other pathogenic bacteria such as *Mycobacterium avium* [2], *Acinetobacter baumanii*, *Methylobacterium* spp. [5], and *Pseudomonas aeruginosa* [6] could also be found in plumbing systems: pipe systems within buildings and towards buildings from the main distribution lines. Common features of these bacteria are their ability to survive in low nutrient environments such as ground water or drinking water, a tolerance for a wider range of temperatures (especially tolerance of higher temperatures up to 60 °C) as well as a resistance towards disinfectants, an affinity towards biofilms or the formation thereof, and a tendency to slow growth (up to 14 days at 37 °C) [7]. While the first two characteristics are crucial for ensuring their survival in these settings, the third helps bacteria to survive disinfection events. Due to the fourth characteristic, contaminations are often overlooked as the incubation time exceeds the standard 48 h incubation time required for most tests.

According to IUPAC (International Union of Pure and Applied Chemistry), a biofilm is an "aggregate of microorganisms in which cells that are frequently embedded within a self-produced matrix of extracellular polymeric substance adhere to each other and/or to a surface" [8]. These biofilms can be formed in general on all kinds of surfaces and in basically any part of the plumbing systems, but connections between different pipe parts

and dead ends where water flow is not constant are contributing factors for biofilm formation [9]. Pipe material also has an influence on the occurrence of biofilm, as indicated by the bacterial species identified on the different materials [10]. This study concluded that stainless steel was better suited due to low corrosion and lower bacterial concentration compared to polyvinylchloride, copper, and steel pipes. Due to the protective nature of the matrix surrounding the bacteria, disinfection or antimicrobial agents cannot enter the cells as easily and removal of the biofilm is complicated [11,12]. It is therefore important to identify contaminated pipes before they are introduced into the system and consequently prevent the formation of biofilms.

One of the bacteria which are very well known for biofilm formation in premise plumbing systems and for its growth under anaerobic conditions is *P. aeruginosa*. *P. aeruginosa* is a rod-shaped, Gram-negative bacterium and a known opportunistic human pathogen [13]. Its pronounced capacity for biofilm-formation is thought to depend on its extracellular appendages like flagella, fimbrial pili and type IV pili [13]. It can cause different diseases such as pneumonia, infections of the urinary and gastrointestinal tract, sepsis and burn wound infections [14]. Currently ranked among the five most frequent microorganisms responsible for nosocomial infections and especially harmful for immunosuppressed patients such as chronically ill patients and those in intensive care units, *P. aeruginosa* is also part of the ESKAPE group of bacteria which are known to “escape” traditional treatment mechanisms [15]. This group consists of six highly virulent and antibiotic resistant pathogens: *Enterococcus faecium*, *Staphylococcus aureus*, *Klebsiella pneumoniae*, *Acinetobacter baumanii*, *P. aeruginosa*, and *Enterobacter* spp. Outbreaks of nosocomial infections linked to *P. aeruginosa* from water systems have been reported for example in 2005 in France in an oncohematology pediatric unit [16], in 2011 – 2012 in Northern Ireland in several neonatal units [17], in 2014 in France in the ear, nose, and throat department of a hospital [18], and in 2017 in the United States in a neonatal intensive care unit [19]. Patients with cystic fibrosis have an even higher risk of infection. Due to the biofilm-forming nature of *P. aeruginosa*, infection in cystic fibrosis patients with an already attacked lung causes a biofilm to form within the lungs which is particularly difficult to treat [20]. Studies show that up to 95% of cystic fibrosis patients have *P. aeruginosa* infections already at age three [21]. As this environment within the lungs is often oxygen depleted, the ability of *P. aeruginosa* to grow under microaerobic or anaerobic conditions is fatal. However, due to its broad spectrum of possible diseases, *P. aeruginosa* can also harm people outside of hospitals as these bacteria have been found in swimming pools, tap water as well as surface water. Moreover, infections can also be related to recreational water use [22]. Another reason why *P. aeruginosa* infections are so dangerous is the intrinsic resistance to a number of readily available antibiotics such as beta-lactam antibiotics. This is due to low membrane permeability and various efflux pumps which hinder antibiotics from entering the bacterial cells or staying in the cells, its genetic capacity to readily express a wide range of resistance mechanisms, and the possibility of mutations in chromosomal genes which regulate resistance genes [23,24]. It has also been reported that *P. aeruginosa* readily incorporates new antibiotic resistance genes which cause

further antibiotic resistance against other antibiotics [25]. Therefore, only few antibiotics remain which are effective in the treatment of in *P. aeruginosa* infections.

P. aeruginosa can use a broad range of organic material as their food source, hence their ability to survive in nutrient-low environments [26]. It is known to degrade hydrocarbons such as diesel, kerosene, and gasoline and has been discussed as a potential candidate for bioremediation after oil spills [27]. The adaptability towards different food sources allows these bacteria to survive in all kinds of surroundings. They can grow in a large temperature range (4 °C – 42 °C) thus requiring a more rigorous regime when decontaminating premise plumbing systems [28]. To prevent the colonization of these systems, a monitoring of tap water is essential. Also, for a fast response to an upcoming contamination, the employed analytical test must be sensitive enough to detect low bacterial cell numbers.

1.1.2 Antibiotic resistance in environmental water sources

As problematic as pathogenic bacteria are to many people, they are an even greater threat when they acquire additional antibiotic resistances. The introduction of widespread antibiotic resistance is one of the best examples of how a discovery that changed the face of medicine may not have the impact it was cut out to be in the long run. It started in 1909 with the discovery of the first antimicrobial drug for treatment of syphilis and gained more attention in 1928 when penicillin was discovered [29,30]. Though this was the start of a revolution in medicine – the antibiotic era – allowing infections to be treated and millions of lives to be saved over the last decades, the long-term consequence poses a great threat to our healthcare system: antibiotic resistance. Through the widespread use and also misuse of antibiotics in human and veterinary medicine, multi-resistant bacteria emerged causing infections that are increasingly difficult to treat. Additionally, reports of infections with so called pan-resistant bacteria - bacteria that are non-responsive to all currently available antibiotics - have risen over the last years [31–33]. It has to be noted that bacteria have developed resistances against naturally occurring compounds with antibiotic properties since thousands of years [34], as studies with permafrost samples showed [35], but the distribution of antibiotics and antibiotic resistant bacteria all over the globe has magnified the spread of antibiotic resistance [36]. While there are continuing efforts to develop new strategies for treating bacterial infections and new antibiotics are entering the pharmaceutical market, experts fear that the end of the antibiotic era may not be too far away [37].

Antibiotic resistance is not only a healthcare crisis with more than 650,000 infections and over 33,000 deaths per year in the European Union (EU), it is also an economic crisis as an estimated 1.5 billion Euro is lost every year in the EU due to productivity losses and healthcare costs arising from infections with antibiotic resistant bacteria [38,39]. With an increasing number of antibiotic resistant bacteria these numbers are expected to rise within the next decades [40]. The reasons behind the spread of antibiotic resistance are manifold. Misuse in human medicine is one of them where antibiotics are wrongfully prescribed to

treat viral infections, the use of wrong antibiotics without sufficient susceptibility testing prior to treatment, or patients stopping to take antibiotics too early [41]. In veterinary medicine huge amounts of antibiotics are used for precautionary measures or as growth promoting agents (although this practice has been banned in the EU since 2006 [42]). Whole stables or herds of animals in factory farming are treated because a few animals have infections. Additionally, drugs of last resort in human medicine are used as standard treatment options for animals (for example colistin [43]) and the prescription of different antibiotics for the same infections in the same herds or farms due to availability are the most pressing reasons [44,45]. As a lot of the manure and slurry is then used to fertilize crops and fields, the antibiotics and resistant bacteria can enter the environment. Food contamination is another possible route of exposure for humans [46]. Through the use of antibiotics in human and veterinary medicine, their metabolites which can have similar effects on bacteria also enter the environment [47]. In addition, antibiotics are often produced in countries with low environmental standards, questionable health and safety standards for workers, and insufficient wastewater treatment resulting in large amounts of antibiotic contaminated water and waste entering the environment causing further spread of antibiotics and thus prompting bacteria to adapt to these surroundings. An overview of the input pathways for antibiotics and antibiotic resistant bacteria as well as their possible concentration behavior in the environment and knowledge gaps therein are given in Figure 1.

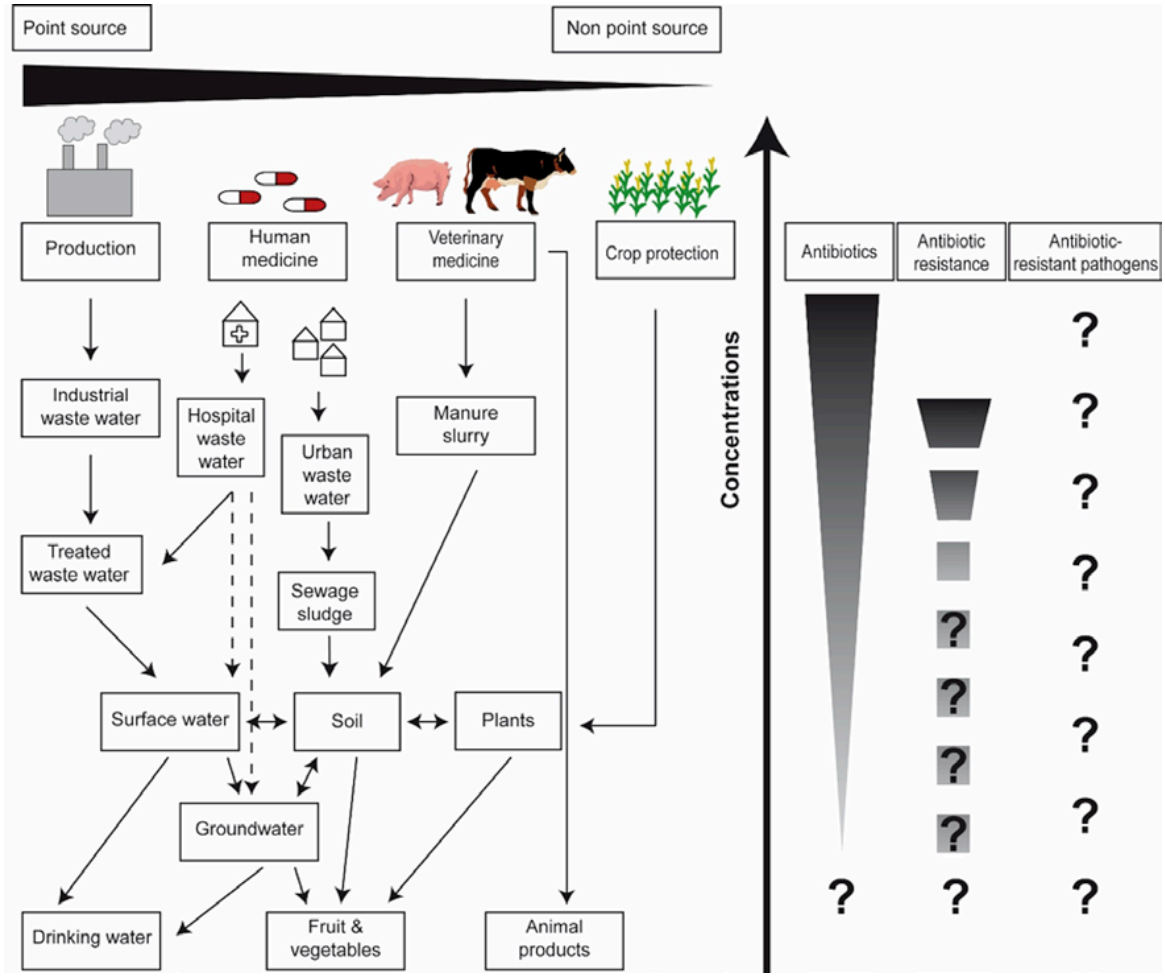

Figure 1: Input pathways of antibiotics, antibiotic resistance, and antibiotic-resistant pathogens into the environment and the food chain (left). Current knowledge gaps about their concentration behavior throughout the process (right) [48].

Monitoring antibiotic resistance in a clinical and environmental context is crucial to understanding the distribution pathways. Knowing the genetic changes responsible allows for even deeper insight into resistance modes and history. Antibiotic resistance genes (ARGs) code for the changes in the bacteria that are responsible for the resistance against antibiotics. Different genes can code for resistance against the same antibiotic and resistance against several antibiotics can be caused by one resistance gene. The occurrence of ARGs varies across countries, continents, and areas [49]. Therefore, detecting ARGs can shed light on where the bacteria and resistances came from and elucidate whether new resistance mechanisms are introduced. ARGs are categorized based on the antibiotic they code resistance against. One of these classes are extended spectrum β-lactamase (ESBL) coding genes. These code for resistances against β-lactam antibiotics which include penicillin and cephalosporins. ESBLs hydrolyze the four membered β-lactam ring thus rendering the antibiotic inactive. ESBL genes have spread worldwide and different types have been identified such as *bla*$_{\text{CTX-M}}$, *bla*$_{\text{SHV}}$, and *bla*$_{\text{TEM}}$, with *bla*$_{\text{CTX-M}}$ being the most common type worldwide [50]. These types or classes are then further broken down into clusters of ARGs where high similarities between the individual genes are found. For *bla*$_{\text{CTX-M}}$ these clusters are cluster 1 (some literature states cluster 3),

cluster 9 (some literature states cluster 14), cluster 2, cluster 8, and cluster 25 [51,52]. The individual genes like *bla*$_{\text{CTX-M-1}}$, *bla*$_{\text{CTX-M-3}}$, *bla*$_{\text{CTX-M-9}}$, *bla*$_{\text{CTX-M-15}}$, *bla*$_{\text{CTX-M-24}}$, and *bla*$_{\text{CTX-M-25}}$ are grouped into these clusters based on their similarities while they are numbered consecutively based on their discovery. The predominant type is *bla*$_{\text{CTX-M-15}}$ which has been detected with increasing frequency all over the world [53]. *bla*$_{\text{CTX-M}}$, so called cefotaximases, are plasmid-mediated and supposedly derived from intrinsic cefotaximases from *Kluyvera* spp. [54,55]. The name *bla*$_{\text{CTX-M}}$ stems from the higher activity against cefotaxime and the city, where it was first discovered in 1990, Munich [56]. ESBL have been identified in different *Enterobacteriaceae* but most frequently in *Escherichia coli* and *Klebsiella pneumoniae* [52]. The spread of *bla*$_{\text{CTX-M}}$ since their discovery and the changing genetic profiles worldwide in clinical and environmental settings can be used to predict the spread of other resistance genes and the implications that follow a widespread occurrence of specific ARGs. Development of assays to detect both - *bla*$_{\text{CTX-M}}$ and their bacterial host (most commonly *E. coli* and *K. pneumoniae*) - in a quick and economic manner is therefore essential.

1.2 Bacterial microplastic degradation in the environment

Some bacteria can be harmful. However, others harbor characteristics which make them useful in the right environment. Among others, the role of bacteria in bioremediation of contaminated sites after oil spills and their ability to degrade certain types of plastics, has been investigated with great interest [57–60]. Artificial plastic compounds have first been synthesized on a larger scale in the early 1900s while plastics derived from natural materials like cellulose and casein have been developed since the mid 1800s [61]. Polyvinyl chloride was first discovered in 1872 by Eugen Baumann but the large scale production did not start until the early 20$^{\text{th}}$ century [62]. With the addition of a seemingly endless variety of plastic compounds for our daily lives and special applications alike, these plastics also entered the environment where bacteria were faced with these new materials [61]. Owing to their evolution and their ability to quickly adapt to changes in the environment, bacteria sought to colonize these new materials. Some bacteria even incorporated certain types of plastics as one of their food sources [63]. It has been shown in several studies that the presence of plastic in a natural environment can change the abundance of specific bacteria and thus the microbial community in these areas [64].

In recent years, smaller plastic particles - so called microplastic – has garnered considerable attention as a potential biohazard from the scientific community and the public. Microplastic is defined as plastic particles with a size ranging from 1 µm to 5 mm. It can either be produced directly for use as granulates or scrubbing agents, e.g. in cosmetics, where it is referred to as primary microplastic. Alternatively, it can form by fragmentation and degradation of larger plastic parts in the environment, referred to as secondary microplastic [65,66]. The so-called “weathering” of plastic in the environment changes the physicochemical properties (e.g. size, mechanical characteristics, and surface chemistry) of these particles and especially the latter is believed to aid

microorganisms in the accessibility of the plastics for degradation [67]. Taking a closer look at microplastic found in the environment, traditional plastic material like polystyrene (PS), polyethylene terephthalate (PET), and polyethylene (PE) are detected frequently while biodegradable plastic materials such as polylactic acid (PLA) and polybutylene adipate terephthalate (PBAT) are not detected as frequently. The latter are thought to degrade in the environment, and also because production numbers are not comparable at the moment [65].

Microplastic has been found in many different environmental compartments and may be present even in remote areas [68]. Most public attention and a prime research focus is directed at microplastic in the marine environment, as plastic debris in oceans is of great concern [68–71]. The introduction of plastics directly into the environment, for example as mulch foils, and their replacement with biodegradable materials has been of great interest as well. Microplastic residues in agriculture are a pressing problem, even with possible implications for human health [72–75]. As most of the traditional polymers like PS and PET are extremely durable in the environment, biodegradable plastic has been discussed as one way to combat microplastic pollution [73,76,77]. Examples of such biodegradable plastic are PBAT, PLA, polyhydroxyalkanoates, and polybutylene succinate among others [78–80]. Although biodegradable plastics do currently not reach the production volume of traditional polymer types, their production volume and market share has been increasing over the last years and is predicted to continue in this direction [80]. Biodegradable plastics are thought to degrade and thus do not remain in the environment as long as conventional polymer types such as the aforementioned PS or PET [63,81,82]. However, the label “biodegradable” is tested under specific conditions resembling industrial composting plants which differ from environmental conditions and thus their degradability under environmental conditions is still not fully understood [83].

It has been shown that bacteria and other microorganisms such as fungi are able to degrade plastic and microplastic particles. The individual species harbor special genes and mechanisms that allow them to degrade certain plastic types of among others (low and high density) PE, PET, and polyamide [57,58,84]. Among the bacterial genera, *Pseudomonas* spp., *Arthrobacter* spp., and *Thermobifida* spp. are responsible for plastic degradation with *Pseudomonas* spp. being found also in aqueous environments [85]. A study also shows, that *Sphingomonas* spp. are able to degrade hydrocarbons and might therefore be able to degrade microplastic as well [86]. It has been recently reported that biofilm formation on microplastic particles induces surface changes and may help to make the particles more accessible for degradation [87]. Additionally, an existing biofilm may promote colonization with further bacteria thus increasing chances of microbial degradation. Identifying new species which are able to colonize plastics and have the potential to degrade microplastic is an important task.

Microbial degradation of microplastic may be a key factor in removing microplastics from the environment. It is important to analyze microplastic from environmental samples in a

fast and precise way to understand degradation and monitor changes in the amount present in the environment. In general, there are two main approaches towards microplastic analysis. On the one hand, mass-spectrometry (MS)-based methods such as thermoextraction desorption gas chromatography MS [88–91] and pyrolysis gas chromatography MS [92–96], on the other hand spectroscopy-based methods like Raman microspectroscopy (RM) alias Raman microscopy [97–104] and focal plane array Fourier-transform infrared spectroscopy (FPA FT-IR) [105–111]. MS-based methods give qualitative information as they identify the type of polymer while also giving quantitative information on the bulk level corresponding to the mass of the sample. RM and FT-IR also give qualitative and quantitative information. For the identification of the polymer type, both RM and FT-IR are comparable to the mass-based methods. However, their quantitative information is based on the single particle level and yields particle size, shape, and number concentration. Both identify microplastic by means of the characteristic vibrational spectra, the so-called fingerprint, of the plastic compounds. As RM uses a small confocal volume at the surface to generate its spectra, it is sensitive to changes on the surface of the microplastic particle. This sensitivity is also the case for FT-IR. Regarding the bacterial degradation of microplastic, it is important to learn more about the process itself than just the result. Key questions are: Knowing how the surface of the particles is changed, where and under what circumstances degradation occurs, and how microplastic is accessible by bacteria. This helps to one day use bacterial degradation as a specific tool for bioremediation of microplastic in the environment. Especially for small particles, RM is the method of choice for monitor these changes on the surface of the microplastic particles [97]. Characterizing these changes may also help to better investigate microplastic in environmental samples as along with the surface the Raman signals may change. Knowing what to look for in monitoring studies is essential and, so far, there is not much known about the altering effects.

2 THEORETICAL BACKGROUND

2.1 Detection methods for pathogens and antibiotic resistant bacteria

When aiming at detecting and monitoring pathogenic bacteria with and without antibiotic resistances in the environment, two different approaches are possible: phenotypic and genotypic detection. While the phenotypic detection relies on different growth of bacteria in selective media and their overall morphology, genotypic detection analyzes the genes present to confirm bacteria. Phenotypic detection has been used for decades and, in the case of standard culture on agar plates, does not require expansive equipment, but distinguishing different bacterial colonies from one another demands a certain expertise. Additionally, the long incubation times make phenotypic methods disadvantageous when immediate results are needed, for example for infection treatment or detection of contaminations in drinking water systems. In recent years, new methods emerged to identify and characterize bacteria. Matrix-assisted laser desorption ionization-time of flight mass spectrometry (MALDI-TOF-MS) identifies bacteria based on the specific ribosomal proteins and its “fingerprint” obtained is then compared to a database [112]. The high-throughput and low-cost analysis of bacteria from culture samples makes MALDI-TOF MS a powerful tool in clinical diagnostics and for identification of bacterial species in environmental samples. RM is able to identify bacteria in a similar way: The distinct pattern of Raman bands acquired either by single cells or bulk analysis is then compared to a database to determine the bacterial species [113]. RM is currently not used as a standard technique for bacterial characterization but the possibility for single cell analysis is one of its main advantages. Regarding the detection of antibiotic resistance, phenotypic methods characterize the whole organism’s response to the antibiotic. This is especially relevant in a clinical context, where the goal is to find an antibiotic the bacteria are susceptible to. Standard phenotypic methods include manual and automatic assays. Manual assays such as culture on antibiotics-containing agar plates, the ETEST® by bioMérieux or the disk diffusion test where the absence of bacterial growth on an agar plate indicates the effectiveness of the antibiotic require overnight incubation. Automatic assay systems such as the VITEK® system by bioMérieux and the Phoenix™ system by Becton Dickinson both provide information on susceptibility and resistance within several hours and, thus, are faster than the manual assays.

The widespread use of genotypic detection also known as DNA-based detection methods started with the development of polymerase chain reaction (PCR) in 1984-1986 [114,115] and has since revolutionized bacterial monitoring in environmental and healthcare surroundings. For analyzing antibiotic resistance, the focus shifts towards the genetic profile responsible for the organism’s resistance and finding the ARGs. These give more insight in distribution patterns and the mode of action of the resistances. Through the amplification of DNA fragments, even low amounts down to one DNA copy, can be visualized and therefore detected within a matter of hours instead of days [116]. With PCR, bacterial strains and gene clusters of ARGs could be identified and the spread and

occurrence of certain ARGs could be traced worldwide. By using DNA intercalating dyes or fluorescent probes, the amount of DNA and in return the number of microorganisms can be quantified in PCR leading to quantitative PCR (qPCR) [117]. DNA amplification requires prior knowledge of the sample as the sequence which is amplified and detected needs to be known. These techniques have been standard laboratory procedures for almost 40 years and are thus cheap and readily available in every biochemical lab. One the other hand sequencing-based techniques, the analysis of existing DNA down to the DNA base sequence, are used more and more frequently [116]. Whole genome sequencing (WGS) reduces the mentioned bias towards known genetic sequences as there the whole DNA information of a sample is gathered and later analyzed. This requires skilled personnel to analyze the large amounts of data generated in a single analysis and, at the moment, is more time consuming per analysis and more expensive. For detecting unknown antibiotic resistances WGS comes into play. It allows for an unbiased look at the whole bacterial DNA in a sample and makes it possible to understand connections within antibiotic resistance in a whole new way [118]. The non-target approach in WGS is more prone to identify targets for monitoring rather than the actual monitoring process itself. For monitoring, on-target approaches for chosen bacterial species or certain antibiotic resistance genes are the method of choice, e.g. (q)PCR or related techniques. Due to these different characteristics both genotypic and phenotypic methods are often combined for a time and cost-efficient analysis to detect bacteria and antibiotic resistance in environmental samples.

2.2 Monitoring challenges and the need for culture-independent techniques

It is well known that microbial communities can adapt to different environmental changes. Therefore, it is crucial to monitor these changes in an unbiased way for a better understanding of the correlations and interactions that lead to these adaptions. However, when bacteria are concerned only a minor fraction of the worldwide bacterial species has been characterized so far and only 1% have been successfully cultured in laboratories [119]. Consequently, research activities have a bias towards bacteria that are culturable, as the rest cannot be detected, leaving the rest unseen and undetected. Additionally, culture-based methods require long incubation times before the bacterial growth can be seen and evaluated (minimum of 16 h, and up to 2 weeks for certain species). For monitoring purposes this means that real-time monitoring is not possible and when investigating outbreak scenarios, critical time for intervention is lost. While culture-based methods have long been the gold standard of bacterial monitoring and characterization because of their easy handling and low cost, culture-independent techniques have gained in importance and popularity over the last decades.

2.3 Concentration from large volume water samples

With culture independent techniques on the rise, new challenges emerge. For water samples with low bacterial contaminations, detection methods are often not suited for the required concentration range. Here, pre-concentration of the sample is necessary to reach the desired limits of detection. One of the areas where this has been of increasing importance is the detection of bacterial pathogens in groundwater or drinking water. The Guidelines for Drinking-water Quality by the World Health Organization (WHO) state that clean water must be available to all residents thus requiring regulators to make sure that no bacteria are to be found [120]. Overall, no bacteria are allowed in concentrations that may be harmful to humans. For fecal indicator bacteria (*E. coli* and *Enterococcus faecalis*) as well as for *P. aeruginosa* this means no colony forming units (CFU) in 100 mL which in turn requires the limit of detection to be 1 CFU 100 mL^{-1}. Considering that single CFU and consequently bacteria need to be detected, analyses with high sensitivity in combination with concentration of large sample volumes, ideally from up to 10 L down to a few mL are needed. An overview of different enrichment methods for bacteria is given in Table 1. Methods and more specifically filter materials for this task should have the following key characteristics: easy production at low cost, tolerance for high pressures to reduce filtration time, long shelf live and easy storage, adaptable surface for concentration of different bacteria, automation possibilities and ability to perform continuous sampling, easy handling for use at diverse settings, and low filter clogging potential to filter large volumes through one filter in a short time.

Monolithic filtration using different materials has been an attractive alternative to the established methods such as centrifugation and membrane filtration because of the high versatility and easy adaptability to enrich different organisms (Table 1). Monoliths, in general, are homogeneous stationary phases with high porosity comprised of organic or inorganic material [121]. Silica is the most prominent and most often used inorganic material with its characteristic high surface. However, the limited pH working range with a stability in a pH range from 2 to 8 excludes it often from applications in adsorption-elution processes in bacterial concentration efforts [122]. In contrast, organic monoliths show a lower surface than silica-based monoliths but compensate this disadvantage with stability at more basic pH and easy synthesis protocols [121,123].

Table 1: Overview of different enrichment methods for microorganisms and especially bacteria [124–127]. Adapted from [128].

Method	Advantages	Disadvantages
Centrifugation	Easy handling	Loss of non-viable cells possible
		Matrix may also be concentrated
		Often only size specific
Immunofiltration	Very specific due to antibody interaction	Cost intensive due to antibodies
		More steps needed for synthesis
Immunomagnetic separation	Very specific due to antibody interaction	Cost intensive due to antibodies
		Low sample volumes
Flocculation	Can enrich multiple microorganisms at once	Time-consuming
		Based on unspecific interactions
Membrane filtration	Automation possible	Dead-end filtration may result in clogged filters
	Defined size range	
	Different materials possible	
Monolithic filtration	Easily adaptable due to functionalization	Sometimes complicated functionalization
	Easy and fast synthesis of unfunctionalized filters	
	Used for different microorganisms	
	Applicable over a wide range of pH values, flow rates and matrices	

Monolithic adsorption filtration for efficient concentration of bacteria and viruses is one application of organic monoliths [129,130]. The monolith used in these studies can be synthesized within 1 h with a defined pore size (21 µm) and present free epoxy groups on the surface [131]. The latter characteristic makes it easy to add specific functional groups to the surface thus changing the adsorption properties. Pore size is dictated by the ratio

between the monomer and the porogen which is a non-polymerizing solvent (mixture). The porogen is responsible for inhabiting free space between the monomer molecules where no polymerization can take place and pores form. The solvents are later evaporated from the system. So far, different surface functionalization types for monolithic adsorption filters (MAFs) have been published which include, among others, MAFs with the antibiotic Polymyxin B (MAF-PmB) being immobilized on the surface [131], hydrolyzed MAFs (MAF-OH) [130], and MAFs with diethyl aminoethyl groups (MAF-DEAE) [132]. All these have in common that the retention of bacteria is based on a complex mixture of different interactions such as ionic or hydrophobic interactions, van der Waals forces, or hydrogen bonds with the exact composition depending on the MAF functionalization and analyte. The macroporous structure of the monolith without mesopores results in filtrations of microorganisms performed at high flow rates (up to 1 L min^{-1}) and with large sample volumes (100 L) [129]. Different height and diameter of MAFs have been published [128]. Dead-end and crossflow filtrations have been reported so far [129,133] and the possibility for automation and batch or continuous sampling is also given.

Traditionally the adsorption elution process is applied to enrich viruses, while first reports of successful transfer to enrichment of *E. coli* and *Salmonella* spp. date back to 1976 (using DEAE cellulose columns) [134]. More recently, *E. coli*, *E. faecalis*, and *Legionella* spp. have been successfully enriched using MAFs [130,131]. However, such an application of MAF for the enrichment of *P. aeruginosa* from drinking water has been missing so far. The development of this method is the first project of this thesis.

2.4 Isothermal nucleic acid amplification techniques and their application for environmental monitoring of antibiotic resistant bacteria

Genotypic characterization of ARGs is commonly done by (q)PCR, thus requiring a thermal cycling device for the different steps. Over the last 30 years, DNA amplification methods have been developed that no longer need thermal cycling but rather depend on different enzymes that make DNA amplification possible at constant temperatures [135]. Therefore, the thermal cycling device can be exchanged for a much cheaper and readily available heating block with fixed temperatures. This allows the analyses to be carried out in-field and in low resource settings. Several isothermal nucleic acid amplification techniques have been developed and the most common ones are briefly described in the following paragraphs.

Loop-mediated amplification (LAMP) is carried out at 60 – 67 °C and uses six primers to create the loop structure which allows for exponential amplification of the DNA [136]. The sensitivity of LAMP is comparable to PCR assays and the typical assay time is 1 h. Due to the high number of primers necessary, it is difficult to multiplex LAMP assays and the primer design requires expertise. Several LAMP assays for pathogen detection have been published in recent years [137].

Strand displacement amplification (SDA) uses an incubation temperature of 37 – 42 °C and two or four primers for first- or second-generation assays, respectively [138]. A recognition site for the restriction endonuclease HincII allows the incorporation of a nick in the DNA strand and leaves an open 3'-OH end which is then elongated by the DNA polymerase.

Helicase dependent amplification (HDA) uses a helicase to denature the double stranded DNA into single strands which are then stabilized [139]. DNA polymerase amplifies the single strands at a temperature of 60 °C. For HDA two primers are required which need to meet more specific requirements than those used for PCR. HDA protocols have been improved steadily to increase sensitivity and provide easier handling [140–142].

Recombinase polymerase amplification (RPA) is done at 37 – 42 °C and requires 20 – 40 min of incubation time [143]. Two primers are needed which are longer than typical PCR primers and require some specific standards to ensure high selectivity and sensitivity [144]. The recombinase and the primers form complexes which invade the double strand, the single strands are stabilized, and DNA polymerase elongates the DNA sequences starting from the primers. Due to the low incubation temperature, there have also been RPA studies working with body heat for incubation [145,146]. RPA assays for detection of different pathogens have been published [145,147] and a recent review covers the development of a diverse set of assays since its discovery [148].

Heterogeneous asymmetrical RPA (haRPA) is a modification of the traditional, homogeneous RPA in reaction tubes, which has been published in 2015, uses a microarray chip to perform the amplification, and subsequent automated detection of the amplified DNA [149]. The haRPA principle is shown in Figure 2. The amplification of the DNA template takes place both on the immobilized reverse (REV) primer and in the liquid bulk phase with limited amount of REV primer available where the amplified DNA is later hybridized to the immobilized primer. Each amplicon is marked with a biotin-labeled forward (FWD) primer. Detection is then performed via chemiluminescence of the horseradish peroxidase catalyzed reaction of luminol and hydrogen peroxide. The high affinity of streptavidin towards biotin allows the streptavidin-labeled horseradish peroxidase to bind selectively to the biotin on the FWD primer, thereby ensuring only complete amplicons are detected. Additionally, the signal is spatially resolved due to the immobilization of the REV primer on specific spots. haRPA assays have so far been developed for human adenovirus, bacteriophages (MS2 and PhiX174), *E.* f*aecalis*, *L. pneumophila*, and for mycotoxin producing fungi [149–151]. Currently available on-chip assays based on RPA include assays for *L. pneumophila*, *Streptococcus pneumoniae*, *Neisseria gonorrhoeae, Salmonella enterica* and methicillin-resistant *Staphylococcus aureus* [152,153]. Hand-held devices for detection of certain pathogens have also been developed [154] as well as assays which combine RPA with immunological detection via enzyme-linked immunosorbent assay (ELISA) [155] and assays performed on digital versatile disks [156]. LAMP and HDA have also been adapted to on-chip assays for

pathogen detection due to the stable incubation temperatures. Detection of *N. gonorrhoeae* and *S. aureus* have been published as on-chip HDA assays [157]. LAMP on-chip applications for pathogenic bacteria in aquatic animals [158] and for viruses as part of point of care diagnostics [159] have also been reported as well as an assay for detection of *Salmonella* spp. in compact disc micro-reactors [160].

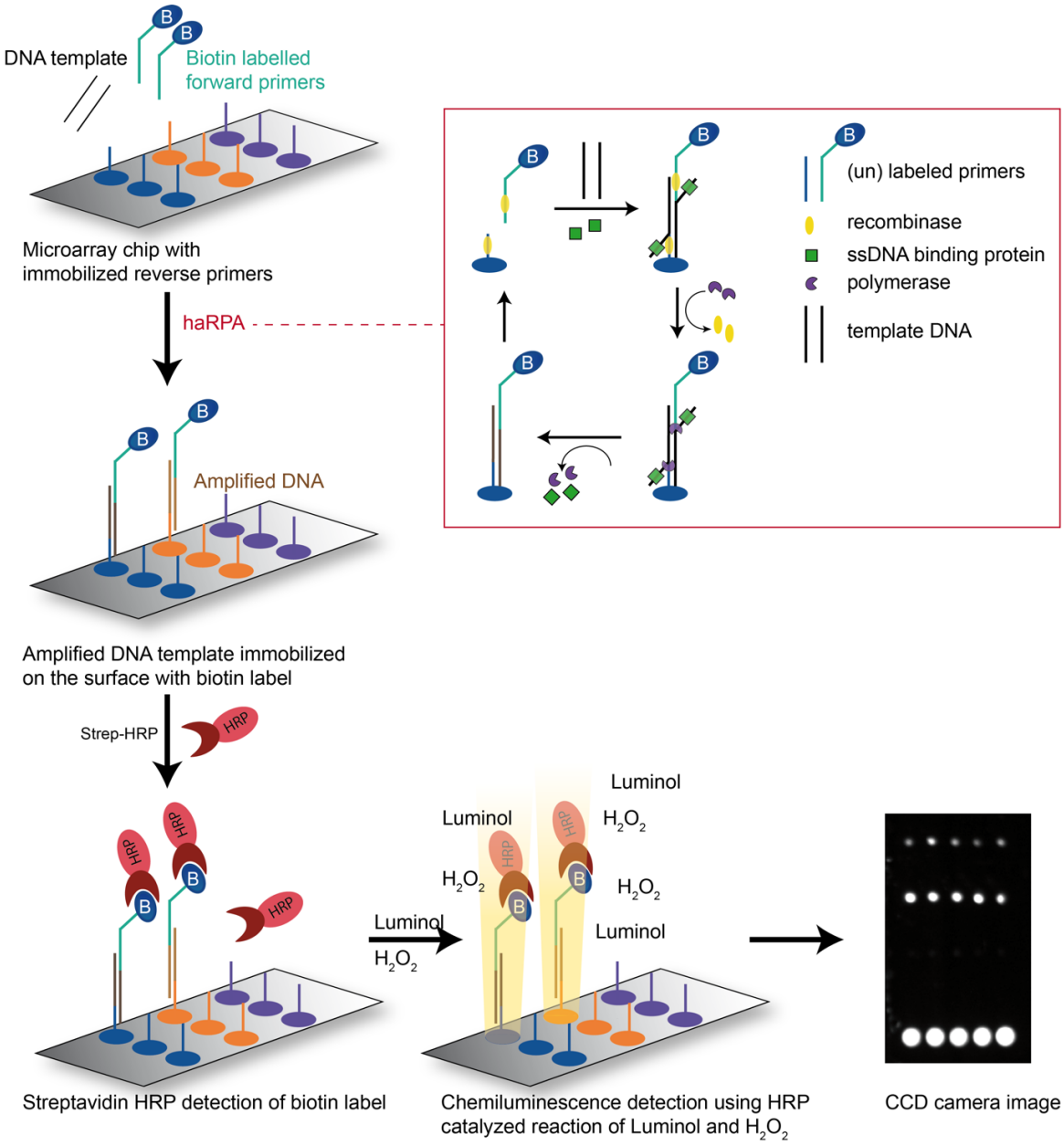

Figure 2: Schematic sketch of the haRPA principle and its detection. DNA amplification takes place on the chip surface as well as in the liquid bulk phase using recombinase and polymerase. The displaced DNA strand is stabilized by single strand DNA (ssDNA) binding proteins to ensure elongation of the primers via polymerase. The immobilized DNA amplicons are then detected by streptavidin horseradish peroxidase (strep-HRP) using the biotin-tag on the forward primers. Through the addition of hydrogen peroxide and luminol a spatially resolved chemiluminescence signal is created.

Taking a closer look at the available isothermal DNA amplification methods for the detection of *bla*$_{CTX-M}$ and bacterial pathogens such as *K. pneumoniae* and *P. aeruginosa*,

several assays have been published in recent years: LAMP assays for the detection of *bla*$_{CTX-M}$ clusters 1, 2, 8, and 9 as well as for the individual gene *bla*$_{CTX-M-9}$ have been published [161–163] as well as assays for the detection of *P. aeruginosa* and *K. pneumoniae* among several other pathogens [164,165]. HDA has been applied for the detection of several different pathogens like *S. aureus*, *E. coli*, and *Salmonella* spp. [166,167], however not the ones of interest for this thesis. A RPA application for *bla*$_{CTX-M}$ has been coupled to electronic detection [168]. For *bla*$_{CTX-M-15}$ RPA assays using microbead dielectrophoresis for detection have been published [169] as well as detection systems using microfluidic devices [170–172]. *K. pneumoniae* and *P. aeruginosa* detection have both been published as RPA assays combined with fluorescence detection [173], however not as haRPA assays. Therefore, RPA and more specifically haRPA assays for the detection of *bla*$_{CTX-M}$ clusters 1 and 9 and for *K. pneumoniae* and *P. aeruginosa* are still missing to facilitate detection of these analytes in low resource settings and for a better monitoring in environmental settings.

2.5 Characterizing bacterial microplastic degradation and its effect on microplastic detection

Spectroscopy-based analysis techniques are an effective tool to get insight into the pressing questions on bacterial degradation of microplastic and what it entails for microplastic detection. RM and FT-IR give qualitative and quantitative information, thus allowing a look at the chemical composition and the number of particles in a sample. While surface changes can be monitored on a single particle level with RM, this in turn means the analysis of thousands of single particles per sample. Here, automation is key to increase sample throughput [174]. Algorithm-assisted particle recognition is used for automatic selection of measurement position followed by subsequent plastic identification via database matching [98,108,175,176]. Using this approach, hands on time for the operator is minimized. The spectra of the particles are acquired, automatically or manually, and matched to the database spectra. When analyzing these spectra, several factors come into play that may infer with this process: Due to the Raman principle, peaks from different compounds within the same confocal volume of the analysis can overlap thus creating a mixed spectrum which hinders specific characterization. Additionally, as Raman is based on vibrational energy changes of chemical bonds, different substances having the same functional groups can show the same Raman spectra. As both Raman and IR spectroscopy share the principle of analyzing the compounds surface, both are expected to change when more oxygen-containing groups (like OH groups) are introduced to the particle surface or organic (humic or bacteria-associated) substances are deposited on the surface. These so-called matrix-effects can be an indication for bacterial microplastic interaction or provide proof for a change in the surface of a plastic compound. This is not only relevant in an environmental context. A recent study used FT-IR to assess PLA degradation in PLA-based implantable medical devices via changes in the IR-spectra [177].

To differentiate between matrix effects from the sample and changes in the plastics chemical structure, sample preparation is necessary for most of the analysis methods for microplastic analysis. Additionally, due to the low concentration of microplastic in environmental samples, concentration methods are essential [71,109,178–180]. To choose the right pre-processing of the sample, the analyte must be known to choose the method accordingly. When dealing with PLA samples as opposed to PS or PET samples, some clean-up methods are not applicable, as these will not only destroy the matrix but the analyte as well or change PLA to such extent that no correct characterization is possible. For example, chemical extraction is one method to reduce matrix effects, but impedes the extraction of additional information such as particle size, shape, and size distribution. RM is a potent method to circumvent these steps for many aqueous samples as minimal sample preparation is needed due Raman signals being insensitive to water. Here, typical sample preparation is the immobilization on a filter surface only thus facilitating a fast analysis after sampling.

Using these analysis techniques, a closer look at MP found in the environment is possible. PLA is in widespread use in food packaging as well as mulch foil where it is seen as a greener alternative to PE [72]. However, to date PLA is not found in the environment, except in burial experiments [181,182]. There are several possible reasons behind this observation. One reason is the proposed instability in the environment as a biodegradable plastic. However, one study in a controlled environment suggests that PLA breaks down in similar ways as traditional plastics [183] and another study found PLA to show almost the same stability as PET when immerged in artificial freshwater and seawater [184]. Another reason is that PLA is degraded so fast by microorganisms or other degradation processes in the environment that no microplastic may be found. The third possible explanation deals with the analysis methods and their bias leading to the conclusion that PLA is altered by the environment due to bacterial colonization, abiotic or bacterial degradation or deposition of humic substances on the surface. This happens to such extent that a correct assignment of the plastic is no longer possible. As database matching is the most commonly used technique to assign samples to specific plastics this pronounced change in the sample's chemical composition and/or degradation could lead to false characterization. The results are false positives (PLA identified as another compound) or false negatives (PLA not discovered). To investigate whether degradation occurs, it is traditionally, assessed either indirectly by monitoring of the degradation products such as the formation of CO_2 or by documenting weight loss of the sample [63,185,186]. Another method is the bulk analysis of the spectral changes via attenuated total refraction FT-IR often combined with a scanning electron microscopy (SEM) visualization of the particle [57,84,187,188]. It is worth noting that biodegradation studies should be carried out with weathered microplastic particles as opposed to pristine particles to mimic environmental conditions and aide bacteria in their efforts. A fast and easy production of artificially weathered microplastic particles has recently been published and is the method of choice for these experiments [99]. Starting with a simple experimental setup (constant temperature, minimal shaking, and ultrapure water), the influences of the surroundings are

kept at a minimum. It will nonetheless allow for a first look into bacterial degradation under conditions that are closer to environmental conditions than a composting plant.

This new approach to achieve a better lateral resolution and, hence, allow single particle analysis, uses RM to characterize the changes happening in the degradation process. It may also help to understand whether PLA is “shielded” from correct identification using RM. This issue has been addressed recently in a study on microplastic from bioplastics in soil [189]. Additional information on particle surface morphology changes is given via field emission SEM (FESEM) images. Using artificially weathered microplastics of traditional plastics like PE and PS and the biodegradable PLA offers the chance to investigate differences in RM and FESEM measurements to answer some of the questions related to biodegradation of (bio)plastics. The investigation of the individual particles surface with RM is of great advantage to achieve this goal and to understand whether bioplastic particles may be under-determined using the current analysis setup. A further combination with culture-based monitoring of the bacteria gives additional insight into the bacterial side of the degradation process. The interaction of RM, FESEM, and bacterial culture for looking at bacterial degradation of microplastic particles from different angles is a new approach to answer important questions on this topic.

3 AIMS OF THIS THESIS

The work detailed in this thesis consists of three individual projects. The first project focusses on the adaptation of the MAF-based filtration process towards *P. aeruginosa* concentration from tap water samples. Starting from existing protocols for other bacterial species, the ideal filter functionalization and elution buffer is to be found and combined with a filtration procedure that ensures easy handling. Culture-independent qPCR analysis is done to guarantee time efficient results for future applications. Providing additional culture-based analysis allows the evaluation of the results with two separate analysis methods. Therefore, culturability of *P. aeruginosa* is assessed for the different conditions present over the course of the filtration procedure. The final objective for this project is a working assay for the detection of P. aeruginosa with a calibration in the desired matrix, tap water.

The second project aims at developing new haRPA assays to detect pathogenic bacteria and antibiotic resistances in one assay. New assays for the ARG clusters *bla*$_{\text{CTX-M}}$ cluster 1 and 9 need to be designed, and existing homogeneous assays for the pathogenic bacterial species *P. aeruginosa* and *K. pneumoniae* are adapted to the heterogeneous haRPA format. The assay for *bla*$_{\text{CTX-M}}$ cluster 1 is then evaluated by comparison to qPCR for sensitivity. As part of the JPI Water project Metawater, bacterial isolates from environmental water sources are tested for *bla*$_{\text{CTX-M}}$ cluster 1 occurrence with an existing PCR protocol and the new haRPA assay, thus providing a specificity comparison for the new assay. The overarching goal to provide a multiplex assay for bacterial species and antibiotic resistances is then first tested with duplex measurements of one bacterial species with one antibiotic resistance, adding additional analytes afterwards. Using this approach, fully evaluated and calibrated assays for detection of single analytes are provided for specific monitoring purposes while a multiplex assay for a broader application is also made available.

The third project tackles two related research questions regarding the interaction between microplastic and bacteria. One aim is to evaluate whether the simple experimental setup chosen is enough to distinguish between microplastic degradation and colonization by monitoring bacterial growth via culture plates and changes in Raman spectra and FESEM images. The other aim is to characterize these changes in the Raman spectra and give insight into how these changes affect correct analysis of microplastic particles subjected to bacteria. For this, three different artificially weathered microplastic polymer types are subjected to different bacterial species and the results after a 21-day incubation period are evaluated. Based on these results, additional experiments using only PLA microplastic particles are done to investigate the observed phenomena in more detail.

4 EXPERIMENTAL PROCEDURES

4.1 Bacteria and DNA samples

Bacterial isolates *E. coli* (CTX-M-2 positive), *E. coli* (CTX-M-3 positive), *E. coli* (CTX-M-9 positive), *E. coli* (CTX-M-14 positive), *E. coli* (CTX-M-27 positive), *K. pneumoniae* (CTX-M-55 positive), *Enterobacter asburiae* (CTX-M-1 positive), and *Enterobacter cloacae* (CTX-M-15 positive) were received from Diagnostic and Research Center for Molecular BioMedicine, Medical University of Graz, Graz, Austria. *K. pneumoniae* (CTX-M-15 positive), *K. pneumoniae* (SHV-18 positive), *E. coli* (CTX-M-15 positive), *E. coli* (TEM-3 positive), and *P. aeruginosa* bacterial isolates were provided by the Bavarian Health and Food Safety Authority, Oberschleißheim, Germany. *E. coli* (5695) without resistance was provided by Institute of Hydrochemistry, TUM, Munich, Germany (IWC-TUM). *Sphingomonas koreensis* and *Pseudomonas libanensis* were isolated from a water sample provided by Elisabeth von der Esch (IWC-TUM) and identified by MALDI-TOF MS as was the case for other bacteria identification needed during the presented work, performed by Jessica Beyerl and Dr. Anna-Cathrine Neumann-Cip, Max von Pettenkofer Institute, Ludwig-Maximilians University, Munich, Germany.

DNA samples and PCR-based ESBL classification for the PCR comparison (according to [190]) were provided by the Bavarian Health and Food Safety Authority, Oberschleißheim, Germany. DNA samples for *L. pneumophila* and *E. faecalis* were provided by Catharina Kober and Sandra Schäfer (IWC-TUM), respectively. Katharina Sollweck (IWC-TUM) provided DNA samples of *Bacillus subtilis*, *Penicillium italicum*, and *Aureobasidium pullulans.*

4.2 Bacteria cultivation

Bacteria from cryo culture (stored at -80 °C for long-term storage or -20 °C for short-term storage (up to 4 weeks)) were cultivated overnight (37 °C) in LB media (with the addition of cefotaxime (1 µg/L), if cefotaxime resistance was present) or NZCYM media (*P. libanensis*, *S. koreensis*, and *E. coli* for microplastic experiments only). OD was quantified using the NanoPhotometer® Classic by Implen (Munich, Germany). Cultivation on LB agar plates (own production) overnight (37 °C) was done with the appropriate dilutions. Cultivation on NZCYM agar plates (own production) for the microplastic study was done overnight (25 °C).

To determine bacterial cell number in liquid culture of *P. aeruginosa*, a calibration model was established based on the linear correlation between optical density measurements at 600 nm (OD_{600}) and the colony forming units on solid nutrient agar. OD from fresh overnight culture was taken and plotted against colony forming unit (CFU) numbers obtained by plating different dilutions on agar plates. This resulted in the following linear

expression: cell number in CFU mL^{-1} = (OD_{600} - 0.0033)/(1.1244 · 10^8). All cell numbers were calculated using this equation.

4.3 MAF disk production

MAFs were produced by self-polymerization of an epoxy-based resin according to literature with minor adjustments [131]. Briefly, a mixture of toluene and *tert*-butyl methyl ether (60:40 (v/v)) used as porogen was tempered at 29 °C. The catalyst trifluoride diethyl etherate ($BF_3 \cdot Et_2O$) in 1,4-dioxane (1:10 (v/v) dilution) was added to the mixture (1.25% (v/v) of the total volume) and mixed thoroughly. The monomer polyglycerol-3-glycidyl ether (CL9) (ratio 20:80 (v/v) monomer/porogen) was added and mixed thoroughly before pouring the mixture into custom-made polytetrafluorotheylene (PTFE) molds (inner diameter 38.6 mm, inner height 10.0 mm) and incubating at 29 °C for 1 h. Afterwards, the MAF disks (38.6 mm diameter, 10.0 mm height) [129] were removed from the polymerization molds, stored in methanol overnight in order to end the polymerization and air-dried at room temperature (Figure 3).

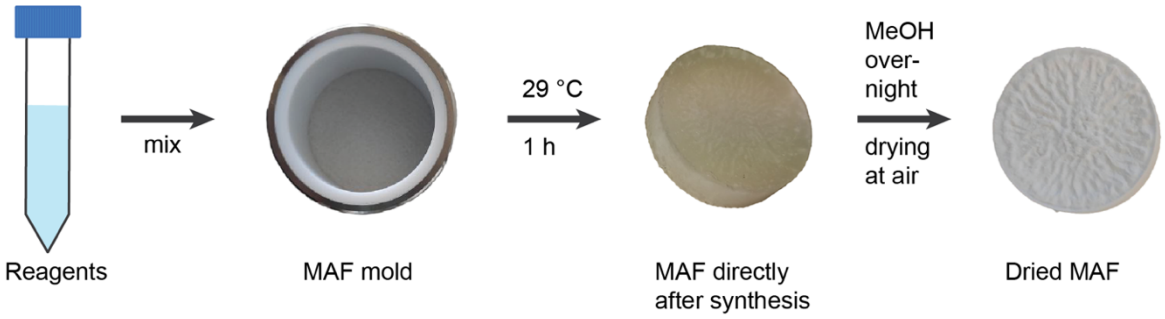

Figure 3: Schematic overview of the MAF production process. The reagents are mixed thoroughly and poured in a MAF mold. After incubation (1 h, 29 °C), the MAF is removed from the mold and put in MeOH to stop the polymerization. After removal from MeOH, the MAFs are air-dried [128].

For functionalization, MAF modules were constructed in 50 mL plastic dispenser tips (PD-tip) consisting of a PTFE support plate with bore holes (diameter 2 mm), an O-ring (38.6 mm in diameter, nitrile butadiene rubber NBR 70), a MAF disk, and a PTFE fitting for connection to tubes. Prior to functionalization, the MAF disks were washed with ultrapure water by connecting the MAF modules to a peristaltic pump and continuously pumping ultrapure water through the system (10 min). The respective functionalization solutions were circulated through the system afterwards according to the functionalization procedures displayed in Table 2. Reaction schemes for the different functionalizations are shown in Figure 4. The functionalized MAF disks were stored in ultrapure water at 4 °C until further use.

Table 2: Overview of functionalization procedures for different MAF disks. MAF-OH: hydrolyzed MAFs; MAF-DEAE: MAFs with diethyl aminoethyl functionalization; MAF-PmB: MAFs with Polymyxin B functionalization [128,130–132]; PBS: phosphate buffered saline.

Functionalization	Functionalization solution	Circulation time	Temperature
MAF-OH	0.5 M sulfuric acid	3 h	60 °C
	ultrapure water	15 min	RT
MAF-DEAE	10% diethylamine in $EtOH/H_2O$ (50/50; v/v)	3 h	60 °C
	ultrapure water	15 min	RT
MAF-PmB	0.5 M sulfuric acid	3 h	60 °C
	Acetonitrile (ACN)	until filtrate was clear	RT
	2 mg mL^{-1} 1,1'-carbonyl-diimidazole in ACN	overnight	RT
	ACN, followed by PBS buffer	until filtrate was clear	RT
	0.02 mg mL^{-1} Polymyxin B in PBS buffer	24 h	RT
	PBS buffer and carbonate buffer	until filtrate was clear	RT

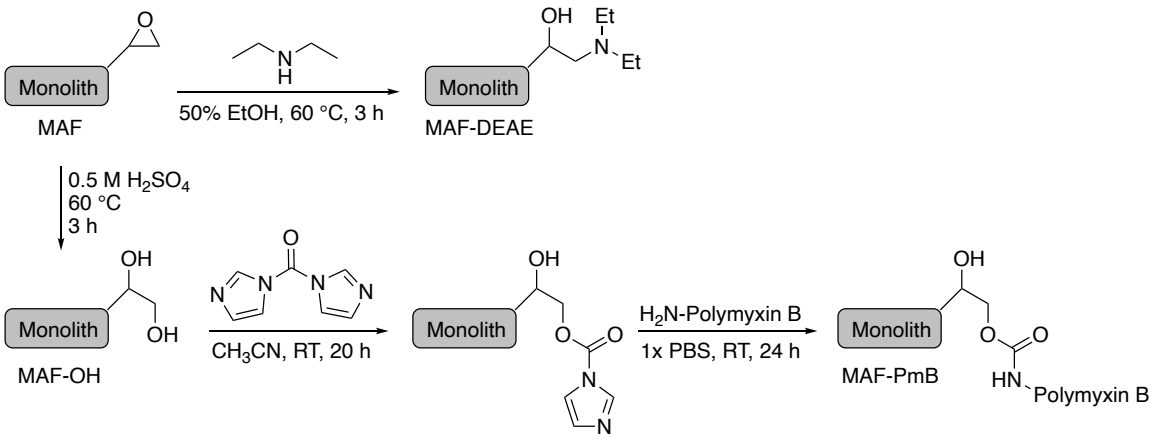

Figure 4: Reaction schemes for functionalization of MAFs to obtain MAF-DEAE, MAF-OH, and MAF-PmB [128].

4.4 Filtration of tap water samples and centrifugal ultrafiltration for enrichment of *P. aeruginosa*

Tap water samples of different volumes were taken at the same location. Tap water was allowed to run for several minutes to ensure comparable samples and collected in different containers (1-L glass bottle, 5-L polypropylene high breast bottle, or 10-L PE canister). If necessary, pH was adjusted to the desired value using 37% hydrogen chloride. Shortly before filtration the samples were spiked with different amounts of *P. aeruginosa*. For all optimization experiments, cells for a final concentration of $1 \cdot 10^8$ CFU L^{-1} were added

whereas for calibration purpose the setup was performed with final cell concentrations ranging from $1 \cdot 10^4$ - $1 \cdot 10^8$ CFU L^{-1}. If heat-inactivated bacteria were used, the inactivation was done at 80 °C for 30 min. A MAF module was connected to a peristaltic pump with a silicone tubing (Maprene Tube) and a 10L PE canister was placed at the MAF module outlet to collect the filtrate. Tap water was used to flush the system prior to filtration and to adjust the flow rate to approx. 180 mL min^{-1}. Filtration was done by inserting the water inlet into the tap water sample and using the adjusted flow rate. After filtration of the whole sample, the MAF module was flushed with air (until no further water exited it) and filled with elution buffer (20 mL). Elution took place in a three-step process with each step consisting of an incubation (2 min) step followed by elution of one third of the elution buffer at a flow rate of approx. 110 mL min^{-1}. Used elution buffers were: carbonate buffer (sodium carbonate (0.150 mM) and sodium bicarbonate (0.350 mM) in ultrapure water; pH 9.6), high salt buffer (sodium chloride (14.99 mM) and HEPES (4-(2-hydroxyethyl)-1-piperazineethanesulfonic acid; 0.500 mM) in ultrapure water; pH 7, adjusted with 32% sodium hydroxide), glycine buffer (5.00 mM in ultrapure water; pH 9.5, adjusted with 32% sodium hydroxide), beef extract glycine buffer (BEG, beef extract (30.0 g) and glycine (0.505 M) in 1 L of ultrapure water; pH 9.5, adjusted with 32% sodium hydroxide), and Pluronic® F68 solution (Pluronic® F68 (1%) in water). After the elution, centrifugal ultrafiltration was performed (5000 rpm) using Vivaspin 20 Membrane 50000 columns to achieve a final volume of 0.5 mL – 1 mL. The filter was washed with sterile phosphate buffered saline (PBS buffer) and the volume was adjusted to 1.5 mL with PBS buffer. 1 mL of the resulting solution was used for DNA extraction while the remaining 0.5 mL were stored at -20 °C. By extracting DNA from 1 mL of culture sample, determining the DNA content in ng μL^{-1} by qPCR, and plating the original sample on agar plates to assess the correct cell number in the culture a correlation could be established. The qPCR was calibrated using a DNA extract of known concentration of total DNA (as determined by micro-volume spectrophotometer analysis using a nanophotometer). Using this approach, $5.75 \cdot 10^6$ *P. aeruginosa* cells per mL of solution before DNA extraction were determined to correspond to 1 ng μL^{-1} DNA in qPCR.

4.5 DNA extraction

For all bacterial extracts used for haRPA optimization and comparison experiments DNA, extraction was done from fresh overnight culture using the QIAamp DNA Mini Kit according to manufacturer's guidelines (elution volume: 200 µL). For haRPA calibration experiments with *bla*$_{CTX\text{-}M}$ cluster 1, 4 mL bacterial cell solution was centrifuged and the resulting pellet was resuspended in 1 mL LB medium before continuing with the manufacturer's protocol. DNA for calibration experiments for *P. aeruginosa* detection using haRPA was done from dilutions of overnight culture containing the desired number of bacterial cells (measured via OD_{600} of the overnight culture). DNA extraction for *P. aeruginosa* for the MAF-study was performed using the GeneJET Genomic DNA Purification Kit following the instruction

manual. For initial cell harvesting of *P. aeruginosa* the sample was centrifuged (5000 × g, 10 min). All DNA extracts were stored at -20 °C until further use.

4.6 DNA chip production

Glass-based DNA microarrays were produced in-house following a procedure published elsewhere in detail [191,192] using the Jeffamine® ED-2003 modification published by Kober *et al*. 2018 [150] with minor adjustments. DNA primers were immobilized on the surface using the SciFLEXARRAYER S1, an inkjet microdispensing system, with an unmodified piezo dispense capillary (PDC 80, P-2040, ID-No. 15842 and 54868) at 20 °C and 55% humidity. Spotting order for singleplex assays started with negative control followed by modified REV primer for the target sequence, negative control, and positive control while 5 replicates, creating a 5 × 4 matrix (number of lines × number of columns). Spotting order for multiplex assays was negative control, modified REV primer for *P. aeruginosa*, negative control, modified REV primer for *K. pneumoniae*, negative control, modified REV primer for *bla*$_{\text{CTX-M}}$ cluster 1, negative control, (modified REV primer for *bla*$_{\text{CTX-M}}$ cluster 9, if needed) and positive control while 5 replicates, creating a 5 × 7 (8 with *bla*$_{\text{CTX-M}}$ cluster 9) matrix. 4.8 ± 0.7 pmol of the REV-primer with 5'-NH_2-C_{12}-tag (sequences in Table 3) was spotted. The spotted negative control was nuclease-free water and positive control was EZ-Link™ amine-PEG2-biotin (0.01 µg mL^{-1}). Assembly of DNA microarrays was carried out according to Kober *et al*. 2018 [150].

4.7 qPCR

The assay was performed according to the manufacturer's guidelines. Briefly, for every reaction 10 µL Luna® Universal qPCR Master Mix, 0.5 µL FWD-primer (10 µM), 0.5 µL REV-primer (10 µM), and 7 µL H_2O was combined in a master mix. This master mix was added together with 2 µL DNA extract of the sample of interest. A non-target control was also included in every qPCR measurement (18 µL of the master mix described above and 2 µL H_2O). Primer sequences for qPCR assays are depicted in Table 3. Table 4 shows the thermocycling conditions for qPCR.

Table 3: Primer sequences for qPCR, haRPA and RPA. *P. aeruginosa* and *K. pneumoniae* species specific haRPA primers were established during the BMBF INIS-EDIT project. All others were designed and tested during this thesis.

Target organism	Gene	Primer	Sequence (5' → 3')	Amplicon length	Assay type
P. aeruginosa	regA gene	PaRegFP	CGCAAGAGCATCGAGTACCT	141 bp	qPCR
	X12366.1	PaRegRP	TAGTGCCTGCCGTGACGG		
P. aeruginosa	regA gene	Pa-RPA-FP	CGCAAGAGCATCGAGTACCT GAACCGGCTGTTG	141 bp	haRPA
	X12366.1	Pa-RPA-RP	CTCCGAATAGTGCCTGCCGT GACGG		
CTX-M carriers	*bla*$_{CTX-M}$ cluster 1	CTX-M-PFP	CTGATGAGCGCTTTGCGATGT GCAGCACCAG	352 bp	haRPA
	X92506.1	CTX-M-RP5	TCACGCGGATCGCCCGGAA TGGCGGTGTTTAACG		
CTX-M carriers	*bla*$_{CTX-M}$ cluster 9	CTX-M-9-PFP	CCGCGTTGCAGTACAGCGAC AATACCGCCAT	372 bp	haRPA
	KP698222.1	CTX-M-9-RP1	TCGTATTGCCTTTGAGCCACG TCACCAACTGCG		
CTX-M carriers	*bla*$_{CTX-M}$ cluster 1	CTX-M-qFP	CGCTTTGCGATGTGCAG	330 bp	qPCR
	X92506.1	CTX-M-qRP	CGGAATGGCGGTGTTTAA		
K. pneumoniae	phoE gene	Kp-RPA-FP	CATAGCTTAACGAGGTGCCG ACGCCGTCGCCGTTC	110 bp	haRPA
	AF064793.1	Kp-RPA-RP	CTTCGGTCTGGTGGATGGCC TGGATCTGACCCTG		

Table 4: Thermocycling conditions for qPCRs using the Luna Universal qPCR Master Mix.

Step	Temperature	Time	Cycles
Initial denaturation	95 °C	60 s	1
Elongation	95 °C	15 s	45
	60 °C	30 s	
		(+ plate read)	
Melt curve	55 – 95 °C	various	1
Hold	37 °C	30 s	1

4.8 Primer design for haRPA and testing in RPA

The design for haRPA primers specific for resistance gene *bla*$_{CTX-M}$ cluster 1 was guided by the published protocol with few adjustments [150]. Five primer pairs were designed based on *E. coli bla*$_{CTX-M-1}$ gene (GenBank number: X92506.1) and an additional pair was based on published qPCR primers for detection of *bla*$_{CTX-M}$ [193]. Homogeneous RPA reactions were performed according to manufacturer's guidelines. Briefly, 2.4 µL of each primer (10 µM), 29.5 µL rehydration buffer, 5 µL DNA sample, and 7.2 µL H_2O were added to the lyophilized reaction component pellet and the reaction was started by addition of 2.5 µL magnesium acetate solution (280 mM). After incubation for 40 min at 39 °C and 800 rpm the RPA product was purified using GeneJet PCR Purification Kit and analyzed on a 3% agarose gel (w/v). The agarose gel was stained with 5 µL Serva Stain Clear G. The amplicons were checked for appropriate size and ranked based on DNA amount. In total, 20 different combinations of FWD and REV primers were tested and the two most promising ones (no cross-reactivities and high amplification efficiency) were chosen for further testing on the haRPA system. The primer pair with the best amplification in haRPA is depicted in Table 3.

4.9 haRPA

haRPA was performed as described elsewhere in detail [149,150] with minor adjustments. Injection was done using a pipette and incubation was done outside the Microarray Chip Reader, 3rd generation (MCR 3) flow cell. The modified REV-primer (5'-NH_2-C_{12}-tag) was immobilized on the chip surface and the biotinylated FWD-primer (5'-biotin-tag) was added to the bulk phase to enable chemiluminescence reaction with streptavidin-labelled horseradish peroxidase (strep-HRP). The running and washing buffer was casein (0.5% (*w/v*)) in PBS. For haRPA reaction in one flow cell, the following reaction mix was used according to manufacturer's guidelines for the TwistAmp® Basic kit: 29.5 µL rehydration

buffer, nuclease free water added to achieve 54 µL total volume, and 5 µL primer mix. Primer mix for singleplex assays consisted of biotinylated FWD-primer and unmodified REV-primer in different ratios (1:5, 1:10, 1:20, and 1:50 REV: FWD) with varying FWD-primer amount (370 nM, 420 nM, and 950 nM) and the according REV-primer amount. The primer mix for duplex or multiplex assays consisted of the different primers for the DNA amplicons which were to be analyzed in the respective ratios and amounts. The reaction mix was added to the lyophilized reagents. Subsequently, 5 µL of DNA extract (for singleplex assay; for duplex/multiplex assays a total volume of 10 µL DNA was not exceeded) was added and the reaction was started using 4 µL of magnesium acetate solution (250 µM). 52 µL of the mixture was injected into the microarray flow cell using a pipette and incubated using a custom-made adapter for microarray chips in a Thermomixer at 39 °C for 40 minutes. Afterwards, the chip was inserted into the MCR 3 (further developed from the original, including a heatable flow cell as published elsewhere [194]) and a dark frame image was taken with the CCD camera for 60 s. The measurement was carried out as published elsewhere [150]. The dark frame image was subtracted from the obtained chemiluminescence image before automated analysis was done using the microarray analysis software MCR Image Analyzer. The ten brightest pixels of each spot were analyzed. Spots with a deviation of more than 15% were not included and marked as outliers. A minimum number of three spots were analyzed per row of immobilized primer.

4.10 Production of microplastic particles

Microplastic particles (PS, PET, and PLA) were produced following a published method [99] with minor adjustments. Briefly, clean microplastic precursor particles (1 cm^2 cut from Activia® yoghurt cups) were sonicated in 0.25 M KOH for 15 h at 35 kHz. The parent particles and the alkaline microplastic suspension were divided, and the alkaline microplastic suspension was processed further. The liquid in the microplastic suspension was changed to ultrapure water using centrifugation (30 min, 3000 rpm, 20 °C) until pH 7 was reached. For the second experiment, as sterile conditions were needed, all lab equipment was autoclaved, when possible, as well as ultrapure water. The PLA precursor particles were sterilized using 70% EtOH and then left to dry at room temperature in a sterile working bench. All necessary steps were carried out either in a sterile working bench or in a laminar flow box. After ultra-sonication the suspensible particles were divided in samples with 30 mL of the particle suspension each.

4.11 Sample preparation of microplastic bacterial suspensions

For the first experiment on microplastic degradation, aliquots of 5 mL of the microplastic suspensions (PLA, PET, and PS) were incubated at room temperature with occasional shaking by hand for 3 weeks. Samples for identification of bacteria were taken on day 28 and plated on NZCYM agar plates (own production). Representative colonies of *S. koreensis* and *P. libanensis* were chosen for identification via MALDI-TOF-MS.

For the second experiment, *S. koreensis*, *P. libanensis*, and *E. coli* cultivated overnight (37 °C) in NZCYM media were subjected to a change of media to ultrapure water by centrifugation (three cycles, 10 min, 5000 rpm) and the number of cells for a final concentration of 10^2 cells mL^{-1} was spiked into the microplastic containing samples. One set of PLA microplastic suspension was not spiked with bacteria, one set was spiked with *E. coli*, one set with *P. libanensis*, one set with *S. koreensis*, and one with both *P. libanensis* and *S. koreensis*. Each set consisted of four individual samples. All samples were incubated at 25 °C for a total of 21 days. Samples for cultivation of bacteria on NZCYM agar plates were taken daily (plated in triplicates) and samples for Raman and FESEM measurements were taken at day 0, 14, and 21.

4.12 Raman measurements of microplastic particles and bacteria

The RM analysis of the microplastic particles and bacteria was conducted on a WITec *alpha300_R* Raman microscope with the help from Elisabeth von der Esch (IWC-TUM). The optical images were produced using a 20× objective. The Raman spectra were acquired manually as well as using the WITec Particle Scout software enabling automated measurement of 70 particles per sample (532 nm laser, 3 mW, 20 s measurement time per particle, 20× objective for automated measurements, 50× objective for manual measurements). Samples were drop cast (10 µL) on CaF_2 carriers under sterile and particle-free conditions before RM analysis.

4.13 FESEM measurements

FESEM images of microplastic particles were recorded with a HD-SE detector and 3 kV acceleration voltage by Christian Schwaferts (IWC-TUM). Samples for MP analysis were drop cast (10 µL) on silicon wafers under sterile and particle-free conditions and imaged without further metal coating. MAFs were imaged in low vacuum mode by Christine Benning (IWC-TUM). For the inner MAF structure, 0.5 × 0.5 cm rectangles were cut out in the center of the MAF and then cut in half horizontally using a scalpel. The upper side of the lower half was investigated in different magnifications and analyzed using ImageJ.

5 RESULTS AND DISCUSSION

5.1 Rapid quantification of *P. aeruginosa* by monolithic adsorption filtration and subsequent detection using qPCR

Using MAFs for filtration of bacteria and viruses has been reported previously [129–131], however, a working assay for the detection of *P. aeruginosa* has been missing so far. The following section sheds light on the development and optimization process of the enrichment of *P. aeruginosa* from tap water samples using MAF, further reduction of the volume by centrifugal ultrafiltration and detection of the final number of *P. aeruginosa* cells using qPCR after DNA extraction (Figure 5).

During the course of the experiments, key factors of the MAF enrichment process were investigated and optimized: functionalization of the MAF disk, elution buffer composition, mode of filtration, initial sample volume, and sample pH. A calibration with the best overall process parameters was then carried out with spiked tap water samples. Further details about the development process can be read in "Quantification of *Pseudomonas aeruginosa* in Tap Water Samples after Concentration by Monolithic Adsorption Filtration" (master's thesis by Julia Klüpfel), which was part of this work.

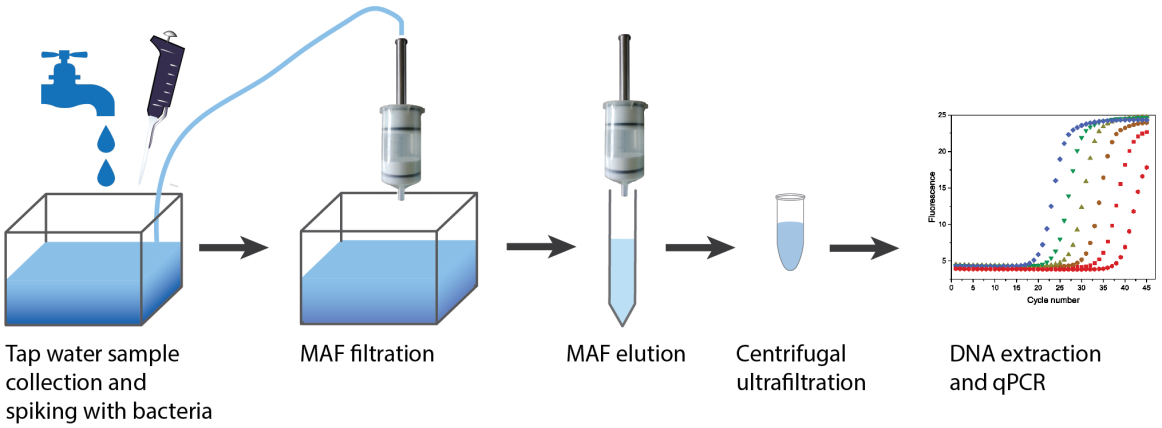

Figure 5: Schematic overview of the total MAF enrichment, elution and subsequent detection procedure. Tap water samples were collected and spiked with bacteria. MAF filtration and elution was followed by centrifugal ultrafiltration and DNA extraction for analysis with qPCR [128].

5.1.1 Quality control of MAFs using FESEM

Batch to batch quality control was done by analyzing FESEM images using ImageJ. The pore sizes as well as the polymer bubble diameters of pristine and OH functionalized MAF were characterized (Figure 6a-c). Figure 6 shows an example of FESEM analysis of batches synthesized for this work. Comparing the observed mean pore size of this work (22.30 ± 6.30 µm) to the literature value of 22.5 ± 9.0 µm [131] indicates good agreement between literature and experiment. The mean pore size of MAF-OH (22.34 ± 5.58 µm) is similar to the mean pore size of pristine MAFs revealing that functionalization does not change the MAF pore size. Analyzing the mean polymer bubble diameter (4.61 ± 0.56 µm) demonstrates a relatively homogeneous size distribution and suggests a homogeneous and continuous polymerization process, as is desired.

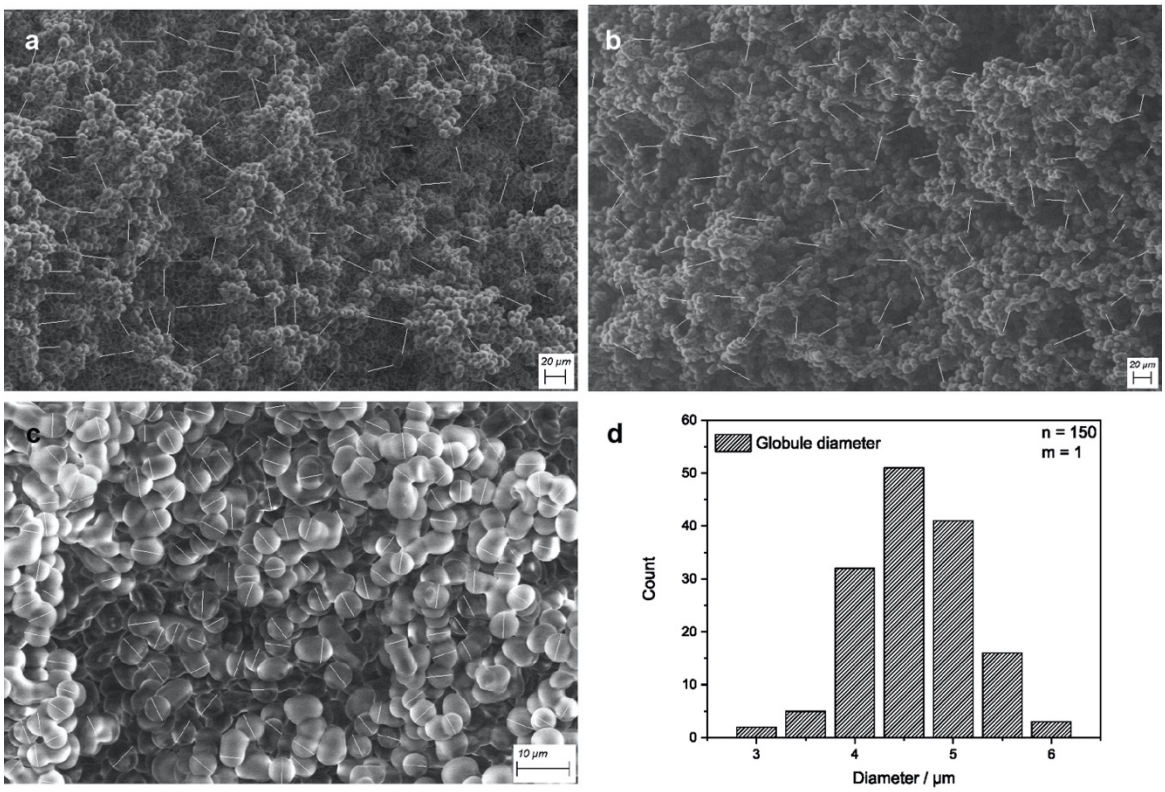

Figure 6: FESEM images for pristine MAF pore size (a), OH functionalized MAF pore size (b), polymer globule diameter (c) with indicated measurement lines (n = 150 for globules) and globule diameter size distribution (d) [128].

5.1.2 Different MAF functionalizations

The first step to adopt the currently available monolithic adsorption filtration procedures for *P. aeruginosa* was to identify the MAF functionalization with the best binding and elution properties. Therefore, three previously published functionalizations (MAF-DEAE [132], MAF-OH [130], and MAF-PmB [131]) were tested with an initial spiked concentration of 10^8 CFU L^{-1}. To quantify the results, a recovery was calculated via the ratio of the total number of cells found in the eluate by qPCR after filtration and the total number of cells in the initial sample. This was necessary as the low number of *P. aeruginosa* cells in the filtrate did not allow a direct determination of the concentration thereof using qPCR and thus hindered direct calculation of the cells retained by the MAF. MAF-DEAE was chosen as the first candidate because of good results for enrichment of *L. pneumophila* in recent years in our laboratory. The literature standard conditions were 1-L sample volume, pH 7, and BEG elution buffer [132]. However, only a very low recovery of 0.04 ± 0.01% could be achieved. Therefore, MAF-OH and MAF-PmB were also tested using the published standard conditions: 10-L sample volume, pH 3, BEG elution buffer for MAF-OH [130] and 1-L sample volume, pH 4, carbonate elution buffer [131] for MAF-PmB. Recovery values of 68.6 ± 7.4% and 4.3 ± 0.3% for MAF-OH and MAF-PmB were achieved, respectively, as depicted in Figure 7. Based on these results, it was concluded that unspecific retention of *P. aeruginosa* cells on the MAF only occurs in very low numbers as is evident by the low recovery with MAF-DEAE. MAF-DEAE recovery was therefore seen as a reference for unspecific binding. The large differences in recovery of these three functionalizations are most likely based on the different forces that allow retention of the bacteria. While MAF-PmB uses the affinity ligand Polymyxin B (a surface-active antibiotic) to hold bacterial cells on the MAF surface, MAF-DEAE and MAF-OH use electrostatic interactions between the bacterial cells and the MAF surface. As the bacteria are positively charged due to acidification in MAF-OH filtration, MAF-OH seems to offer them significantly higher interaction possibilities compared to MAF-DEAE. At neutral pH (which is used for MAF-DEAE filtration) almost no interaction takes place between the MAF surface and the negatively charged bacterial cell surface due to the lipopolysaccharide structures presented on the surface of the bacteria. This structure is positively charged at pH 3 and negatively charged at pH 7. As *P. aeruginosa* possess a typical lipopolysaccharide structure (detailed information in [195]) hydrogen bonds are believed to be the main form of interaction. Due to these results, MAF-OH seems to present the best option for establishing a MAF-based enrichment procedure of *P. aeruginosa*, however further experiments with MAF-DEAE and MAF-PmB were carried out to get a deeper understanding of the MAF filtration process.

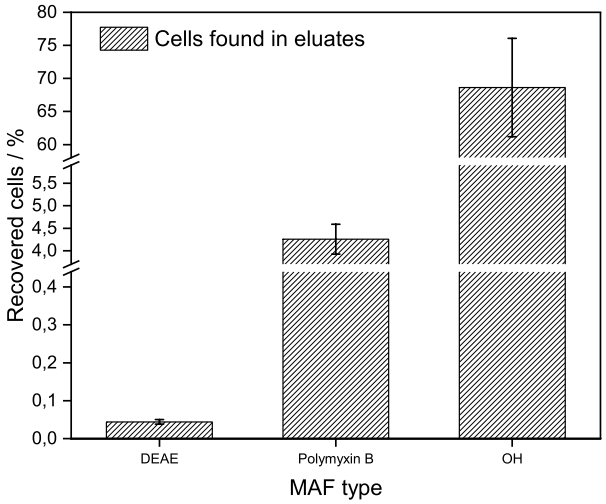

Figure 7: Recoveries for different MAF functionalization types at literature conditions (MAF-DEAE: 1-L sample volume, pH 7, BEG elution buffer; MAF-OH: 10-L sample volume, pH 3, BEG elution buffer; MAF-PmB: 1-L sample volume, pH 4, carbonate elution buffer); DEAE (MAF-DEAE), Polymyxin B (MAF-PmB), OH (MAF-OH), n = 3 [128].

5.1.3 Elution buffer comparison for MAF-DEAE and MAF-OH

MAF-OH and MAF-DEAE were further investigated by testing of different elution buffers to see which change in properties resulted in the most efficient elution of the bacterial cells from the monolith surface. Therefore, five different elution buffers (BEG buffer, high salt buffer, carbonate buffer, glycine, and Pluronic® F68 solution) were tested. The initial spiked *P. aeruginosa* cell concentration was the same for all tests (10^8 CFU mL^{-1} in the bacterial solution used for spiking, resulting in 10^8 CFU L^{-1} initial sample concentration) and the applied MAF process was also the same for all tests using the same MAF functionalization: For MAF-OH 10-L initial sample volume, sample pH 3, 20-mL elution volume and for MAF-DEAE 1-L initial sample volume, sample pH 7, 20 mL elution volume were used. An overview of the recoveries for MAF-OH is given in Figure 8a. The aforementioned standard elution buffer, BEG buffer, yields the highest recovery (57.0 ± 3.0%) while the other tested buffers show similar, significantly lower recovery values. These are 8.6 ± 0.3% for Pluronic® F68 solution, 8.8 ± 0.7% for carbonate buffer, 11.6 ± 0.6% for high salt buffer, and 17.5 ± 1.5% for glycine buffer. It seems that the combination of a change in pH (from an initial sample pH of 3 to elution buffer pH of 9.5) and the presence of proteins (from the beef extract) results in the best desorption und thus breaks the interactions between the cells and the monoliths surface most efficiently. The change in pH results in a change in the net charge of the bacteria while van der Waals forces and hydrophobic interactions by the protein help to remove the cells from the MAF surface. As a consequence, BEG buffer was chosen for elution of *P. aeruginosa* from MAF-OH.

A different picture presented itself when comparing the same elution buffers for MAF-DEAE (displayed in Figure 8b). Here, the standard elution buffer BEG showed the lowest recovery (0.04 ± 0.01%) and the carbonate buffer was only slightly better with a recovery

of 0.054 ± 0.00%. Glycine buffer and Pluronic® F68 solution showed improved recoveries with 1.23 ± 0.08% and 1.30 ± 0.10%, respectively. The highest recovery for MAF-DEAE was achieved with high salt buffer (1.66 ± 0.23%) meaning that high ion strength resulted in the best elution from the MAF-DEAE surface. High salt buffer was therefore used for all further experiments with MAF-DEAE. However, MAF-DEAE showed significantly lower results with all elution buffers than even the least promising combination of elution buffer with MAF-OH. Thus, it was concluded that MAF-OH is better suited for enrichment of *P. aeruginosa*.

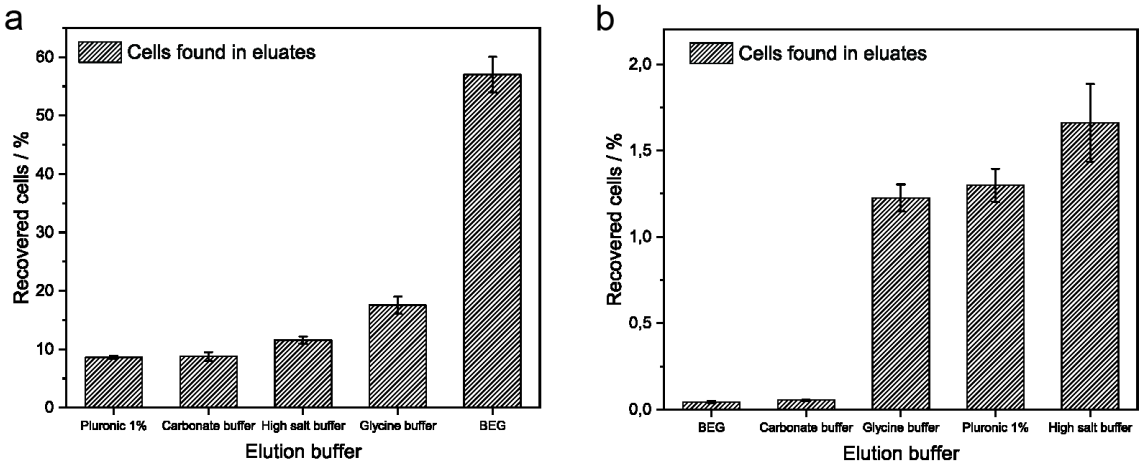

Figure 8: Recoveries determined using different elution buffers for MAF-OH (a) and MAF-DEAE (b), n = 3 [128].

5.1.4 Filtration mode variation for MAF-DEAE

Due to the low initial sample volume of 1 L, MAF-DEAE filtration at pH 7 and elution with high salt buffer was further investigated for changes in the filtration mode. The standard filtration mode, 1-L sample and a single filtration at constant flow, was compared to circulating filtration (circulating the 1-L sample through the MAF for 1 h) and repeated filtration (5 × filtration of the same 1-L sample through the same MAF) to evaluate whether an increase in contact time of the sample with the MAF also increased the adsorption efficiency. Additionally, a 10 × higher initial sample volume (10 L) was also tested. The results are shown in Figure 9a. All three tested alterations from the standard technique resulted in unsatisfactory recoveries of 0.28 ± 0.04%, 0.58 ± 0.07%, and 0.49 ± 0.01% for repeated, circulating, and higher initial sample volume filtration, respectively. The standard MAF-DEAE filtration showed a recovery of 1.66 ± 0.23%. Due to these results, MAF-DEAE was excluded from further optimization efforts. The improvement of the MAF-OH procedure was pushed further.

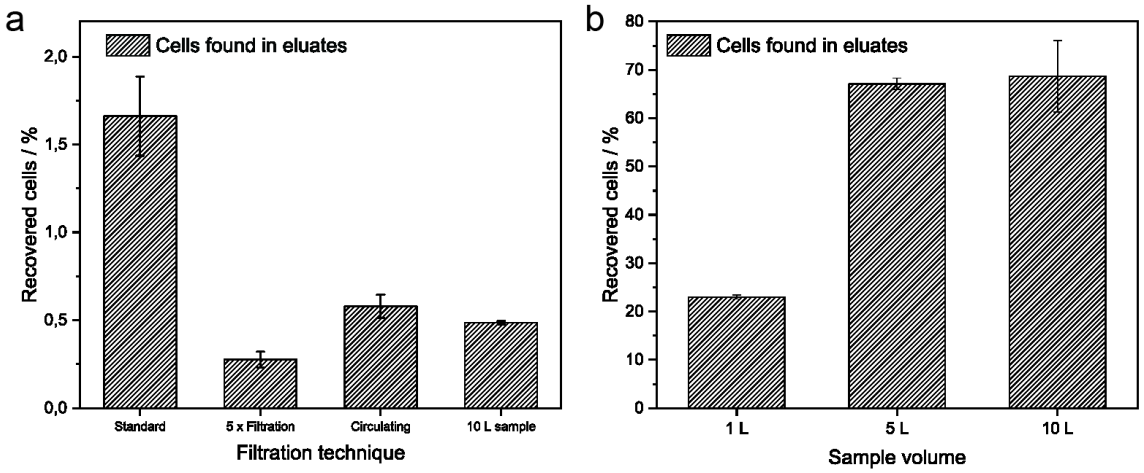

Figure 9: Recoveries found with (a) different filtration techniques and initial sample volumes using MAF-DEAE (pH 7, elution with high salt buffer) and (b) different initial sample volumes using MAF-OH (pH 3, elution with BEG buffer), n = 3 [128].

5.1.5 Sample volume optimization for MAF-DEAE and MAF-OH

While the MAF diameter (3.86 cm) and height (1 cm) is the same for all functionalizations, the optimal sample volume differs between MAF-DEAE and MAF-OH. Optimizing this parameter may further increase recovery. For MAF-DEAE, the original protocol states 1-L initial sample volume [132] and, due to the low recoveries, 10-L initial sample volume was also tested with 10^8 CFU L^{-1} spiked *P. aeruginosa* at a sample pH of 7and with high salt elution buffer (Figure 9a). However, a recovery of only 0.49 ± 0.01% could be achieved while the standard (1 L) sample volume reached 1.66 ± 0.23% recovery. This revealed that the original procedure using different bacteria [132] showed the same trend as the new experiments with *P. aeruginosa*. An explanation for this behavior is that MAF-DEAE do not provide sufficient adsorption properties for *P. aeruginosa* which are therefore swept out of the MAF with increasing volume instead of accumulating on the filter. This matches the assumption that MAF-DEAE can be seen as a proxy for unspecific retention of the bacterial cells on the MAF-surface.

For MAF-OH, the standard protocol states 10-L initial sample volume. As the goal was to facilitate easy sampling and rapid enrichment, a reduction in initial sample volume with still reasonably high recovery was aimed at. Therefore, 1 L and 5 L initial sample volume was also tested under the conditions stated above (10^8 CFU L^{-1} *P. aeruginosa* spiked at a sample pH of 3 and BEG elution buffer). Reducing the sample volume from 10 L to 5 L did not change the recovery significantly (from 68.6 ± 7.4% to 67.1 ± 1.2%, respectively) while further reduction to 1 L lead to a recovery of only 23.0 ± 0.4% (Figure 9b). This result confirms that among the tested volumes MAF-OH are best suited for filtration of 10-L samples. However, due to insignificant reduction in recovery, better reproducibility (indicated by lower standard deviation), easier handling of the samples with 5 L volume, and reduced processing time, it was decided to continue with a sample volume of 5 L. A possible explanation for this behavior is the distribution of *P. aeruginosa* within the MAF over time: The bacteria seem to only attach to the first part of the MAFs cylindrical structure

with a lower sample volume and thus are not completely eluted from the MAF using the current elution procedure. With higher sample volume, several adsorption and desorption events seem to occur before the bacterial cells stick to the MAF surface in the end. Therefore, the distribution of the *P. aeruginosa* cells over the whole filter is more even and consequently leads to a higher recovery using the current elution protocol. Having a second look at the different recoveries using 10-L sample volume for MAF-OH filtration reveals a measurable inter-batch variance (e.g., 68.6 ± 7.4% to 57.0 ± 3.0%) with a relatively low intra-batch variance (for each individual parameter tested). It is therefore crucial to perform quality control of each MAF batch to reduce the influence of MAF quality on the recovery results.

5.1.6 Optimization of sample pH for MAF-OH

The final parameter in MAF filtration to be optimized was the sample pH. Literature sample pH for MAF-DEAE was 7.0 and for MAF-OH 3.0 [130,132] and these values were set as the higher and lower limit for optimization. With *P. aeruginosa* as the model organism here, culturability in tap water needed to be assessed as no reliable literature data could be found. Cultivation as a confirmative detection method after filtration should be used which required the bacteria to be alive and detectable. With the possibility of cultivation as an additional detection method the results of this work would be even more comparable as detection via culture is still the gold standard. Unfortunately, this could not be achieved with pH 3 tap water samples, where no growth could be observed even if the bacteria were only left in acidic solution for a very short time (10 min). Growth of *P. aeruginosa* was observed on all agar plates where the pH value was above pH 3.3 with overgrown plates after overnight incubation. In contrast, no growth (no colonies visible) was observed for pH below 3.2 (down to 3.0, which was the lowest pH tested). This indicates a change in physiology of the bacteria at these low pH values. Literature data showed one study investigating the effect of low pH values on the survival of *P. aeruginosa* [196] while a different study found good bacterial growth for pH higher than 3.8 [197] thus confirming the findings of the culturability study in this work.

To test for a combination of culturability and good enrichment of bacteria, different pH values between pH 3 and pH 7 for filtration with MAF-OH were tested. All filtrations were carried out using the optimized protocol (MAF-OH, 5-L initial sample volume, BEG elution buffer). *P. aeruginosa* were spiked to a final cell concentration of 10^8 CFU L^{-1} and the cultivated *P. aeruginosa* samples used for spiking were acidified just prior to filtration. Good retention and subsequent elution could only be achieved with a sample pH of 3 (as depicted in Figure 10a with the recovery for a sample pH of 3 set to 100%). Filtrations of samples at pH 3.2 or higher resulted in significantly lower recoveries with the highest being at pH 3.6 and the lowest at pH 4.0 (pH 3.2: 26.7% ± 5.3%; pH 3.4: 32.5% ± 12.72%; pH 3.6: 34.4% ± 15.45%; pH 3.8: 17.7% ± 8.4%; pH 4: 11.6% ± 9.3%). Higher sample pH values did not show better relative recoveries with 23.2% for pH 5, 17.0% for pH 6, and 10.6% for pH 7. In conclusion, no good retention on the MAF and subsequent elution was

possible at filtration conditions that allowed for later *P. aeruginosa* detection via culture. However, the recovery values are higher than those of unspecific binding meaning a specific interaction between the MAF surface and the bacterial cells takes place. Spiked cultivated *P. aeruginosa* cells which were culturable at pH values higher than 3 seem to be adsorbed onto the surface of MAF-OH to a significantly lower extent than non-culturable cells at a pH of 3. This finding of a possible correlation between filtration efficiency and culturability required further investigation which was carried out by using viable *P. aeruginosa* cells and heat-inactivated cells for spiking into the tap water samples at different sample pH.

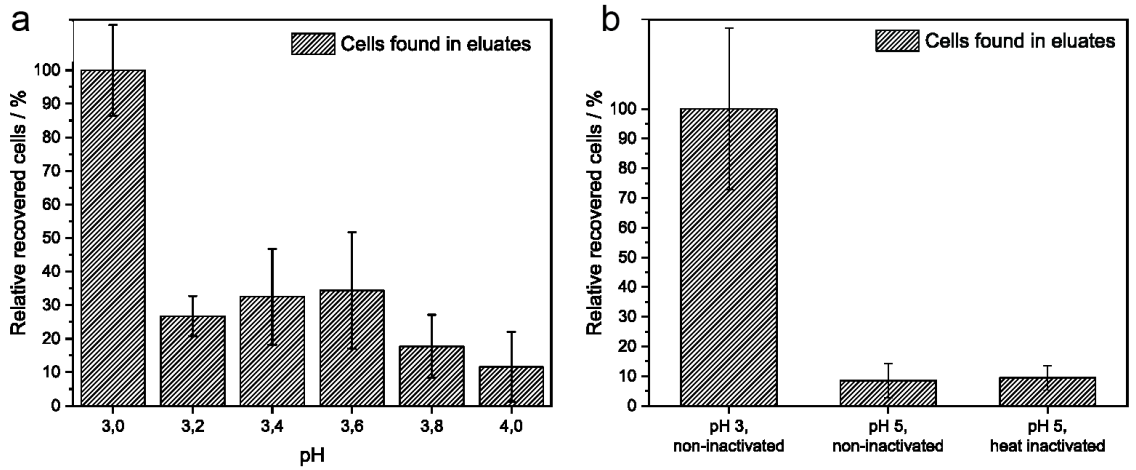

Figure 10: Relative recoveries (recovery for pH 3 and viable cells was set to 100%) found with (a) different initial sample pH and with (b) viable or heat-inactivated cells at pH 3 and pH 5 using MAF-OH (pH 3, elution with BEG buffer, 5 L initial sample volume), n = 3 [128].

As is shown in Figure 10b, no significant difference between heat-inactivated cells and non-inactivated cells at pH 5 could be determined with a relative recovery of 9.4% ± 4.1% and 8.5% ± 5.7%, respectively. Recovery at pH 3 with non-inactivated cells was set to 100% (standard deviation ± 27.2%) for comparison. Due to these results, it was concluded that contrary to the original theory, there is no correlation between culturability status of the bacteria and filtration efficiency but rather between filtration efficiency and sample pH. The higher retainability of the cells at a sample pH of 3 on the MAF surface seems to stem from a change in outer membrane chemistry of the bacteria which in turn induces a change in interactions between the outer membrane of the cells and the monolith's surface. These findings result in the conclusion that the current set-up does not allow for a detection via culture or a live-dead discrimination as *P. aeruginosa* cells are not culturable after acidification to pH 3. However, successful quantification after filtration can be done by culture-independent detection methods such as qPCR.

5.1.7 Calibration of filtration at optimal conditions with MAF-OH

After the optimization process covering different aspects of MAF filtration, a calibration using the optimized filtration conditions for highest recovery of *P. aeruginosa* from tap water samples was carried out. The conditions were as follows: initial sample volume of

5 L at a sample pH of 3 with MAF-OH and elution with BEG buffer. Five different concentrations of *P. aeruginosa* ($1 \cdot 10^4$ - $1 \cdot 10^8$ CFU/L) were spiked in tap water and concentrated using MAF filtration. As a blank, tap water was used and the linear range of the calibration is depicted in Figure 11. As the initial volume was reduced from 5 L to a final volume of 1.5 mL after MAF filtration and centrifugal ultrafiltration, a concentration factor of $3 \cdot 10^3$ in under 1 h was achieved. The calibration line includes the filtration efficiency (recovery rate: 67.1 ± 1.2%) and can therefore be used to calculate the concentration in the initial sample from the total number of detected cells in the eluate with the respective quantification method of choice.

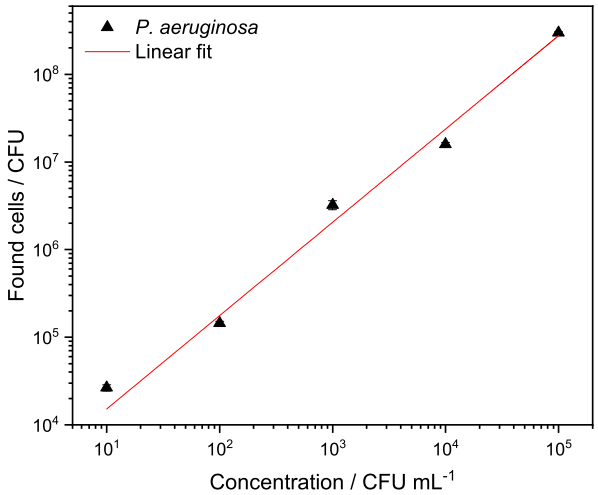

Figure 11: Linear range of cells found in 1.5 mL eluate against concentration in 5-L initial sample volume at pH 3 concentrated with MAF-OH and eluted with BEG buffer. y = (3.11 ± 0.20) + (1.07 ± 0.04) · x. n = 3, the error bars are smaller than the symbols indicating the values and thus are not clearly visible [128].

As the limit of detection is based on the detection method of choice, introducing a probe-based qPCR approach could lower the detection limit further. The MAF process, adsorption and later elution, also lends itself to a continuous sampling approach where the filters are installed in a cross-filtration mode within the plumbing system and removed regularly for analysis. The short filtration time (1 h) combined with fast, culture-independent detection (DNA-based) allows for a significant drop in analysis time compared to traditional culture-based techniques and can help to identify contaminations sooner.

5.2 haRPA for ESBL genes and bacterial pathogens

Several microorganisms, bacteria and viruses, can already be detected via haRPA [149,150]. Therefore, the detection of additional bacterial pathogens and ARG clusters, namely ESBL gene clusters, is based on this detection assay.

This chapter details the process and results of the development of haRPA assays for detection of the ESBL gene cluster *bla*$_{CTX-M}$ cluster 1 and the species *P. aeruginosa* in singleplex assays. The detection of *bla*$_{CTX-M}$ cluster 1 in haRPA was started from scratch, from the design of the primers to the evaluation of the final assay via comparison to two standard laboratory procedures, qPCR for sensitivity and PCR for selectivity. A calibration of haRPA for *P. aeruginosa* detection was carried out before these singleplex assays were included in duplex and multiplex experiments to provide a quick and easy monitoring tool for future research endeavors. The duplex and multiplex assays also included *K. pneumoniae* as an additional species to *P. aeruginosa* and *bla*$_{CTX-M}$ cluster 9 as an additional ESBL cluster. A schematic overview of the assay workflow for all haRPA detection systems is shown in Figure 12.

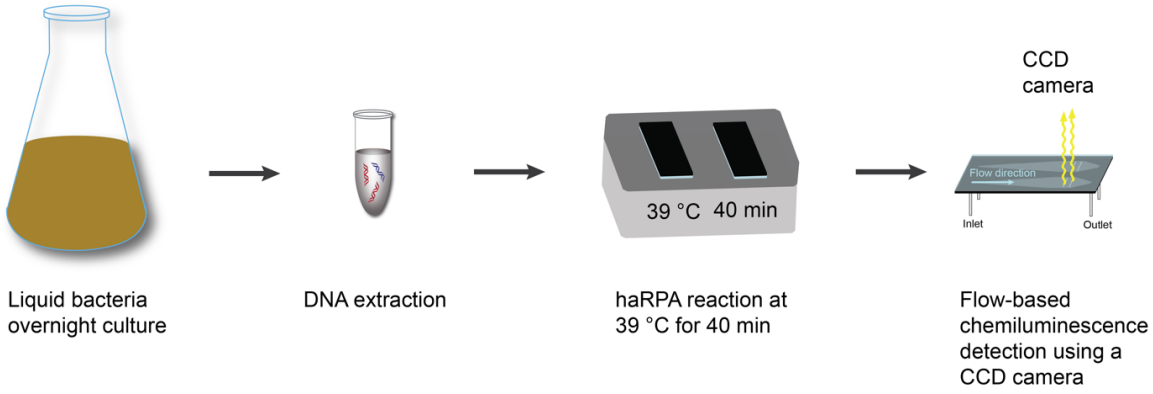

Figure 12: Schematic overview of the haRPA assay workflow. The DNA of liquid bacteria overnight culture is extracted. haRPA reaction is carried out (39 °C, 40 min) and the DNA amplicons are detected using chemiluminescence, adapted from [198].

5.2.1 Development of haRPA for bla_{CTX-M} cluster 1

The first step towards a new haRPA assay is the design and testing of a sensitive and selective primer set. The primer design was carried out as described in Figure 13 to maximize the options of haRPA primer pairs within the testing set (step 1). Step 2, the primer testing, was done by selecting one column e.g., REV primer and testing all FWD primers with this REV primer. The best primer pair (with the highest amplification efficiency) was then the basis for the second round of testing (all REV primers against the best forward primer of the previous round). This allows a fast assessment of many different primer pair combinations while reducing labor time and keeping resources spent at a minimum. Two primer sets which have shown similar amplification efficiencies in homogeneous RPA were tested in the heterogeneous assay where only one primer pair gave detectable chemiluminescence signal. This primer pair was then used for further experiments. The final assay showed no cross reactivities towards other *bla*$_{CTX-M}$ clusters (clusters 2 and 9), other ESBL genes (*bla*$_{TEM-3}$ and *bla*$_{SHV-18}$), or non-resistant bacterial species (*P. aeruginosa*, *L. pneumophila*, and *E. faecalis*) in homogeneous and heterogeneous RPA assays. In haRPA, no signal above the limit of detection could be detected for all different tested DNA samples in cross-reactivity testing.

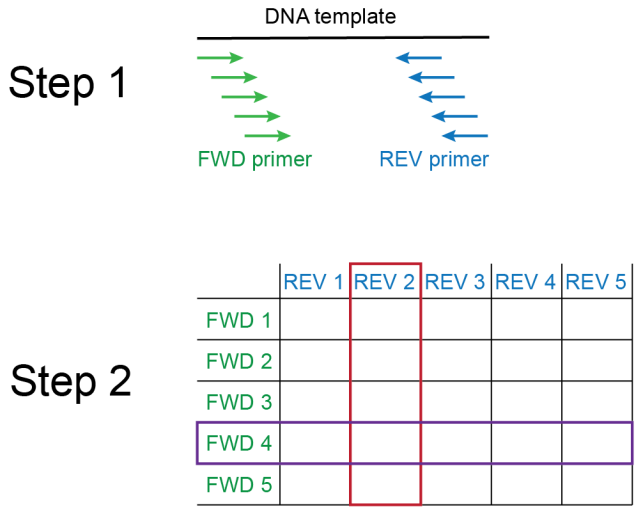

Figure 13: Overview of the primer design and testing process. Step 1, primer design, aimed at providing many different combination possibilities with a limited number of primers to test. Step 2, primer testing, was done by first testing for example the combinations in the red rectangle and then, based on performance, the purple rectangle.

The haRPA assay with the chosen primer pair was then optimized using DNA from *K. pneumoniae* with *bla*$_{CTX-M-15}$ resistance. The first parameter under investigation was the amount of primer in the liquid bulk phase. Here, three different concentrations were tested (370 nM, 420 nM, and 930 nM of the FWD primer with REV primer in 10:1 ratio). The chemiluminescence signal increased with primer concentration, however, due to the goal of developing a duplex or multiplex assay, 420 nM concentration of the FWD primer was ultimately chosen as the compromise between signal intensity and primer load in the assay. The second parameter investigated was the ratio between the FWD and REV

primer in the bulk phase. Four different ratios (1:5, 1:10, 1:20, and 1:50 REV:FWD primer, respectively) were analyzed with 1:10 giving the highest signal (Figure 14). This correlates with earlier findings where 1:10 was also the ratio resulting in the highest chemiluminescence signal [199]. The final assay set-up was a ratio of FWD to REV primer of 420 nM to 42 nM (final concentration in the assay) and this was used for all subsequent experiments.

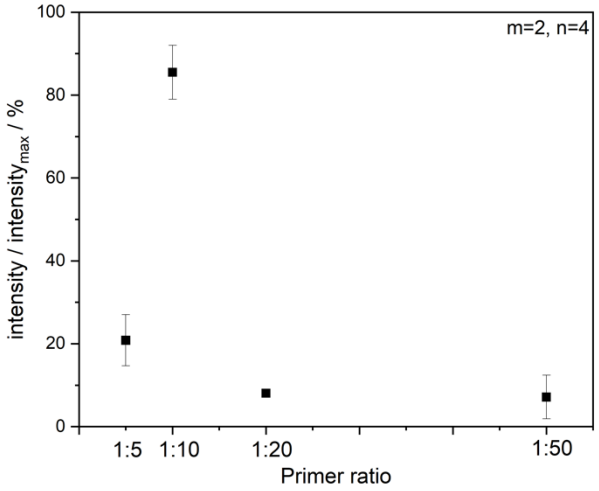

Figure 14: Relative signal intensities (signal to maximum signal) of different primer ratios (REV:FWD) of haRPA for *bla*$_{CTX-M}$ cluster 1 detection.

5.2.2 Evaluation of qPCR based on haRPA for bla$_{CTX-M}$ cluster 1

To achieve high comparability of haRPA and qPCR in terms of sensitivity, new qPCR primers were designed, based on the haRPA primers for detection of *bla*$_{CTX-M}$ cluster 1. These new qPCR primers were then tested for specificity by conducting a specificity study with 14 DNA samples of different bacterial strains and with a diverse ESBL resistance pattern. Except for the *K. pneumoniae* and *P. aeruginosa* reference strains, all other bacterial strains were isolated from water samples. The classifications in terms of ESBL occurrence and the corresponding bacterial species are depicted in Table 5.

Table 5: Overview of bacterial strains used for qPCR specificity tests with the ESBL gene and positive or negative characterization for cluster 1 [198].

Bacterial species	ESBL gene	Cluster 1 positive/negative
Enterobacter asburiae	$bla_{\text{CTX-M-1}}$	Positive
Enterobacter cloacae	$bla_{\text{CTX-M-15}}$	Positive
E. coli	$bla_{\text{CTX-M-1}}$	Positive
E. coli	$bla_{\text{CTX-M-2}}$	Negative
E. coli	$bla_{\text{CTX-M-3}}$	Positive
E. coli	$bla_{\text{CTX-M-9}}$	Negative
E. coli	$bla_{\text{CTX-M-14}}$	Negative
E. coli	$bla_{\text{CTX-M-15}}$	Positive
E. coli	$bla_{\text{CTX-M-27}}$	Negative
E. coli	$bla_{\text{TEM-3}}$	Negative
K. pneumoniae	$bla_{\text{CTX-M-15}}$	Positive
K. pneumoniae	$bla_{\text{CTX-M-55}}$	Positive
K. pneumoniae	$bla_{\text{SHV-18}}$	Negative
P. aeruginosa	No ESBL	Negative

For all non-target sequences tested in the experiment, no cross-reactivities were detected as amplification occurred after cycle 30, representing unspecific amplification or formation of primer dimers, and the designed primer pair is, therefore, specific for detection of $bla_{\text{CTX-M}}$ cluster 1 independent of the bacterial species (Figure 15). The blank cut-off was set at 30 cycles to eliminate any unspecific interactions.

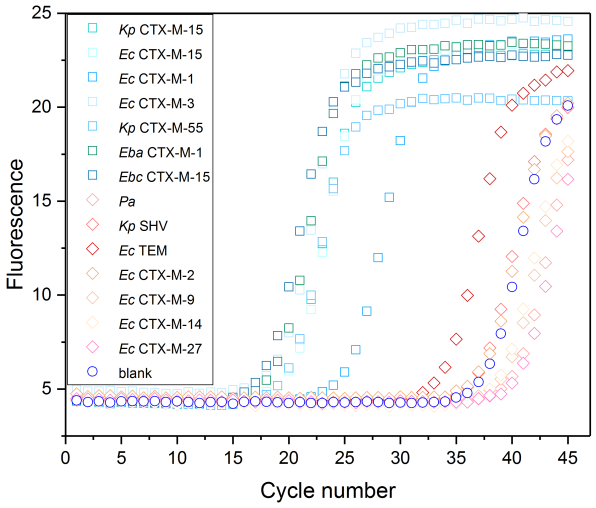

Figure 15: Overview of qPCR specificity test for *bla*$_{CTX-M}$ cluster 1 with 0.1 ng µl^{-1} DNA samples. Kp: *K. pneumoniae*; Ec: *E. coli*; Eba: *E. asburiae*; Ebc: *E. cloacae*; Pa: *P. aeruginosa*; CTX-M-number: with *bla*$_{CTX-M}$ number gene; SHV: with *bla*$_{SHV}$ gene; TEM: with *bla*$_{TEM}$ gene; blank: non-target control [198].

5.2.3 Comparison of the working range and limit of detection between haRPA and qPCR for bla$_{CTX-M}$ cluster 1

As a first step in evaluating the haRPA assay the sensitivity of haRPA and qPCR were compared. Therefore, the same DNA samples from *K. pneumoniae* and *E. coli* (both with *bla*$_{CTX-M-15}$) were used with DNA concentrations between 0.0001 ng µL^{-1} and 50 ng µL^{-1}. The complete calibration for haRPA is plotted in Figure 16a including the limit of detection and the linear working range while for qPCR only the linear range (Figure 16b) is plotted. For both diagrams, two different bacterial species (*K. pneumoniae* and *E. coli*) and two technical replicates (2 individual measurements using the same DNA), meaning 4 individual measurements in total, are included in each measurement point shown in the graph. The limit of detection in haRPA is calculated as blank measurement (332.7 ± 62.5 a.u.) plus three times the standard deviation. This results in a concentration of 0.013 ng µL^{-1} or 520.1 a.u. (Figure 16a). Therefore, the limit of detection is calculated much easier in haRPA than for qPCR. For qPCR, the cycle cut-off at 30 cycles limits the working range (Figure 16b). All error bars shown in the graphs represent the standard deviation of the individual measurements.

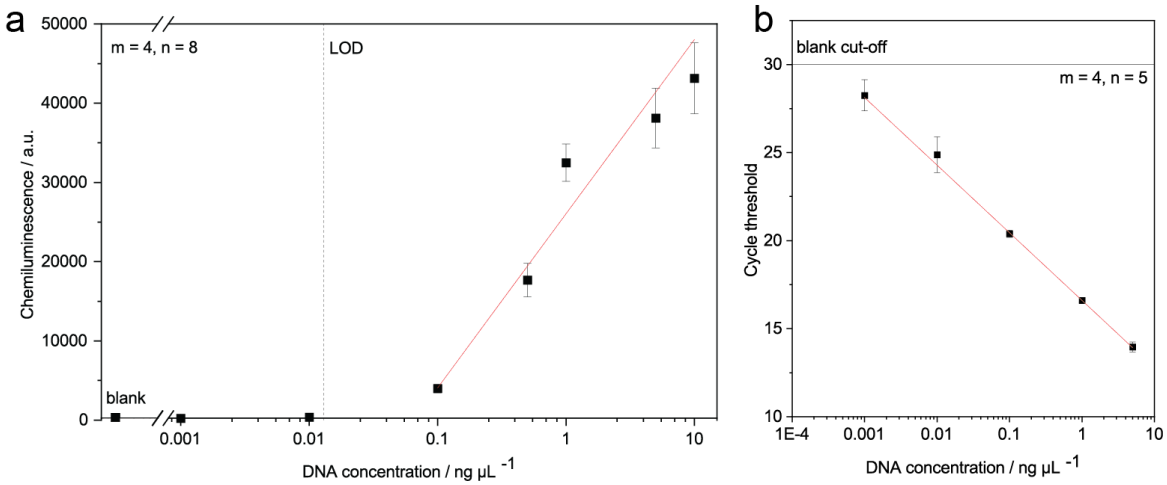

Figure 16: Calibration of haRPA (a) with indicated blank and limit of detection (LOD) with linear range/working range and linear range of qPCR (b). Two biological replicates were measured in duplicates for each measurement point (*E. coli* and *K. pneumoniae*, both with $bla_{CTX\text{-}M\text{-}15}$ genotype). Blank cut-off for qPCR at cycle 30. Error bars are shown for all measurement points (sometimes smaller than the symbols and thus not clearly visible) [198].

As is depicted in Figure 16, the new haRPA assay shows a linear concentration dependency in the range of 0.1 ng µL^{-1} to 10 ng µL^{-1} (Figure 16a). The linear range of the qPCR is 0.001 ng µL^{-1} to 5 ng µL^{-1} (Figure 16b). Concentrations of 10 ng µL^{-1} cannot be quantified in qPCR, because the initial fluorescence signal is already elevated. In contrast, quantitative results can be obtained from higher DNA concentrations in haRPA. Here, the chemiluminescence signal saturates at around 50 ng µL^{-1} (data not shown). A comparison of the working range reveals a greater sensitivity, as is indicated by a higher slope of the calibration curve, for haRPA resulting in a higher and smaller working range. haRPA is nevertheless sensitive enough, but also good suitability for quantification of DNA extracts from culture. The difference in limit of detection can have several possible reasons. With haRPA being a heterogeneous assay, the ratio between reaction volume and spot area is unfavorable and only a smaller part of the amplified DNA is immobilized on the chip surface. This haRPA assay is furthermore based on a commercially available lyophilized reaction mix, where no individual ratio of the different enzymes and reaction components can be set with respect to the heterogeneous assay. A sensitivity loss due to a change in the reaction mix has been reported previously [200], which may also have affected this study. In general, the difference in read-out (fluorescence in qPCR vs. chemiluminescence in haRPA) and reaction mechanism with different enzymes can also have effects on the limit of detection. Nevertheless, other comparisons between RPA assays and qPCR also showed a similar difference in detection limit [200,201]. While qPCR is prone to unspecific contaminations and thus requires a clean bench environment, haRPA can be performed in the field while still maintaining sufficient sensitivity. Moreover, several studies on RPA report on the absence of any interference from substances of more complex matrices has been reported in different studies [202,203]. Additionally, another study states that qPCR requires cleaner DNA meaning less contamination with proteins, humic substances, or salts than RPA [204] which is another advantage of RPA-based techniques.

5.2.4 Specificity test for haRPA for bla$_{CTX-M}$ cluster 1 by comparison with PCR

The second step in the haRPA performance evaluation was a specificity test conducted between the haRPA method and a well-established PCR protocol. This was done as part of the JPI Water project METAWATER where 37 bacterial isolates from surface, irrigation and wastewater effluent from Germany, Denmark, Spain, and Cyprus were collected. Overall, 23 *E. coli* isolates and 14 *K. pneumoniae* with different ESBL profiles were chosen. The DNA extracts were first characterized for *bla*$_{CTX-M}$ cluster 1 by PCR by the Bavarian Health and Food Safety Authority (according to a published method [190]). Afterwards, haRPA was done by measuring all DNA extracts in duplicates. 10 different ESBL genetic profiles were grouped into 6 different classifications and analyzed resulting in 100% agreement between the haRPA set-up and the PCR qualification (Table 6).

Table 6: Overview of ESBL classification from PCR- and haRPA-based results [198]. ESBL neg.: no ESBL gene could be detected; other ESBL pos.: *bla*$_{TEM}$ and *bla*$_{SHV}$ positive; other *bla*$_{CTX-M}$ pos.: *bla*$_{CTX-M-9}$, *bla*$_{CTX-M-14}$, *bla*$_{CTX-M-27}$ positive; *bla*$_{CTX-M}$ cluster 1 pos.: *bla*$_{CTX-M-1}$, *bla*$_{CTX-M-3}$, *bla*$_{CTX-M-15}$ positive; K. p. *K. pneumoniae*, E. c. *E. coli*.

ESBL classification	**# of samples**	**PCR result**	**haRPA result**
ESBL neg.	5 (2 *K. p.*, 3 *E. c.*)	Neg.	Neg.
ampC pos.	2 (2 *K. p.*, 0 *E. c.*)	Neg.	Neg.
other ESBL pos.	3 (0 *K. p.*, 3 *E. c.*)	Neg.	Neg.
other *bla*$_{CTX-M}$ pos.	10 (5 *K. p.*, 5 *E. c.*)	Neg.	Neg.
bla$_{CTX-M}$ cluster 1 pos.	6 (0 *K. p.*, 6 *E. c.*)	Pos.	Pos.
bla$_{CTX-M-15}$ *pos.*	11 (5 *K. p.*, 6 *E. c.*)	Pos.	Pos.

As is confirmed by these results, haRPA is able to detect *bla*$_{CTX-M}$ cluster 1 genes as specific as the well-established PCR assay. The haRPA assay proved to identify diverse genes within cluster 1 from two different bacterial species. Both PCR and haRPA could detect the presence of *bla*$_{CTX-M}$ cluster 1 genes in DNA from cultured bacterial isolates. In regard to the source of the bacterial isolates, *bla*$_{CTX-M}$ cluster 1 harboring bacteria were found in all three different water sources (surface water, wastewater effluent, and irrigation water) and in all investigated countries. Albeit a study with a limited data set, it confirms the claim that antibiotic resistance is widespread and antibiotic resistant bacteria can be found in various environmental water sources.

5.2.5 haRPA for detection of *P. aeruginosa*

In addition to the haRPA assay for *bla*$_{CTX-M}$ cluster 1, an assay for the detection of *P. aeruginosa* was also of interest. Here, an RPA primer set was already available from a previous project (EDIT project, tested for cross reactivity and high amplification efficiency) which has never been tested in the haRPA assay before. With the experiences from the *bla*$_{CTX-M}$ cluster 1 assay development, the first step was to successfully transfer the working and tested primer pair from homogeneous to heterogeneous amplification. After successful completion of this task, a calibration using DNA extracts of *P. aeruginosa* from liquid media with different bacterial cell concentrations (10^2 to 10^8 cells mL^{-1} plus a blank) was carried out. The primer composition in the liquid bulk phase was set at 420 nM / 42 nM for FWD / REV primer.

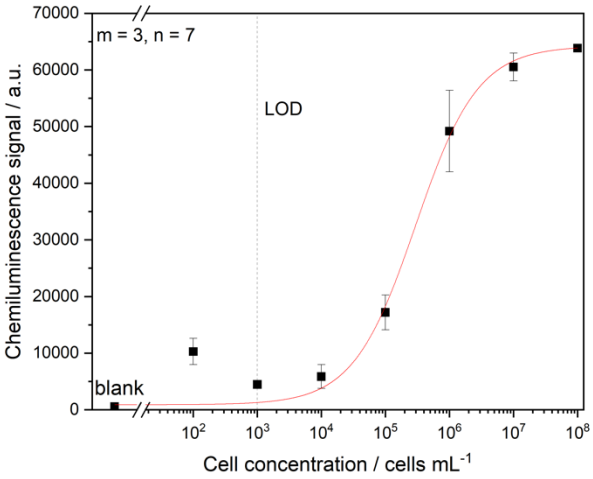

Figure 17: Calibration of haRPA for *P. aeruginosa* detection.

As is depicted in Figure 17, the limit of detection for this assay is calculated with 10^3 cells mL^{-1} which is comparable to other haRPA assays for bacteria detection [149]. The signal saturates at a concentration of 10^8 cells mL^{-1}. The working range of the assay is between 5×10^4 and 10^7 cells mL^{-1}. The measurement point at 10^2 cells mL^{-1} is deemed an outlier.

5.2.6 Investigation of multiplex haRPA for simultaneous detection of bacterial pathogens and *bla*$_{CTX-M}$ cluster 1

The overall goal was to develop a haRPA assay that would allow for the detection and quantification of bacterial pathogens and ARGs on a single chip. Two exemplary bacteria, *K. pneumoniae* and *P. aeruginosa* were chosen together with *bla*$_{CTX-M}$ cluster 1 and *bla*$_{CTX-M}$ cluster 9 as the model ARGs. The development of *bla*$_{CTX-M}$ cluster 9 was carried out similar to that of *bla*$_{CTX-M}$ cluster 1 (Chapter 5.2.1) and resulted in one primer pair that showed good amplification in homogeneous application. The primer pair for *K. pneumoniae* was designed in a previous project (INIS-EDIT project) and had been previously tested for high amplification efficiency without cross-reactivity. First individual

measurements for *K. pneumoniae* and *bla*$_{CTX-M}$ cluster 9, respectively, with haRPA proved successful by showing detectable chemiluminescence signal (Figure 18).

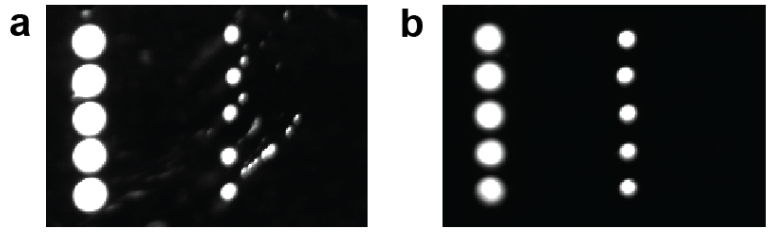

Figure 18: Chip image for qualitative detection of *K. pneumoniae* (a) and *bla*$_{CTX-M-9}$ (b) with haRPA.

5.2.6.1 Investigation of primer interaction

The first step was to exclude primer-primer interactions occurred between the different primer pairs by performing (ha)RPA experiments without addition of DNA. This was first tested in homogeneous RPA where no primer duplets could be detected using agarose gel electrophoresis. As has been experienced previously during the development of the *bla*$_{CTX-M}$ cluster 1 primer pair, primers tend to behave differently in homogeneous and heterogeneous reaction environments. Therefore, the same experiments were repeated on the chip (heterogeneous reaction environment). As highlighted by the results in Table 7, interaction between the primers is detected when combining all 4 primer sets (1:10 ratio REV: FWD, FWD primer in 420 nM). The chemiluminescence signal intensities for *K. pneumoniae* and *bla*$_{CTX-M}$ cluster 1 are significantly higher (36,453 and 4,105, respectively, compared to the value of 597 for *bla*$_{CTX-M}$ cluster 9) indicating unwanted primer interactions. The next set of experiments aimed at identifying the primers responsible for these interactions. At the beginning of this identification process, to reduce the overall primer load, only FWD primers were used as these are crucial for DNA amplification. This resulted in removal of the intense *K. pneumoniae* signal while the *bla*$_{CTX-M}$ cluster 1 signal was persistent. The *bla*$_{CTX-M}$ cluster 1 signal could be eliminated by excluding the *bla*$_{CTX-M}$ cluster 9 FWD primer from the mix. This means in turn, that using these primers, no *bla*$_{CTX-M}$ cluster 9 could be detected in the multiplex assay as no biotin-labelled FWD primer was present in the mix. The next step was to reintroduce the REV primers into the mix (1:10 REV:FWD), as previous studies had shown, that a small amount of REV primer significantly enhances the chemiluminescence signal [149]. As is evident from the signal values in Table 7, an interaction between the immobilized REV primer for *K. pneumoniae* and one of the other REV primers is present, resulting in the high signal intensity. Through elimination experiments, this primer was identified as the unmodified REV primer for *K. pneumoniae*. Eliminating this primer from the primer mix results in negative signals for all spotted primers, hence excluding any primer interaction. The final primer mix for multiplex measurements consisted of FWD primers for *P. aeruginosa*, *K. pneumoniae* and *bla*$_{CTX-M}$ cluster 1 and unmodified REV primers for *P. aeruginosa* and *bla*$_{CTX-M}$ cluster 1. Duplex measurements were carried out with the desired primer pairs except for *K. pneumoniae*, where only the FWD primer was added.

Table 7: Overview of primer interaction chemiluminescence signals with haRPA (without addition of DNA). Gray numbers are negative signals, black bold numbers are positive signals. Best primer mix compositions are indicated with gray background. Pa: *P. aeruginosa* primer, Kp: *K. pneumoniae* primer, a.u.: arbitrary units, PP: primer pair. Higher negative signals stem from overloaded signal from neighboring spots which influences the automatic signal detection without a signal from the primer spot visible or from spotting impurities.

	Chemiluminescence signal in a.u.			
Primer mix composition	***P. aeruginosa***	***K. pneumoniae***	***bla*$_{\text{CTX-M-1}}$**	***bla*$_{\text{CTX-M-9}}$**
FWD and REV	4 344	**36 453**	**4 105**	597
FWD only	1 564	753	**7 448**	945
FWD only – Pa	324	619	**8 181**	350
FWD only – Kp	403	376	**6 034**	365
FWD only – *bla*$_{CTX\text{-}M\text{-}1}$	808	341	**24 856**	498
FWD only – *bla*$_{CTX\text{-}M\text{-}9}$	735	534	520	401
FWD and REV – *bla*$_{CTX\text{-}M\text{-}9}$ PP	5 873	**20 689**	641	1 561
FWD and REV – *bla*$_{CTX\text{-}M\text{-}9}$ PP, *bla*$_{CTX\text{-}M\text{-}1}$ REV	2 448	**46 102**	586	6 939
FWD and REV – *bla*$_{CTX\text{-}M\text{-}9}$ PP, Pa REV	3 015	**58 696**	5 452	7 203
FWD and REV – *bla*$_{CTX\text{-}M\text{-}9}$ PP, Kp REV	859	845	949	3 920

5.2.6.2 Duplex measurements of one bacterial species with the resistance gene *bla*$_{\text{CTX-M}}$ cluster 1

The second step in developing the multiplex assay was then to test duplex measurements of one of the bacterial species with the respective resistance gene. As the available *P. aeruginosa* strain did not have a *bla*$_{\text{CTX-M}}$ cluster 1 gene, *E. coli* DNA with *bla*$_{\text{CTX-M-15}}$ was added to allow detection of both the species (*P. aeruginosa*) and the resistance gene (*bla*$_{\text{CTX-M-15}}$). This first test was successful for both duplex assays, one for each bacterial species, and a preliminary calibration with concentrations from 10^2 cells mL^{-1} to 10^8 cells mL^{-1} was performed to see, whether both assays were concentration dependent. As is shown in Figure 19, concentration dependency was given in both assays (*P. aeruginosa* Figure 19a, *K. pneumoniae* Figure 19b) for both DNA amplicons each proving a successful next step towards a haRPA assay for simultaneous quantification of multiple DNA samples in one assay. It is, nonetheless, evident for both assays that the

bla$_{CTX-M}$ cluster 1 gene signal intensities (indicated in blue in both graphs; 15,953 a.u. and 21,291 a.u. for measurements with *P. aeruginosa* and *K. pneumoniae*, respectively) are significantly lower than those of the bacterial species (indicated in black in both graphs; 63,306 a.u. and 38,764 a.u. for *P. aeruginosa* and *K. pneumoniae*, respectively). One explanation is the abundance of the species-specific genes in comparison to the ESBL genes which are not necessarily as abundant in the bacterial genome and might be present in lower copy numbers in relation to the cell number (which is the calibration standard).

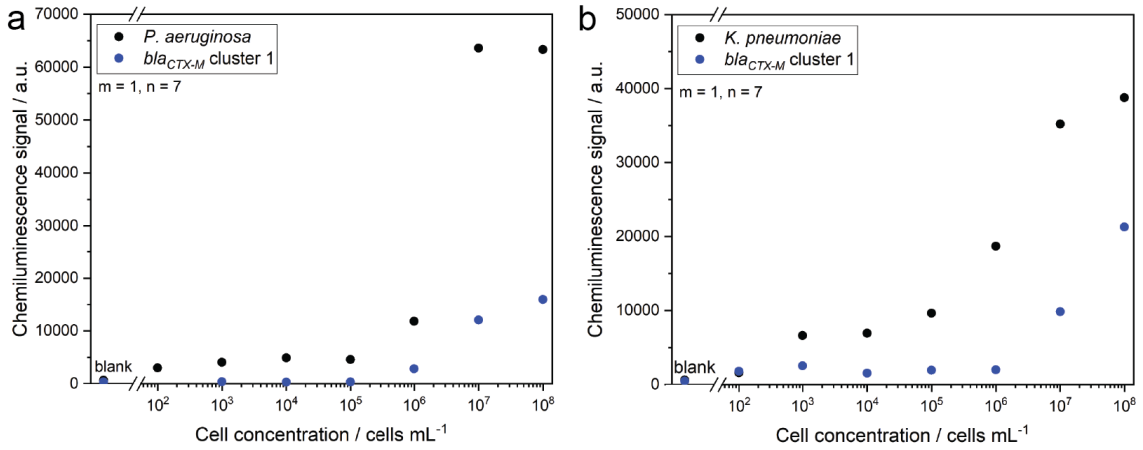

Figure 19: Concentration dependency of haRPA duplex measurements of *bla*$_{CTX-M}$ cluster 1 with (a) *P. aeruginosa* and (b) *K. pneumoniae*. *bla*$_{CTX-M}$ cluster 1 is indicated in blue, bacteria in black.

However, as is depicted in Figure 20a, repeating the same assay for *P. aeruginosa* detection with (blue measurement points) and without (red measurement points) the addition of *E. coli* DNA showed differences in signal response for the same concentrations (63,306 a.u. and 49,237 a.u., respectively). The intensity of the chemiluminescence signal is significantly lower in the duplex assay compared to the singleplex assay (black measurement points; where not only the DNA load but also the primer load is reduced). For *bla*$_{CTX-M}$ cluster 1 identification which is depicted in Figure 20b there is a large difference visible between the singleplex assay (black measurement points; 60,893 a.u.) and the two different duplex measurements (red for duplex measurement with *P. aeruginosa*, blue for duplex measurement with *K. pneumoniae*; 15,953 a.u. and 21,291 a.u., respectively). It was concluded that the large differences in signal intensity for the same DNA concentrations stem from the higher primer and DNA load which seems to interfere with the haRPA assay. While the primer load can be controlled easily, doing so for the DNA load from samples is much more difficult, especially if the goal is to identify unknown samples. Additionally, it was observed that the species related DNA amplicons have higher signals than the *bla*$_{CTX-M}$ cluster 1 specific signals at the same DNA concentration. There are two probable reasons for this behavior: First, ARG specific genes might not be as abundant as species specific genes which results in lower concentrations of the target DNA and consequently lower signal of the *bla*$_{CTX-M}$ cluster 1 amplicon. Second, the quality of the primer pair for *bla*$_{CTX-M}$ cluster 1 is not as good as those for the species-specific genes. The primers for the species-specific genes were designed in a previous

project and tested extensively by several project partners and thus might have a higher amplification efficiency as the primer pair for *bla*$_{CTX-M}$ cluster 1.

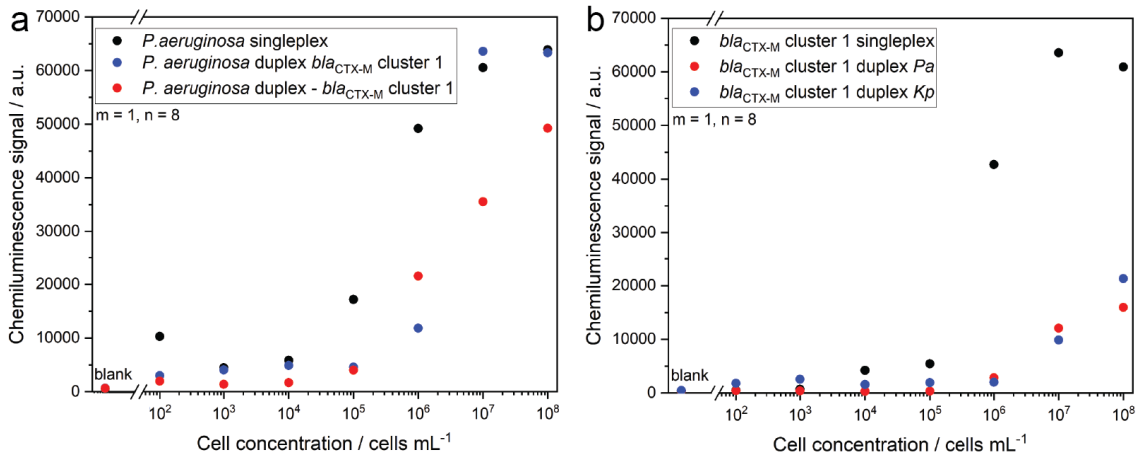

Figure 20: Comparison of concentration behavior of haRPA for *P. aeruginosa* (a) and *bla*$_{CTX-M}$ cluster 1 (b) for singleplex (black) and different duplex measurements (blue and red). Pa: *P. aeruginosa*, Kp: *K. pneumoniae*.

The third step in developing the multiplex assay was to try to overcome these drawbacks by two different strategies. Strategy A was to add DNA that does not include the desired sequences but adds to the overall DNA load in the assay to facilitate comparable signal intensities between singleplex and duplex assays (ideally within the range of the standard deviation of the singleplex assays, ± 10%). Salmon sperm DNA (as single strand DNA) was chosen for these tests. While an effect of introducing a large amount of DNA to the system (reduction of the overall signal intensity and visible smear of chemiluminescence over the whole chip at very high salmon sperm DNA concentrations) was seen, no effect of the additional DNA to harmonize quantification between duplex and singleplex assays could be observed (data not shown). Additional experiments were not carried out as the barrier of varying DNA load could not be overcome and resources were needed elsewhere. It was therefore decided to use the assay without the addition of single strand DNA as a qualitative assay.

Strategy B was a change in primer mix composition to enhance the signal of the *bla*$_{CTX-M}$ cluster 1 amplicon while reducing the signal of the species-specific amplicon in comparison. DNA concentration was kept constant for testing of different primer mix compositions (extracts from 10^5 cells mL^{-1}). Experiments with increased *bla*$_{CTX-M}$ cluster 1 primer amount and reduced species-specific primers did improve comparability between the different assays. The signal intensity of *P. aeruginosa* and *bla*$_{CTX-M}$ cluster 1 was comparable while chemiluminescence signal intensities for *K. pneumoniae* were significantly higher for the optimized assay. This is illustrated by the chip image displayed in Figure 21. The final primer ratios were 3:30:2:20:20 of REV *bla*$_{CTX-M}$ cluster 1 / FWD *bla*$_{CTX-M}$ cluster 1 / REV *P. aeruginosa* / FWD *P. aeruginosa* / FWD *K. pneumoniae*, respectively.

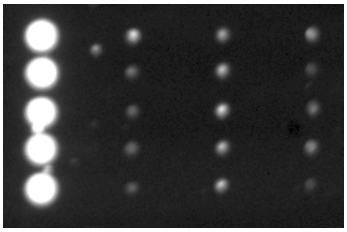

Figure 21: Chip image for multiplex measurements with optimized primer mix (3:30:2:20:20 of REV *bla*$_{CTX-M}$ cluster 1 / FWD *bla*$_{CTX-M}$ cluster 1 / REV *P. aeruginosa* / FWD *P. aeruginosa* / FWD *K. pneumoniae*, respectively) with DNA from *P. aeruginosa* and *K. pneumoniae* with *bla*$_{CTX-M-15}$ resistance. From left to right: positive control, *P. aeruginosa*, *K. pneumoniae*, *bla*$_{CTX-M}$ cluster 1.

5.2.6.3 Detection of two bacterial species and one resistance gene

Based on the results obtained with the improvement experimental parameters, it was decided that the goal of a quantitative multiplex assay would have to be realized in a different approach. Nevertheless, the present assay using *P. aeruginosa* and *K. pneumoniae* species-specific detection combined with *bla*$_{CTX-M}$ cluster 1 resistance gene detection represents an optimized, easy to handle, multiplex assay for fast, qualitative analysis (Table 8). The presence of the target genes (DNA from extracts of 10^5 to 10^7 cells mL^{-1}) was successfully detected using model organisms (*P. aeruginosa*, *K. pneumoniae*, and *E. coli*) and non-target control (salmon perm DNA, single stranded). Chemiluminescence signals were deemed positive upon visual determination, if a visible signal (distinguishable from the background) in the spotted area was seen. In contrast, no visible signals in the spotted area were deemed negative. Spotting artefacts from the positive control (as seen in Figure 21 between the first and second column from the right) were excluded from analysis. An example of a chip image for the multiplex measurements is given in Figure 21.

Table 8: Overview of qualitative measurements for bacterial species identification in combination with *bla*$_{CTX-M}$ cluster 1 characterization. Bacterial species without ARG denomination do not carry known ARGs. Pos. means positive signal with visible spot; neg. means negative with no spot visible.

DNA in the sample	***P. aeruginosa* spot**	***K. pneumoniae* spot**	***bla*$_{CTX-M}$ cluster 1 spot**
P. aeruginosa, *E. coli*$_{CTX-M-15}$	Pos.	Neg.	Pos.
P. aeruginosa, *K. pneumoniae*$_{CTX-M-15}$	Pos.	Pos.	Pos.
K. pneumoniae$_{CTX-M-15}$	Neg.	Pos.	Pos.
E. coli$_{CTX-M-15}$	Neg.	Neg.	Pos.
P. aeruginosa, *K. pneumoniae*$_{SHV-18}$	Pos.	Pos.	Neg.
Salmon sperm DNA	Neg.	Neg.	Neg.

Possible solutions for the DNA and primer load issue could be the implementation of hybrid DNA targets where only one biotin labelled FWD primer is added to the bulk phase and the REV primers (for different target sequences) are immobilized on the chip. Using this set-up, although introducing an additional step for generating DNA fusion sequences, the overall DNA load in the bulk phase is lowered while simultaneously keeping the ability to detect several target sequences on one chip. In general, the RPA kits used for the haRPA assays are optimized for homogeneous amplifications and an increase in sensitivity and selectivity for haRPA could be achieved by altering the ratio of the reaction mix components (enzymes, nucleic bases, etc.). A recent study suggested that a change in reaction component ratio had an influence on the sensitivity of the RPA reaction [200]. Increasing the enzyme amount, for example, could counteract the microfluidic disadvantage of the heterogeneous assay. Both strategies should be investigated in the future to increase sensitivity and selectivity for the haRPA assay as the full potential of this rapid and easy DNA detection assay has not yet been exhausted.

5.3 Characterization of chemical and morphological changes of microplastic particles during bacterial colonization/degradation at environmentally relevant conditions

Although it is widely recognized that monitoring of microplastic particles in environmental surroundings is crucial for establishing its burden for environment, no study known to us investigated the effects bacteria can have on the detection and identification process has been done so far. This aspect is as crucial as understanding the degradation process itself. Thus, this chapter details two sets of experiments which aim to answer pressing questions on biodegradation of microplastics in a simplified environment and on how bacteria influence the characterization of microplastic particles using RM. Additionally, a broad outline is given where future research efforts should be focused on to further investigate the observed effects.

First, three different polymers (PLA, PET, and PS) were incubated under non-sterile conditions in ultrapure water for 3 weeks and analyzed with RM and SEM showing significant differences between the plastic types in RM analysis. The isolated bacteria were subsequently identified as *Pseudomonas libanensis* and *Sphingomonas koreensis*. Then, based on these results, a second study was done with sterile aqueous PLA solutions and a defined number of bacteria added to each sample. The samples were monitored closely over an incubation period of 21 days using culture on agar plates to monitor the bacterial growth, RM measurements to detect bacteria-induced changes in the Raman spectra of PLA, and FESEM measurements to characterize morphological changes of PLA. A schematic overview of the process is given in Figure 22.

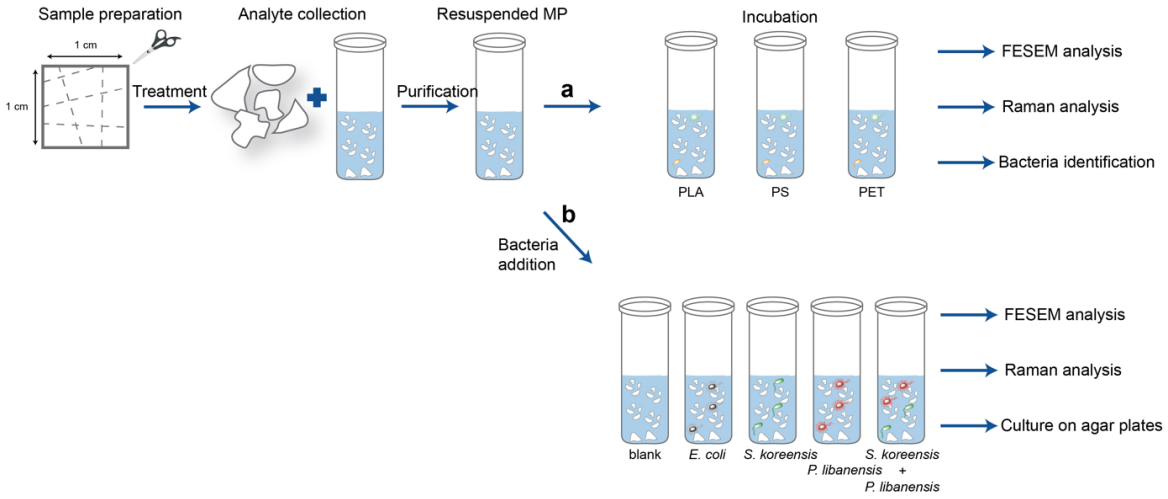

Figure 22: Overview of the involved experimental steps to investigate (a) the differences between the polymers (PLA, PS, and PET) and (b) the influences of bacteria on PLA microplastic. The microplastic sample is prepared and the suspended microplastic particles are then incubated with bacteria (except for the blank) over the course of 21 days at 25 °C. For (a) samples were taken at day 21 only, for (b) samples from bacterial cultures were taken daily, for FESEM and Raman analysis was performed on samples collected on day 0, 7, 14 and 21.

5.3.1 Comparison of different plastic types

In the first set of experiments, different polymer types (PS, PET, and PLA) were analyzed first with FESEM and later with RM after an incubation time of 3 weeks in non-sterile ultrapure water. FESEM analysis revealed the presence of bacteria in the samples (Figure 23) and more pronounced roughness of the PLA particles was observed in the presence of bacteria whereas the morphology of PS and PET did not change significantly. The aqueous microplastic suspension was plated on agar plates to allow for identification of their species. Successful cultivation on solid agar plates and in liquid media gave the opportunity to identify these bacteria as *P. libanensis* and *S. koreensis* based on MALDI-TOF-MS analysis.

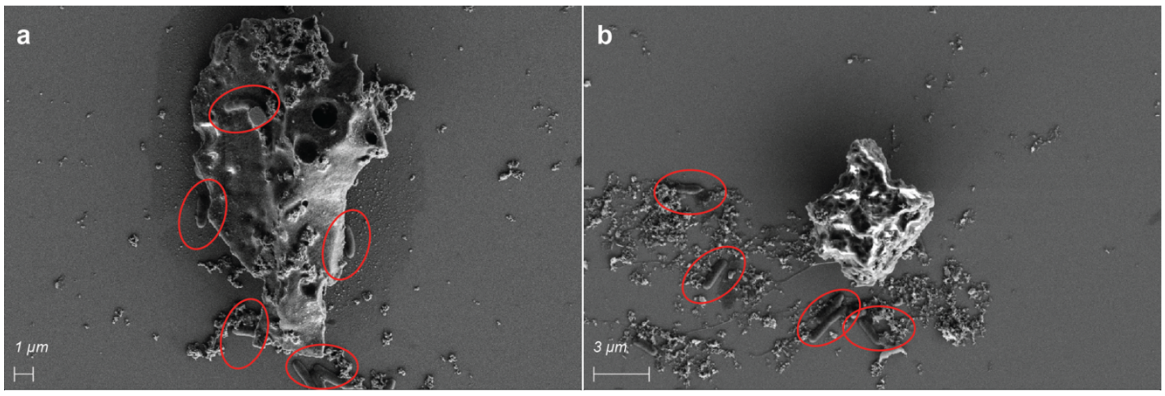

Figure 23: FESEM images of PLA samples with bacteria after 21-day incubation. Bacteria are visible in both images (a and b) on and next to the PLA particle (indicated in the red circles). Images taken by Christian Schwaferts.

5.3.1.1 Differences in changes observed via RM between plastic types

Looking at the Raman spectra, changes in the spectral fingerprint upon incubation compared to the plastic reference spectrum are detected for all three types of plastic (Figure 24 and Figure 25). However, when trying to match the observed spectra to the database, only PS and PET delivered matches (examples of the hit quality index (HQI) for each spectrum are listed in Figure 24). The HQI is a correlation coefficient between the measured spectrum of the particle and the database spectrum of the plastic. To calculate the HQI only the characteristic bands in specific regions are taken into account to reduce in influence of background noise on the identification process. These regions are marked in green in the spectra shown in this thesis. Although the HQI differs between the individual spectra depicted, a correct database match was possible for all PS and PET particles measured.

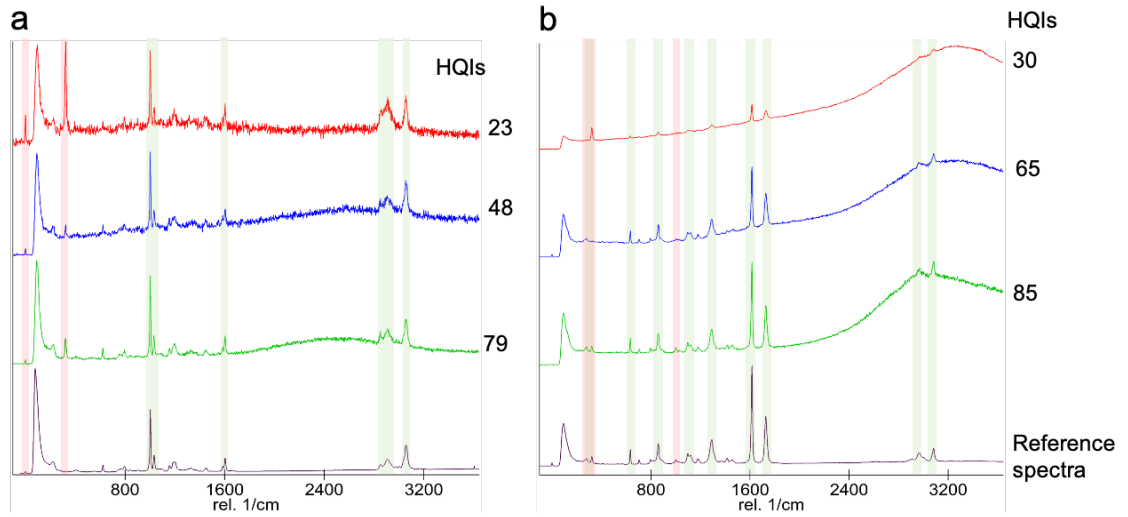

Figure 24: Spectra comparison for PS (a) and PET (b) Raman spectra after 21-day incubation with bacteria from different, individual particles (red, blue, and green spectra). Bottom spectra (black) are the reference spectra for each plastic type. HQI were calculated from the areas marked in green. Changes between the spectra are marked in red.

For PLA, on the other hand, the expected database assignment could not be achieved. Here, the spectral fingerprint changed to an extent that identification based on specific marker bands was not possible. While some bands disappeared compared to the spectra of pristine PLA, additional bands emerged at different wavelengths or existing bands changed their shape creating spectra that were no longer recognized as PLA by the algorithms of the database matching software (Figure 25). Database matching for PLA is based on two spectral regions: ~ 1520 to 1900 cm^{-1} for C=O and ~ 2800 to 3000 cm^{-1} for C-H stretching vibrations. However, these regions are also subject to significant changes in the presence of bacteria. Recognizing these changes offers a possible explanation as to why biodegradable plastic remnants are underestimated in environmental samples due to incorrect classification.

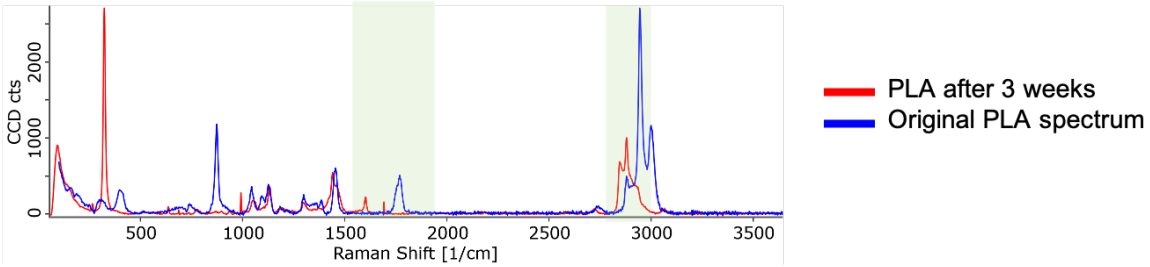

Figure 25: Comparison of spectra for PLA particles before (blue) and after incubation with bacteria (red). HQI areas which are important for database matching are marked in green.

5.3.1.2 Analysis of bacteria on microplastic particles with RM

During the investigation it was possible to distinguish bacterial spectra from polymer spectra, thanks to the confocal nature of the Raman microscope system, even when the bacteria were attached to the microplastic particle. Depending on the z-axis focus, a mixture of the bacteria and PS spectra or a pure PS spectrum can be acquired (Figure 26a). To the best of our knowledge, Raman spectra of a bacterium on top of a PS microplastic particle were collected for the first time. Figure 26b shows the corresponding microscope image. The spectrum showed characteristics of both the plastic (green areas) and the bacterium (red areas) thus creating a combined spectrum of both inputs. As can be seen, changes in Raman spectra can also originate from the colonization of (micro)plastic particles (as seen for the example of the PS particle) or by accumulation of organic matter produced by the bacteria on the (micro)plastic. Therefore, these changes do not necessarily indicate degradation, as is the case in this experiment. Only when the bacteria and the PS particle are within the confocal volume that delivers the Raman signal, modifications in the spectrum become visible thus clearly indicating that colonization alone can also result in changes in the signal. Consequently, this poses the question, if bulk spectroscopic assessments of degradation can actually show the modification of the chemical structure of the particles within the sample, thus referring to degradation events. Or they rather show a complex mixture of colonization and/or degradation events by bacteria on the surface of the microplastic particle.

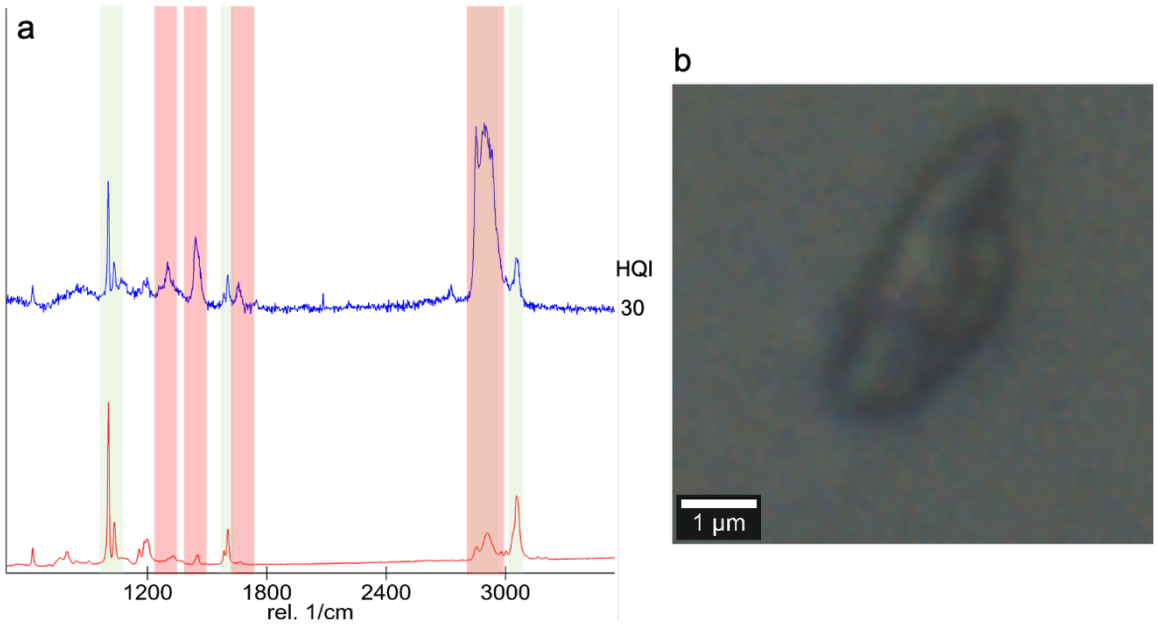

Figure 26: Raman spectrum (a) of a bacterium on PS particle (blue spectrum) and reference spectrum of PS (red spectrum) with indicated HQI areas marked in green and additional bands (red areas). (b) Microscope image of the bacterium sitting on top of the PS particle.

This combined spectrum has a prominent band at ~ 2800 cm^{-1} characteristic for bacteria (Figure 26) which interferes with the detection of PLA as the C-H-stretch vibration in this spectral region is crucial for correct database matching (green area in Figure 25). As all

the prominent PS bands are present in the spectrum of PS incubated in the presence of bacteria without noticeable band shifts or change in relative band ratios, the assumption that only chemical modification of the plastic itself causes a change in Raman spectra, is not supported by this data. This observation is especially crucial for PLA which is designed to be biodegradable and a clear distinction using Raman measurements between degradation and colonization by bacteria is not yet possible. Examining the differences in availability as a substratum towards bacteria, the biodegradable PLA was designed to offer bacteria a handle for degradation and thus is more accessible than PET and PS. Together with the more pronounced roughness of the PLA particles surfaces in comparison to PET and PS particles makes PLA microplastic a preferred substrate for bacteria. However, further studies were not carried out with PET and PS to focus resources on biodegradable PLA microplastics.

These results prompted the conduction of a second set of experiments to evaluate the changes in the Raman spectra of the PLA particles and gain insight into possible solutions for the under-representation of PLA in environmental samples. Additionally, bacterial growth changes over the course of the experiment were monitored via the culture method and morphological changes were tracked using FESEM.

5.3.2 PLA subjected to bacteria

The follow-up experiments included five samples with four identical replicates each. For the first experiment, bacteria were added to the PLA microplastic suspension with one sample containing *E. coli*, one *S. koreensis*, one *P. libanensis*, and one with both *S. koreensis* and *P. libanensis*. A sterile aqueous suspension of PLA microplastic without the addition of bacteria served as negative control. All samples were incubated over a 21-day period, treated identical, and samples for the different analysis techniques were taken at the respective time points (daily for bacterial growth observation, at day 7, 14, and 21 for RM and FESEM analysis). The second experiment, incubation of ultrapure water with the same bacteria, was done as a control to check whether the presence of PLA microplastic particles influenced the bacterial growth behavior in the aqueous microplastic suspensions (analysis via culture on agar plates).

5.3.2.1 Bacterial growth behavior in the presence of PLA microplastic

Based on the bacterial growth data acquired by plating the PLA microplastic suspension on agar plates, a fundamental prerequisite for experiments with bacteria and microplastic particles could be demonstrated: The production of sterile PLA reference particles was successful following the afore mentioned protocol as no bacteria were culturable in the samples which contained MP suspension only. Additionally, *E. coli* growth was not observed in the course of the 21 days of incubation time (apart from day 0, directly after starting the experiment) which is expected, as *E. coli* cannot survive in these nutrient stripped conditions. *P. libanensis* and *S. koreensis* are, however, able to survive and strive under these conditions. This has also been reported in previous studies using different

Sphingomonas and *Pseudomonas* species [205–208]. Both *P. libanensis* and *S. koreensis* showed growth over the whole time of the experiment and did not reach a steady state. A large intra-set variability was seen for the replicates in all five different sample sets resulting in the decision to view each sample individually and not as replicates. The data for *S. koreensis* is shown in Figure 27 and is discussed in more detail below as the data for *P. libanensis* shows similar trends.

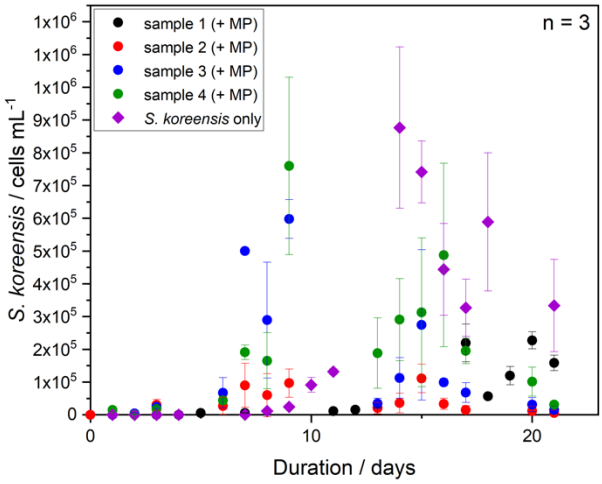

Figure 27: Change of S. *koreensis* cell numbers over 21-day incubation period in PLA microplastic suspension (black, red, blue, and green represent the four replicates) and in ultrapure water (purple).

This experiment was planned as a preliminary first glance at what happens to biodegradable microplastic particles subjected to bacteria and over the course of the experiment, several drawbacks became apparent. The drops in the number of counted cells which can be seen in Figure 27 (for the green and blue graphs between day 9 and 13, for example) are generated by the adjustment of the dilution factors for plating to ensure good countability of the colonies. The time points varied for each sample and were decided for each sample separately. For *S. koreensis*, this adjustment of dilution could only be done with a one-day delay, as these colonies needed to grow for 2 days to show colonies large enough for counting. This effect skewed the results, as, for analysis purposes only, a number of colonies greater than what was countable was assumed and the high numbers are likely overestimated. This specific problem was not encountered with *P. libanensis*. As is the case for many *Pseudomonas* species, their biofilm-forming nature complicates counting efforts as insufficient mixing prior to plating on the agar plates results in uneven distribution and formation of a biofilm which hampers manual counting. Although extensive measures were taken to ensure a sterile working environment, a contamination with *Methylobacterium rhodesianum* was detected in different samples starting for some at day 6. *M. rhodesianum* was identified using MALDI-TOF MS. The colonies of *M. rhodesianum* show a distinct pale pink coloring and grow at a rather slow pace [209,210]. These bacteria need 3 days to grow to a countable colony size under the conditions of the experiment, hence, the delay in detection. However, *M. rhodesianum* did not outgrow the spiked bacteria in any way or inhibit the growth of either of our chosen

bacteria, the rest of the experiment was carried out as originally planned and the growth of *M. rhodesianum* was monitored as well.

Collecting Raman spectra of the single bacteria themselves was also attempted. However, due to the high fluorescence induced by *P. libanensis* which is also visible by naked eye (visible fluorescence of the colonies after incubation for 2 days) no Raman spectrum could be obtained [211]. For *S. koreensis*, spectra could be obtained but showed mainly carotenoid characteristic bands which is plausible as these bacteria produce yellow to orange-colored colonies and therefore produce large amounts of carotenoids [212].

5.3.2.2 Particle and bacteria visualization with FESEM

FESEM samples were taken at day 7, 14, and 21. As is visible in Figure 28, microplastic particles were successfully imaged using FESEM (Figure 28a-c). Bacteria could be shown in the samples with spiked *P. libanensis* and *S. koreensis* (Figure 28b-d) but not in the sample with microplastic suspension only (Figure 28a). This confirms the bacterial culture results, where the negative control containing only microplastic suspension does not show any growth. Both bacteria were visible in the sample with *P. libanensis* and *S. koreensis*, as is shown in Figure 28d. This supports the results from the bacterial culture surveillance. Additionally, bacteria on top of the PLA particles as well as in the vicinity of the microplastic particles (Figure 28c) could be visualized. PLA particles in different shapes and with different surface structure (rough edges as well as a smooth surface) could be observed. While the rough edges are typical for PLA particles [99], the smooth surface seems to originate from bacterial colonization. In the samples with increasing bacterial population, more nano-sized particles, probably PLA, are present compared to the microplastic suspension without bacteria (Figure 28a and d). Degradation products of the larger particles could be one explanation for this observation. It has been previously reported, that under controlled weathering conditions it is possible to form nano-sized PLA particles from way larger particles, which supports our theory of the small particles being nano-sized PLA particles [183]. These observations lead to the conclusion that some form of bacterial degradation of the PLA particles happened, although the extent of this cannot be quantified and the FESEM images provide only empirical evidence.

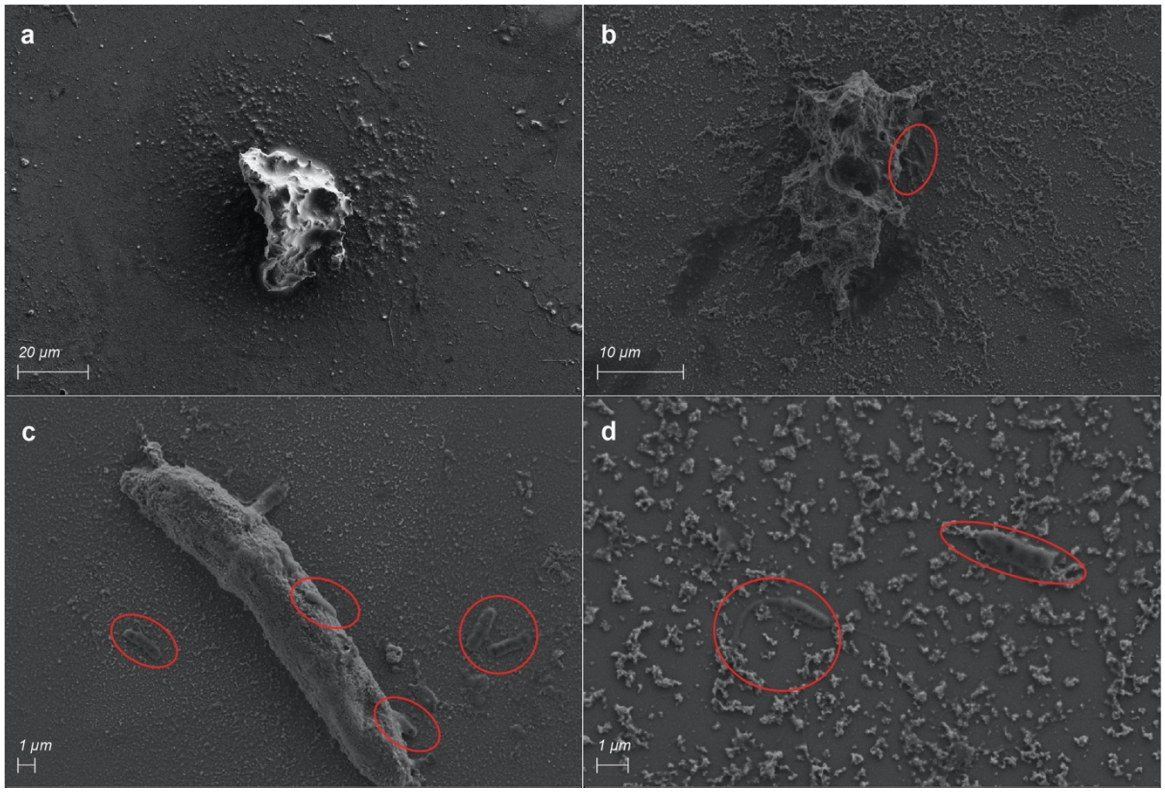

Figure 28: FESEM images of PLA suspension samples. (a) PLA particle after 7 days without bacteria; (b) PLA particle after 7 days with *S. koreensis*; (c) PLA particle at day 14 with P. *libanensis* in vicinity; (d) *S. koreensis* and *P. libanensis* in sample at day 14 with nano-sized particles. Bacteria are marked in red. Images taken by Christian Schwaferts.

5.3.2.3 Changes in Raman spectra due to PLA-bacteria interaction

The samples taken at day 7, 14, and 21 were analyzed with RM single particle analysis. The existing automated protocol by von der Esch et al. [98] was adapted to the task at hand. First, an image of the entire droplet residue was taken for each sample and all particles were morphologically characterized yielding the total particle number of each sample as well as the shapes and sizes of the particles within each sample. Comparing the microscope images of the individual samples revealed a great heterogeneity between the different samples and between the same samples at different sampling times (Figure 29). While some samples showed a great heterogeneity over the course of the experiment (Figure 29a) with good quality for automated analysis on some days (day 14, in this example) and bad quality on other days (day 7 and day 21), others showed a greater homogeneity during the incubation period of 21 days (Figure 29b and c). As is evident from the samples depicted as examples in Figure 29b and c, some were not suited for automated analysis, since this approach requires isolated structures with good contrast compared to the background (Figure 29b). Others could be analyzed easily using the developed automated analysis (Figure 29c). One explanation for this behavior is the occurrence of drying artefacts as the samples were drop-cast onto CaF_2 carriers and then left to dry under sterile conditions. As all samples were handled in the same way by the same operator, an explanation as to why these artefacts appeared for some samples and

not for others could not be given. Further studies addressing this issue are envisaged to ensure a better automated processing of the samples.

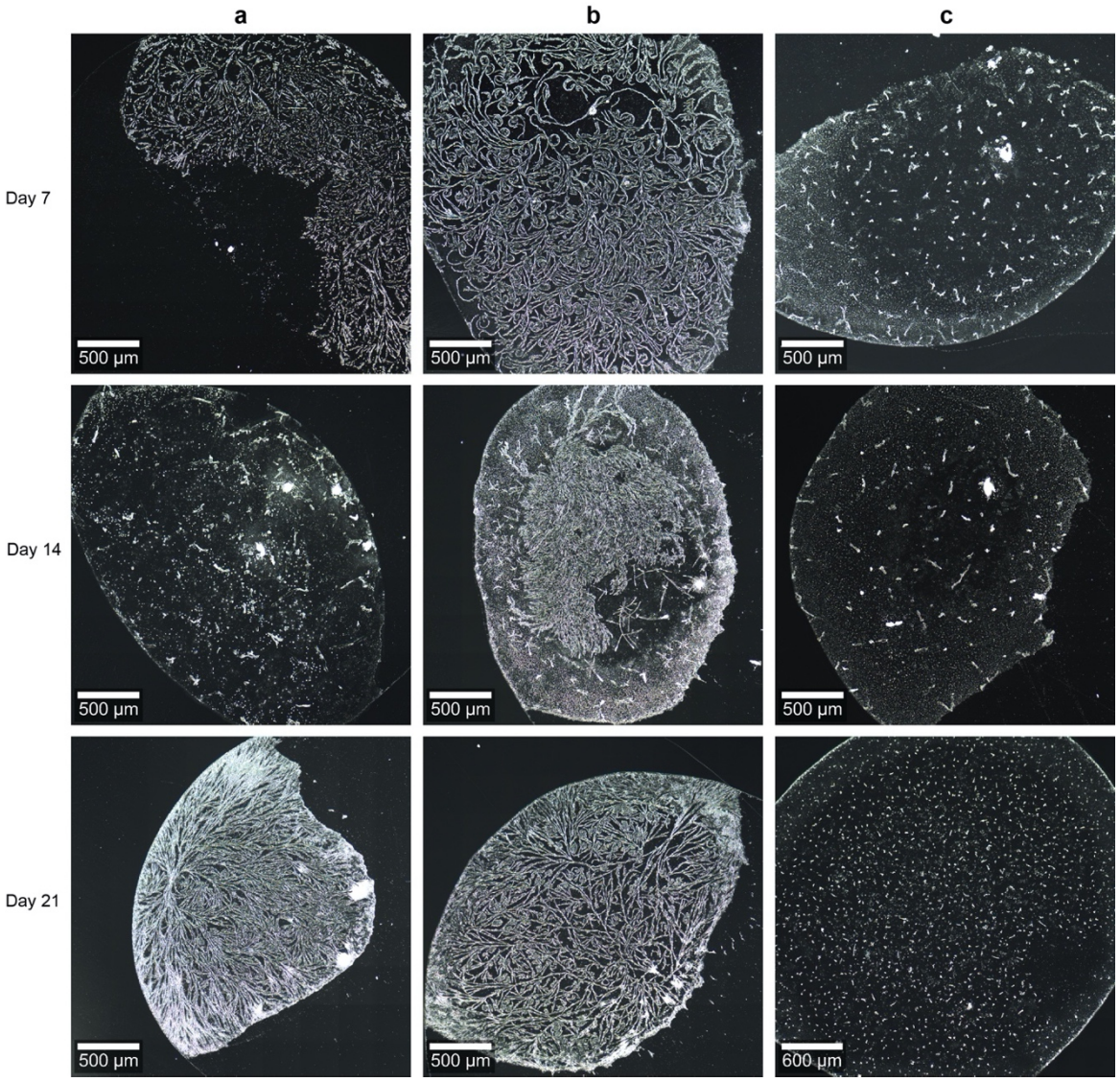

Figure 29: Overview of Raman microscope images for automated detection of different samples at different time points. (a) PLA microplastic suspension, replicate 3; (b) PLA microplastic suspension with *S. koreensis*, replicate 2; (c) PLA microplastic suspension with *S. koreensis*, replicate 3.

Due to these impediments the number of particles within each sample at each measurement point also differs greatly. Analyzing the metadata of the Raman analysis gives further indication that although single particle analysis is an excellent tool for microplastic analysis, it also hinders a more in-depth look without analysis of a sufficiently large number of particles to ensure statistically sound results. In this study, 70 of the particles recognized by the WITec Particle Scout (selected via random sampling [97]) were chemically analyzed by RM. The focus of the metadata lies on four key aspects: total particle number recognized by the algorithm, ratio of PLA-assigned particles to total particles measured, average HQI for PLA database assignment, and average fluorescence. The corresponding graphs are shown in Figure 30.

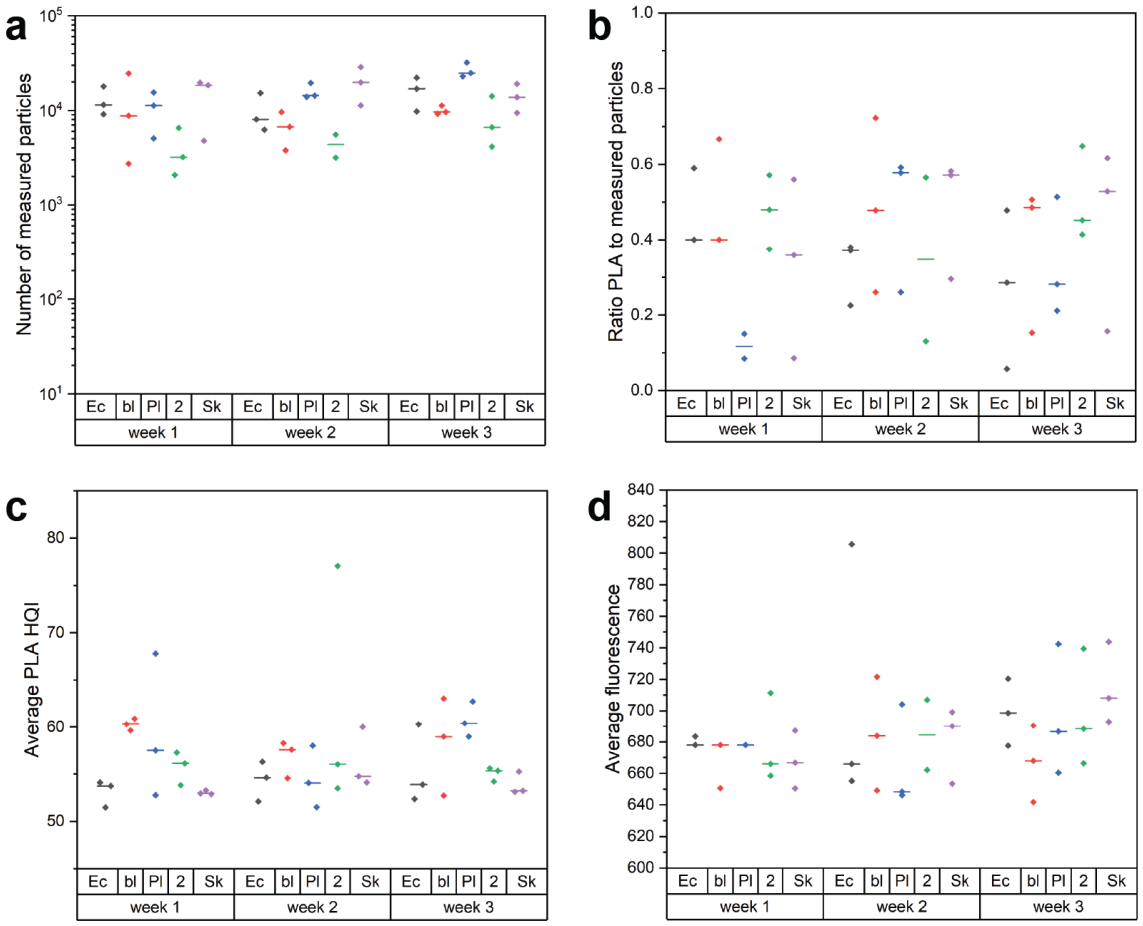

Figure 30: Overview of metadata for Raman spectra analysis. (a) number of total particles detected by the WITec Particle Scout, (b) ratio of particles assigned to PLA to total number of particles identified, (c) average HQI for particles identified as PLA, and (d) average fluorescence for all particles analyzed. Dots: individual measurements; lines: median of the replicates; Ec: *E. coli* samples (black); bl: blank (without bacteria; red); Pl: *P. libanensis* samples (blue); 2: *P. libanensis* and *S. koreensis* samples (green); Sk: *S. koreensis* samples (purple).

The total particle number (Figure 30a) does not show a significant trend overall but rather great homogeneity with no clear changes visible when looking at all available sample sets. Examining only the samples with *P. libanensis* and *S. koreensis* (blue and green, respectively) shows an increase in particle number (11,237 to 24,706 particles for *P. libanensis* and 3,208 to 6,617 particles for *S. koreensis*) which is in contrast to the sample containing both bacteria where no increase is visible (purple). While an increase in total particle number was originally expected, the agglomeration of microplastic particles due to organic matter disposal has the opposite effect. Depending on which effect is stronger in each sample, the number of total particles is influenced accordingly. The ratio of PLA-assigned particles to measured particles (Figure 30b) does not show any trend but again underlines the great heterogeneity found in all analyses. Here, two factors come into play that are expected to have opposing effects on the total particle number: fragmentation into smaller particles leads to more, smaller particles thus increasing the number of PLA particles found in the samples while the formation of biofilm decreases the number of PLA particles assigned correctly. A closer look at the average HQI of the PLA assigned particles

(Figure 30c) also shows a great heterogeneity without a clear trend. Here, again, several factors that affect this data need to be considered: When more particles are identified as PLA, the statistical value of the average HQI data increases. Thus, this data relies heavily on the number of particles assigned as PLA. For example, a small number of PLA particles assigned with different HQI values (as is seen in the second week for the green graph) influences the overall heterogeneity impression to a large extent. While a higher number of analyzed particles could prevent this bias, this was not possible during this study due to time and instrument restrictions. While the average fluorescence was expected to rise over the course of the study for all samples with bacterial influence (Figure 30d), this could only be observed for the *S. koreensis* and *S. koreensis* with *P. libanensis* samples. The two negative controls, without any bacteria and with the initial addition of *E. coli* also showed changes in fluorescence which might be due to the contamination of some of the samples with *M. rhodesianum* over the course of the study. To overcome these limitations, future studies in this area should include more particles to be measured to increase statistical significance of the data and possibly overcome the heterogeneity problem that hindered a better analysis of the current data.

Figure 31 reveals distinct changes in the Raman spectra of the PLA in the presence of bacteria. The green graph spectrum was collected from a selected PLA particle that was incubated in the presence of bacteria while the reference PLA spectrum is depicted in red and the carotenoid reference spectrum is shown in blue. Analyzing the individual bands further, it became clear that the most prominent bands pertaining to the carotenoids present on the surface of the PLA particles correspond nicely with those of a carotenoid reference (blue) whereas only the C-H stretching vibration around 2900 cm^{-1} indicates the presence of PLA. This observation is plausible as the bacteria *S. koreensis* shows yellow-pigmented colonies on agar plates and is known to produce large amounts of carotenoids [212]. However, the heterogeneity mentioned previously between the samples also comes into play here. Each particle measured exhibited differing Raman spectra and varied over time for the same samples revealing no clear pattern. This confirms the widely stated hypothesis that microplastic particles act as islands, as not all PLA particles in this experiment may be subjected to the same amount of bacterial colonization or degradation - just like expected in nature. In turn, the particles sampled at a specific time point show great heterogeneity in terms of whether degradation/colonization occurred and how strong the related effects are and thus the Raman spectra reflect that. However, this gave the unique opportunity to look at particles at different stages of bacterial colonization and degradation in one sample. While some particles do not show any changes in Raman spectra compared to the PLA reference, other Raman spectra have changed to such an extent that no correct identification as PLA particles was possible. One possibility, which has not been explored yet due to technical difficulties, would be to look at fixed microplastic particles (similar in size to the ones produced in this study, ~ 10 µm) over a longer period of time to identify the changes happening on a time-resolved scale. An additional observation of the individual Raman spectra revealed an increase in fluorescence for particles with increasing deviation from the PLA reference Raman spectra. Here, the

influence of the bacteria and the associated organic matter comes into play, as especially *P. libanensis* shows strong fluorescence (also visible by naked eye) and no Raman spectrum could be obtained due to the large fluorescent background [211].

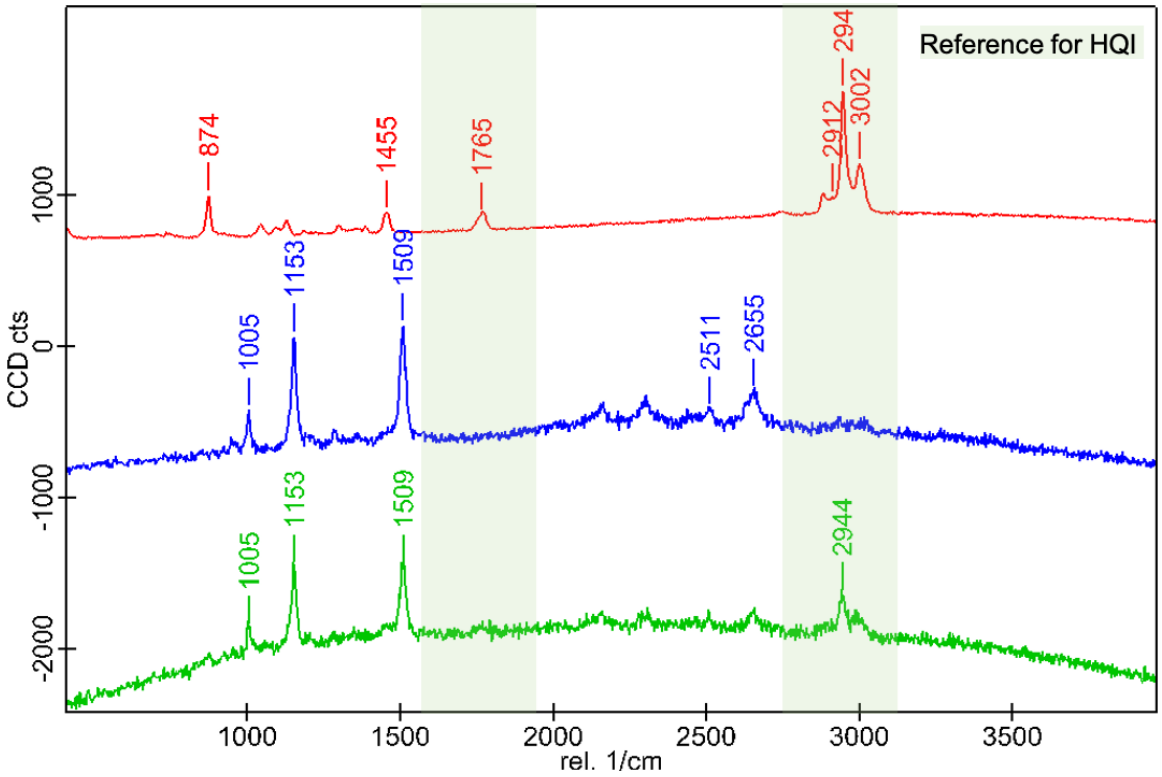

Figure 31: Comparison of different Raman spectra: PLA reference spectrum (red), carotenoid spectrum (blue) and the example of a PLA spectrum in the presence of bacteria (green). HQI reference areas for PLA are indicated as green-shaded areas.

Due to the significant changes of the Raman spectra, the correct assignment of PLA by database matching was not possible for many particles. Interestingly, most of these particles were then identified as polyamide by the database matching software (blue spectrum in Figure 32 shows the polyamide database spectrum). This stems from the change in the shape of the C-H-stretch band which is typically used for PLA identification (green region in Figure 32). Due to the change of the three distinct bands at 2912 cm^{-1}, 2944 cm^{-1}, and 3002 cm^{-1} (red spectrum in Figure 32) to slightly shifted band positions with an additional change in the relative ratio between the bands (green spectrum in Figure 32), polyamide is the closest match in the database. However, due to the experimental set-up it is impossible to obtain polyamide as only PLA particles were added to the sample vials and a change in polymer type is not possible. Furthermore, a reevaluation of the spectra in question by experts often results in a change of qualification. As the overall appearance of polyamide and protein Raman spectra are similar and organic matter is ubiquitously found in environmental samples, this preliminary observation supports the possibility that PLA and in consequence biodegradable microplastic in the environment might be under-estimated.

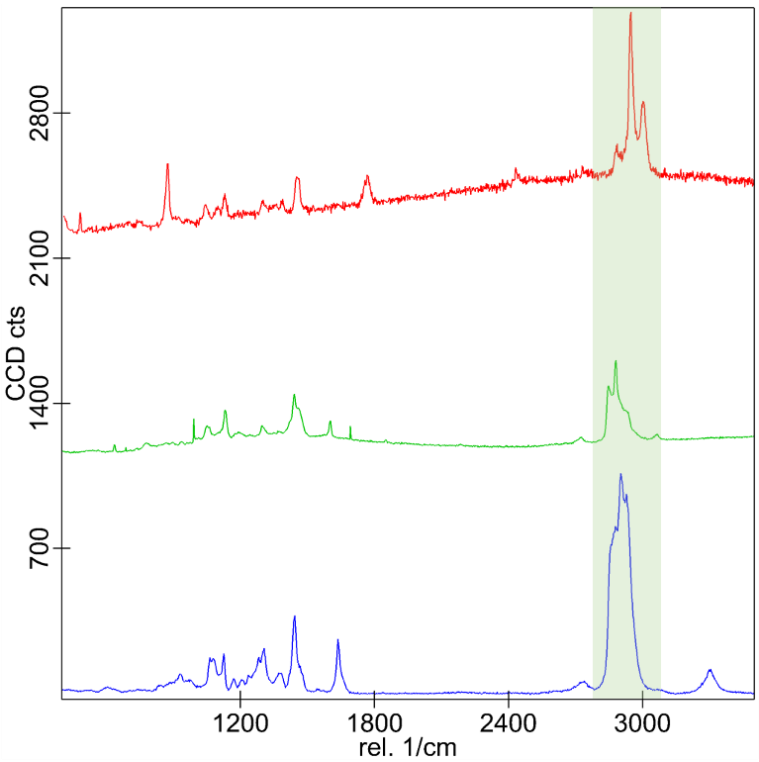

Figure 32: Comparison of different Raman spectra: pristine PLA particle (red), PLA particle under influence of bacteria (green), polyamide reference spectrum (blue).

Summarizing the different aspects of the studies conducted here on microplastic and bacterial degradation thereof, it became apparent that the preliminary setup chosen for this experiment may have been too simple. This study suggests bacteria preferred to attach to the biodegradable PLA rather than PET and PS and in turn use PLA as a substratum to adhere to, and, likely also as a substrate to grow on. However, further studies investigating the degradation effect will have to be done to support this finding. Using the limited 21-day time frame no complete elimination of PLA particles was seen, which would support the association of the bacteria with the PLA. FESEM data suggests the formation of nano-sized PLA particles during this process, giving a strong indication towards degradation events occurring. Interestingly, the PLA particles still present in the samples were not all correctly assigned to PLA using RM with database matching. This is in contrast to PET and PS samples which were assigned correctly, even when measuring a bacterium on top of a microplastic particle. Consequently, the effects leading to the shift in PLA Raman spectra were investigated further and revealed, that PLA may be underestimated in natural environments when in the presence of bacteria. Additionally, with RM as the analysis technique for investigation of microplastics, not differentiation between colonization and degradation can be made. The most likely hypothesis is a combination of both occurring for PLA and supporting experiments in this direction were not conducted to focus on investigating the effects on RM analysis.

Currently, PLA particles are at the moment not adequately recognized using RM. Most prominently, single particle analysis from environmental samples via RM is currently facing the challenge of using database matching as approach since these databases mostly

include Raman spectra of pristine plastics. Since these are rarely found in the environment, the result is a bias in the outcome of the analysis. A more in depth look at the data on a case-by-case basis, extension of existing databases using aged microplastic or microplastic subjected to different microbial communities, and correcting factors in the automatic detection pipeline are possible workable approaches and areas to direct future research efforts on. Including the presence of carotenoid and amide bands and an increase in fluorescence as indicators for bacterial interaction with the microplastic particles should also be investigated further and considered when analyzing bio-based microplastic particles from environmental samples.

6 CONCLUSION AND OUTLOOK

Aqueous environments may harbor antibiotic resistant bacterial pathogens which may cause infections and can also help to reduce the antibiotic burden by breaking down these compounds. Providing improved enrichment methods for bacteria to facilitate culture-independent analysis, establishing new assays for detection of bacterial pathogens and antibiotic resistance genes, are important elements to move analysis methods forward. Gaining insight into how bacteria interact with biodegradable microplastic and the challenges for analysis of these compounds are additional interesting analytical questions.

To ensure time efficient detection of the opportunistic bacterial pathogen *P. aeruginosa* from tap water, an enrichment method is needed to be able to detect the low amounts using qPCR. The optimized MAF filtration procedure (MAF-OH, BEG elution buffer, 5-L initial sample volume, sample pH 3) was calibrated in the range of $1 \cdot 10^4$ - $1 \cdot 10^8$ CFU L^{-1} and resulted in an enrichment factor of $3 \cdot 10^3$ in under 1 h (combined with centrifugal ultrafiltration). An additional culturability study of *P. aeruginosa* revealed, that no growth was observed under a pH of 3.2 thus eliminating the possibility of culture-based detection or live-dead discrimination using the evaluated setup. To achieve the latter goal, new MAF functionalizations would have to be established as the currently available modifications did not provide promising results. Future research efforts should be directed at a detailed understanding of the mechanisms behind the retention of the bacterial cells on the MAF surface and the elution process of the bacteria from the MAF to streamline optimization processes for other microorganisms. The developed method of elution for *P. aeruginosa* cells can also be used for continuous sampling MAF which are then eluted later on to monitor premise plumbing systems. This fast and culture-independent approach cuts down on precious time between sampling and detection to minimize the impact on residents.

Detecting opportunistic bacterial pathogens and antibiotic resistance in a fast and low resource manner allows for a broader monitoring of these traits of bacteria in the environment. The isothermal DNA amplification method haRPA offers a new approach to detect the ARG $bla_{\text{CTX-M}}$ cluster 1. The established assay was compared against PCR and qPCR protocols with the same high selectivity and lower sensitivity, respectively. A haRPA assay for *P. aeruginosa* (limit of detection: 10^3 cells mL^{-1}) was also established and combined with the detection of *K. pneumoniae* for a multiplex assay to detect the opportunistic bacterial pathogens and the antibiotic resistance simultaneously. This qualitative assay is a promising first step to a field-application friendly monitoring of both pathogenicity and antibiotic resistance. Future research efforts in haRPA development should shed light on a feasible multiplex assay composition for example generating fusion products and thus lowering the DNA load in the bulk phase. Combining this isothermal DNA amplification and detection method with enrichment processes is one way to provide culture-independent detection of bacterial pathogens and ARGs. To improve the sensitivity of the haRPA assay, changing the enzyme ratio from the mixture provided by the manufacturer might be one way as the current mixture is not optimized for the

heterogeneous setup the haRPA uses. In adjusting the enzyme ratio for example, the sensitivity of the assay could be improved. For in-field applications, a simpler detection device with minimal power consumption and optimized reagent use would be more suitable and thus, research efforts should also be directed there.

In the environment, microorganisms such as bacteria are thought to degrade microplastic particles. Understanding this process is critical to aid bacteria in their efforts to decontaminate the environment from microplastic. In this study using RM, FESEM, and bacterial culture, we gathered evidence that the bio-based PLA is indeed degraded to some extent, even in the very simple setup used (21-day incubation, ultrapure water, stable temperature, mild shaking). Two bacterial species previously unknown to grow under these circumstances and probably use PLA as a food source were identified, *P. libanensis* and *S. koreensis*. Changes in the Raman spectra of the PLA particle analyzed complicated the correct assignment of the remaining particles as PLA. This was not seen for PS and PET, which were still identified correctly using database matching, even when measuring a bacterium on top of a PS particle. There similar shifts in Raman signals were observed as for the altered PLA particles. It is therefore currently not possible to distinguish between colonization and degradation using RM. The results of this study also suggest that PLA microplastic particles are “shielded” from correct assignment using RM and database matching as the surface of these particles seems to change under the influence of bacterial colonization/degradation. This reveals a possible underdetermination PLA in environmental samples. The proposed method to counteract this bias is to reevaluate Raman spectra with indicators for bacterial activity (carotenoid bands, amide bands) and especially those that were assigned as polyamide. Forthcoming projects should further elucidate these findings for example by using isotope-labelled plastics for a similar study and implementing stable isotope Raman spectroscopy to differentiate between degradation and colonization from bacteria. A more elaborate study using carbon mass ratio experiments, a minimal-media environment for the bacteria, and a higher number of particles measured to increase statistical value should be carried out to get a more complete picture of the process. Also, it became apparent that the current plastic database needs to be extended by reference spectra of environmental samples and polymers subjected to different environmental influences to overcome the observed bias in analysis.

Understanding where pathogenic bacteria are present in our urban environment and how antibiotic resistance is spread throughout different water sources is important to help decrease infection risks with hard to combat bacteria. On-site analysis with minimal time spent between sampling and final results helps to ensure a continuous monitoring and to detect threats at an early stage. Revealing how bacteria degrade bio-microplastic and how this process might interfere and/or hinder the detection of this analyte is crucial to ensure that an environmental sample is analyzed and classified correctly and to draw the right conclusions from it. Working on these tasks in the future can help combat the spread of antibiotic resistance and pathogenic bacteria in critical infrastructure while also ensuring that the plastic pollution problem is dealt with and may lead to a better future.

LIST OF FIGURES

LIST OF TABLES

LIST OF ABBREVIATIONS

ARG	Antibiotic resistance gene
BEG	Beef extract glycine
CFU	Colony forming unit
ESBL	Extended spectrum beta-lactamase
ESKAPE	*Enterococcus faecium*, *Staphylococcus aureus*, *Klebsiella pneumoniae*, *Acinetobacter baumanii*, *Pseudomoas aeruginosa*, and *Enterobacter* spp.
EU	European Union
FESEM	Field emission scanning electron microscopy
(FPA) FT-IR	(Focal plane arrier) Fourier-transform infrared spectroscopy
FWD	Forward
haRPA	Heterogeneous asymmetric recombinase polymerase amplification
HDA	Helicase dependent amplification
HQI	Hit quality index
IUPAC	International Union of Pure and Applied Chemistry
IWC-TUM	Institute of Water Chemistry, Technical University of Munich
LAMP	Loop-mediated isothermal amplification
MAF	Monolithic adsorption filter
MAF-DEAE	MAF with diethyl aminoethyl groups on the surface
MAF-OH	Hydrolyzed MAF
MAF-PmB	MAF with Polymyxin B on the surface
MALDI-TOF-MS	Matrix assisted laser desorption/ionization time of flight mass spectrometry

MS	Mass spectrometry
OD	Optical density
OD_{600}	Optical density at 600 nm
PBAT	Polybutylene adipate terephthalate
PBS	Phosphate buffered saline
PCR	Polymerase chain reaction
PE	Polyethylene
PET	Polyethylene terephthalate
PLA	Polylactic acid
PS	Polystyrene
PTFE	Polytetrafluoroethylene
qPCR	Quantitative polymerase chain reaction
REV	Reverse
RM	Raman microspectroscopy
RPA	Recombinase polymerase amplification
SDA	Strand displacement amplification
SEM	Scanning electron microscopy
ssDNA	Single strand DNA
WGS	Whole genomes sequencing
WHO	World Health Organization

Devices and consumables

Activia yoghurt cups in PS, PLA, and PET	Danone (Paris, France)
Autoclave Laboklav	SHP Steriltechnik (Peißenberg, Germany)
Balloons	Carl Roth (Karlsruhe, Germany)
Beakers	Schott (Mainz, Germany)
Bench-top centrifuge	Carl Roth (Karlsruhe, Germany)
Blue Light Table	SERVA electrophoresis GmbH (Heidelberg, Germany)
Bottles	Schott (Mainz, Germany)
Canula: size 1, G 20 × 1 ½" / ø 0,90 × 40 mm, yellow; size 2, G 21 × 1 ½" / ø 0,80 × 40 mm, green; Sterican®	B Braun (Melsungen, Germany)
Centrifuge 5804 R	Eppendorf (Hamburg, Germany)
Colony counter sc6+	Cole-Parmer (Staffordshire, UK)
Cuvettes	BRAND GmbH (Wertheim, Germany)
Disposable pipettes	Carl Roth (Karlsruhe, Germany)
DNA/RNA UV-Cleaner Box	SIA biosan (Riga, Latvia)
Drying cabinet	Memmert (Schwabach, Germany)
Field emission scanning electron microscope *Sigma VP 300*	Carl Zeiss (Jena, Germany)
Gel electrophoresis unit	Bio-Rad Laboratories (Munich, Germany)
Gloves	Carl Roth (Karlsruhe, Germany)
High Breast bottles GL 45, 5 L	Carl Roth (Karlsruhe, Germany)

Ice machine	Wessamat (Kaiserslautern, Germany)
Incubator	Heraeus (Hanau, Germany)
	Brunswick scientific (Nürtingen, Germany)
	Memmert (Büchenbach, Germany)
LightCycler 480	Roche Diagnostics GmbH (Mannheim, Germany)
LightCycler 480 Multiwell plate 96	Roche Diagnostics GmbH (Mannheim, Germany)
Magnetic stirrer	Heidolph (Schwabach, Germany)
	IKA Labortechnik (Staufen im Breisgau, Germany)
MCR 3	gwk Präzisionstechnik (Munich, Germany)
Microchip assembly equipment	Institute of Hydrochemistry (Munich, Germany)
Milli-Q plus 185	Millipore (Bedford, MA, USA)
Nano-Photometer	IMPLEN (München, Germany)
Parafilm	Sigma-Aldrich (Taufkirchen, Germany)
PE sealing film	Excel Scientific (Victorville, CA, USA)
Peristaltic pump	Heidolph (Schwabach, Germany)
	Watson Marlow Sci (Falmouth, UK)
Petri dishes glass	Carl Roth (Karlsruhe, Germany)
Petri dishes PS	Carl Roth (Karlsruhe, Germany)
pH-meter FiveEasy	Mettler-Toledo (Columbus, OH, USA)

Piezo dispense capillary, unmodified, PDC 80, P-2040	Scienion AG (Berlin, Germany)
Pipette tips: 0.1 – 10 µL, 10 – 200 µL, 100 – 1000 µL, 1 – 5 mL	Eppendorf (Hamburg, Germany) Sarstedt (Sevelen, Switzerland) Sorenson BioScience (Salt Lake City, UT, USA) Carl Roth (Karlsruhe, Germany)
Pipettes: 0.5 – 10 µL, 10 – 100 µL, 100 – 1000 µL, 1 – 5 mL	Eppendorf (Hamburg, Germany)
Polypropylene tube CELLSTAR: 15 mL, 50 mL	Greiner Bio-One (Kremsmünster, Austria)
Precision balance	Mettler (Columbus, OH, USA)
Precision dispenser tips 50 mL	Carl Roth (Karlsruhe, Germany)
Reaction tubes: 0.2 mL, 0.5 mL, 1,5 mL, 2 mL	Carl Roth (Karlsruhe, Germany)
Roti® Store Cryo Tubes	Carl Roth (Karlsruhe, Germany)
Rotilabo® canister 10 L	Carl Roth (Karlsruhe, Germany)
Rotilabo® syringe filters 0.22 µm	Carl Roth (Karlsruhe, Germany)
Scale	Kern (Balingen, Germany)
sciFLEXARRAYER S1	Scienion AG (Berlin, Germany)
sciSOURCEPLATE-384-PP	Scienion AG (Berlin, Germany)
Snap cap vials: 5 mL, 10 mL, 25 mL	Carl Roth (Karlsruhe, Germany)
Standard microscope slides, soda lime glass, 26 × 76 × 1mm, ± 0.1 mm	Carl Roth (Karlsruhe, Germany)
Sterile bench	BCK Luft- & Reinraumtechnik GmbH (Sonnenbühl-Genkingen, Germany) Kendro Laboratory Products GmbH (Langenselbold, Germany)
Syringes: 1 mL, 5 mL, 10 mL, 50 mL	B Braun (Melsungen, German

ThermaSeal RT™ Sealing Films	Excel Scientific (Victorville, CA, USA)
ThermoMixer® C	Eppendorf (Hamburg, Germany)
Tissues	Carl Roth (Karlsruhe, Germany)
Ultrasonic bath Sonorex RK510S	Bandelin (Berlin, Germany)
Vivaspin® 20, Membrane 50 000	Sartorius (Stonekouse, UK)
Vortexer	Fisher Scientific (Pittsburgh, PA, USA)

Software

Adobe Illustrator 2017 – 2020	Adobe Inc. (San Jose, CA, USA)
Adobe Photoshop 2017 – 2020	Adobe Inc. (San Jose, CA, USA)
Avis FITS Viewer	MSB di F. Cavicchio (Ravenna, Italy)
ChemDraw Professional 19	PerkinElmer (Waltham, MA, USA)
Image J 1.49	Rasband (NIH, Bethesda, USA)
MCRImageAnalyzer	gwk Präzisionstechnik (Munich, Germany)
Microsoft Excel 2016	Microsoft (Redmond, WA, USA)
Microsoft Power Point 2016	Microsoft (Redmond, WA, USA)
Microsoft Word 2016	Microsoft (Redmond, WA, USA)
Origin 2017 – 2020	OriginLab (Northampton, MA, USA)
Mendeley 1.19	Elsevier (Amsterdam, Netherlands)

Chemicals

(3-Glycidyloxypropyl)-trimethoxysilane	Sigma-Aldrich (Taufkirchen, Germany)
1,1'-Carbonyldiimidazole	Carl Roth (Karlsruhe, Germany)
1,4-Dioxane	Sigma-Aldrich (Taufkirchen, Germany)
4-(2-hydroxyethyl)-1-piperazineethane-sulfonic acid	Sigma-Aldrich (Taufkirchen, Germany)
Acetonitrile	Sigma-Aldrich (Taufkirchen, Germany)
Agar Agar	Carl Roth (Karlsruhe, Germany)
Agarose	Carl Roth (Karlsruhe, Germany)
Beef extract	Sigma-Aldrich (Taufkirchen, Germany)
Boron trifluoride diethyl etherate	Sigma-Aldrich (Taufkirchen, Germany)
Casein (from milk)	Sigma-Aldrich (Taufkirchen, Germany)
Cefotaxim	Sigma-Aldrich (Taufkirchen, Germany)
Diethylamine	Carl Roth (Karlsruhe, Germany)
Dimethylaminopyridine	Sigma-Aldrich (Taufkirchen, Germany)
Dimethylformamide	Sigma-Aldrich (Taufkirchen, Germany)
Dipotassium hydrogen phosphate	Carl Roth (Karlsruhe, Germany)
Disuccinimidyl-carbonate	Sigma-Aldrich (Taufkirchen, Germany)
DNA ladder	Carl Roth (Karlsruhe, Germany)
DNA Stain Clear G	Serva Electrophoresis GmbH (Heidelberg, Germany)
EDTA	Carl Roth (Karlsruhe, Germany)
Ethanol, ≧ 99.8%	Sigma-Aldrich (Taufkirchen, Germany)
EZ-Link ™ amine-PEG2-biotin	Thermofisher Scientific (Waltham, MA, USA)
Glacial acetic acid	Carl Roth (Karlsruhe, Germany)
Glycerin	Carl Roth (Karlsruhe, Germany)

Glycine	Sigma-Aldrich (Taufkirchen, Germany)
Hellmanex III	Hellma GmbH (Mühlheim, Germany)
Hydrochloric acid, 37%	Sigma-Aldrich (Taufkirchen, Germany)
Jeffamine ED-2003	Huntsman (USA)
LB Media	Carl Roth (Karlsruhe, Germany)
Luminol-enhancer solution	Cyanagen (Bologna, Italy)
Magnesium chloride	Sigma-Aldrich (Taufkirchen, Germany)
Methanol	Sigma-Aldrich (Taufkirchen, Germany)
Methyl *tertiary*-butyl ether, 99.8%	Sigma-Aldrich (Taufkirchen, Germany)
Nuclease-free water	Invitrogen AG (Carlsbad, USA)
NZCYM Media	Carl Roth (Karlsruhe, Germany)
Orange G 6 × loading buffer	Carl Roth (Karlsruhe, Germany)
Pluronic F-68	Sigma-Aldrich (Taufkirchen, Germany)
Polyglycerol-3-glycidyl-ether (CL9)	Ipox chemicals (Laupheim, Germany)
Polymyxin B	Sigma-Aldrich (Taufkirchen, Germany)
Potassium dihydrogen phosphate	Sigma-Aldrich (Taufkirchen, Germany)
Potassium sulfate	Carl Roth (Karlsruhe, Germany)
sciClean 8	Scienion AG (Berlin, Germany)
Sodium azide	Sigma-Aldrich (Taufkirchen, Germany)
Sodium carbonate	Sigma-Aldrich (Taufkirchen, Germany)
Sodium chloride	Carl Roth (Karlsruhe, Germany)
Sodium hydrogen carbonate	Sigma-Aldrich (Taufkirchen, Germany)
Sodium hydroxide solution, 32%	Carl Roth (Karlsruhe, Germany)
Sodium hypochlorite	Carl Roth (Karlsruhe, Germany)
Soy peptone	Carl Roth (Karlsruhe, Germany)
Streptavidin horseradish peroxide	Biozol (Eching, Germany)

Sulfuric acid, 97%	Sigma-Aldrich (Taufkirchen, Germany)
Toluene, 99.8%	Sigma-Aldrich (Taufkirchen, Germany)
Triethylamine	Sigma-Aldrich (Taufkirchen, Germany)
Tris(hydroxymethyl)-aminomethane Sigma 7-9®	Sigma-Aldrich (Taufkirchen, Germany)

Reaction kits

GeneJET PCR Purification Kit	Thermofisher Scientific (Waltham, MA, USA)
GeneJET Genomic DNA Purification Kit	Thermofisher Scientific (Waltham, MA, USA)
Luna® Universal qPCR Master Mix	New England Biolabs (Ipswitch, MA, USA)
QIAamp DNA Mini Kit	QIAGEN (Hilden, Germany)
TwistAmp basic®	TwistDx (Cambridge, UK)

REFERENCES

1. Falkinham JO, Pruden A, Edwards M. Opportunistic Premise Plumbing Pathogens: Increasingly Important Pathogens in Drinking Water. Pathogens. 2015;4(2):373–86.

2. Falkinham III JO, Hilborn ED, Arduino MJ, Pruden A, Edwards MA. Review Epidemiology and Ecology of Opportunistic Premise Plumbing Pathogens : *Legionella pneumophila*, *Mycobacerium avium* and *Pseudomonas aeruginosa*. Environ Health Perspect. 2015;123(8):749–58.

3. Fields BS, Benson RF, Besser RE. *Legionella* and Legionnaires' Disease: 25 Years of Investigation. Clin Microbiol Rev. 2002;15(3):506–26.

4. Kaufmann AF, McDade JE, Patton CM, Bennett J V, Skaliy P, Feeley JC, et al. Pontiac fever: Isolation of the etiologic agent (*Legionella pneumophilia*) and demonstration of its mode of transmission. Am J Epidemiol. 1981;114(3):337–47.

5. Szwetkowski KJ, Falkinham III JO. Methylobacterium spp. as Emerging Opportunistic Premise Plumbing Pathogens. Pathogens. 2020;9(149).

6. Bédard E, Prévost M, Déziel E. *Pseudomonas aeruginosa* in premise plumbing of large buildings. Microbiologyopen. 2016;5:937–56.

7. Falkinham JO. Common Features of Opportunistic Premise Plumbing Pathogens. Int J Environ Res Public Health. 2015;12(5):4533–45.

8. Vert M, Doi Y, Hellwich K-H, Hess M, Hodge P, Kubisa P, et al. Terminology for biorelated polymers and applications (IUPAC Recommendations 2012). Pure Appl Chem. 2012 Jan 11;84(2):377–410.

9. Manuel CM, Nunes OC, Melo LF. Dynamics of drinking water biofilm in flow/non-flow conditions. Water Res. 2007;41(3):551–62.

10. Hyun-Jung J, Choi YJ, Ka JO. Effects of Diverse Water Pipe Materials on Bacterial Communities and Water Quality in the Annular Reactor. J Microbiol Biotechnol. 2011;21(2):115–23.

11. De Beer D, Srinivasan R, Stewart PS. Direct Measurement of Chlorine Penetration into Biofilms during Disinfection. Appl Environ Microbiol. 1994;60(12):4339–44.

12. Wang H, Masters S, Hong Y, Stallings J, Falkinham JO, Edwards MA, et al. Effect of disinfectant, water age, and pipe material on occurrence and persistence of *Legionella*, mycobacteria, *Pseudomonas aeruginosa*, and two amoebas. Environ Sci Technol. 2012;46(21):11566–74.

13. Cai X, Wang R, Filloux A, Waksman G, Meng G. Structural and Functional Characterization of *Pseudomonas aeruginosa* CupB Chaperones. PLoS One. 2011;6(1).

14. Streeter K, Katouli M. *Pseudomonas aeruginosa*: A review of their Pathogenesis and Prevalence in Clinical Settings and the Environment. Infect Epidemiol Med. 2016;2(1):25–32.

15. Pendleton JN, Gorman SP, Gilmore BF. Clinical relevance of the ESKAPE pathogens. Expert Rev Anti Infect Ther. 2013;11(3):297–308.

16. Aumeran C, Paillard C, Robin F, Kanold J, Baud O, Bonnet R, et al. *Pseudomonas*

aeruginosa and *Pseudomonas putida* outbreak associated with contaminated water outlets in an oncohaematology paediatric unit. J Hosp Infect. 2007;65:47–53.

17. The Regulation and Quality Improvement Authority Independent Review of Incidents of *Pseudomonas aeruginosa* Infection in Neonatal Units in Northern Ireland Final Report. 2012.

18. Costa D, Bousseau A, Thevenot S, Dufour X, Laland C, Burucoa C, et al. Nosocomial outbreak of *Pseudomonas aeruginosa* associated with a drinking water fountain. J Hosp Infect. 2015;91(3):271–4.

19. Kinsey CB, Koirala S, Solomon B, Rosenberg J, Robinson BF, Neri A, et al. *Pseudomonas aeruginosa* Outbreak in a Neonatal Intensive Care Unit Attributed to Hospital Tap Water. Infect Control Hosp Epidemiol. 2017;38(7):801–8.

20. Høiby N, Ciofu O, Bjarnsholt T. *Pseudomonas aeruginosa* biofilms in cystic fibrosis. Future Microbiol. 2010;5(11):1663–74.

21. Burns JL, Gibson RL, McNamara S, Yim D, Emerson J, Rosenfeld M, et al. Longitudinal Assessment of *Pseudomonas aeruginosa* in Young Children with Cystic Fibrosis. J Infect Dis. 2001;183(3):444–52.

22. Lutz JK, Lee J. Prevalence and Antimicrobial-Resistance of *Pseudomonas aeruginosa* in Swimming Pools and Hot Tubs. Int J Environ Res Public Health. 2011;8:554–64.

23. Lambert PA. Mechanisms of antibiotic resistance in *Pseudomonas aeruginosa*. J R Soc Med. 2002;95(41):22–6.

24. Breidenstein EBM, de la Fuente-Núñez C, Hancock REW. *Pseudomonas aeruginosa*: All roads lead to resistance. Trends Microbiol. 2011;19(8):419–26.

25. Botelho J, Grosso F, Peixe L. Antibiotic resistance in *Pseudomonas aeruginosa* – Mechanisms, epidemiology and evolution. Drug Resist Updat. 2019;44(April):100640.

26. Moradali MF, Ghods S, Rehm BHA. *Pseudomonas aeruginosa* Lifestyle: A Paradigm for Adaptation, Survival, and Persistence. Front Cell Infect Microbiol. 2017;7(39).

27. Wongsa P, Tanaka M, Ueno A, Hasanuzzaman M, Yumoto I, Okuyama H. Isolation and Characterization of Novel Strains of *Pseudomonas aeruginosa* and *Serratia marcescens* Possessing High Efficiency to Degrade Gasoline, Kerosene, Diesel Oil, and Lubricating oil. Curr Microbiol. 2004;49(6):415–22.

28. LaBauve AE, Wargo MJ. Growth and Laboratory Maintenance of *Pseudomonas aeruginosa*. Curr Protoc Microbiol. 2012;1–11.

29. Gensini FG, Conti AA, Lippi D. The contributions of Paul Ehrlich to infectious disease. J Infect. 2007;54:221–4.

30. Ligon BL. Penicillin: Its Discovery and Early Development. Semin Pediatr Infect Dis. 2004;15(1):52–7.

31. Molinaro M, Morelli P, De Gregori M, De Gregori S, Giardini I, Tordato F, et al. Efficacy of intraventricular amikacin treatment in pan-resistant *Pseudomonas aeruginosa* postsurgical meningitis. Infect Drug Resist. 2018;11:1369–72.

32. Nichols L. Death from pan-resistant superbug. Autops CaseReports. 2019;9(3).

33. Nishida S, Ono Y. Genomic analysis of a pan-resistant *Klebsiella pneumoniae* sequence type 11 identified in Japan in 2016. Int J Antimicrob Agents. 2020;55(4).

34. Perry J, Waglechner N, Wright G. The Prehistory of Antibiotic Resistance. Cold Spring Harb Perspect Med. 2016;6(6):1–8.

35. D'Costa VM, King CE, Kalan L, Morar M, Sung WWL, Schwarz C, et al. Antibiotic resistance is ancient. Nature. 2011;477(7365):457–61.

36. Dodds DR. Antibiotic resistance: A current epilogue. Biochem Pharmacol. 2017;134(December):139–46.

37. Livermore DM. Has the era of untreatable infections arrived? J Antimicrob Chemother. 2009;64(SUPPL.1):29–36.

38. Cassini A, Högberg LD, Plachouras D, Quattrocchi A, Hoxha A, Simonsen GS, et al. Attributable deaths and disability-adjusted life-years caused by infections with antibiotic-resistant bacteria in the EU and the European Economic Area in 2015: a population-level modelling analysis. Lancet Infect Dis. 2019;19(1):56–66.

39. European Centre for Disease Prevention and Control. The bacterial challenge: time to react. 2009.

40. Ahmad M, Khan AU. Global economic impact of antibiotic resistance: A review. J Glob Antimicrob Resist. 2019;19:313–6.

41. Ventola CL. The Antibiotic Resistance Crisis Part 1: Causes and Threats. Pharm Ther. 2015;40(4):277–83.

42. Castanon JIR. History of the Use of Antibiotic as Growth Promoters in European Poultry Feeds. Poult Sci. 2007;86(11):2466–71.

43. Gharaibeh MH, Shatnawi SQ. An overview of colistin resistance, mobilized colistin resistance genes dissemination, global responses, and the alternatives to colistin: A review. Vet World. 2019;12(11):1735–46.

44. Teuber M. Veterinary use and antibiotic resistance. Curr Opin Microbiol. 2001;4(5):493–9.

45. Schwarz S, Kehrenberg C, Walsh TR. Use of antimicrobial agents in veterinary medicine and food animal production. Int J Antimicrob Agents. 2001;17(6):431–7.

46. Heuer H, Schmitt H, Smalla K. Antibiotic resistance gene spread due to manure application on agricultural fields. Curr Opin Microbiol. 2011;14(3):236–43.

47. Manzetti S, Ghisi R. The environmental release and fate of antibiotics. Mar Pollut Bull. 2014;79(1–2):7–15.

48. FAO & IAEA. Antimicrobial movement from agricultural areas to the environment: The missing link. A role for nuclear techniques. Rome; 2019.

49. Doi Y, Iovleva A, Bonomo RA. The ecology of extended-spectrum β-lactamases (ESBLs) in the developed world. J Travel Med. 2017;24(1):S44–51.

50. Bush K, Jacoby GA. Updated Functional Classification of β-Lactamases. Antimicrob Agents Chemother. 2010;54(3):969–76.

51. Zhao W-H, Hu Z-Q. Epidemiology and genetics of CTX-M extended-spectrum β-lactamases in Gram-negative bacteria. Crit Rev Microbiol. 2013;39(1):79–101.

52. Cantón R, González-Alba JM, Galán JC. CTX-M enzymes : origin and diffusion. Front Microbiol. 2012;3(110).

53. Bevan ER, Jones AM, Hawkey PM. Global epidemiology of CTX-M β-lactamases: temporal and geographical shifts in genotype. J Antimicrob Chemother. 2017;(72):2145–55.

54. Olson AB, Silverman M, Boyd DA, McGeer A, Willey BM, Pong-Porter V, et al. Identification of a Progenitor of the CTX-M-9 Group of Extended-Spectrum β-Lactamases from *Kluyvera georgiana* Isolated in Guyana. Antimicrob Agents Chemother. 2005;49(5):2112–5.

55. Decousser JW, Poirel L, Nordmann P. Characterization of a Chromosomally Encoded Extended-Spectrum Alass A β-Lactamase from *Kluyvera cryocrescens*. Antimicrob Agents Chemother. 2001;45(12):3595–8.

56. Bauernfeind A, Schweighart S, Grimm H. A New Plasmidic Cefotaximase in a Clinical Isolate of *Escherichia coli*. Infection. 1990;18(5):294–8.

57. Kale SK, Deshmukh AG, Dudhare MS, Patil VB. Microbial degradation of plastic: a review. J Biochem Technol. 2015;6(2):952–61.

58. Yuan J, Ma J, Sun Y, Zhou T, Zhao Y, Yu F. Microbial degradation and other environmental aspects of microplastics/plastics. Sci Total Environ. 2020;715:136968.

59. Amobonye A, Bhagwat P, Singh S, Pillai S. Plastic biodegradation: Frontline microbes and their enzymes. Sci Total Environ. 2020;759.

60. Ławniczak Ł, Woźniak-Karczewska M, Loibner AP, Heipieper HJ, Chrzanowski Ł. Microbial Degradation of Hydrocarbons—Basic Principles for Bioremediation: A Review. Molecules. 2020;25(4):1–19.

61. Geyer R, Jambeck JR, Law KL. Production, use, and fate of all plastics ever made. Sci Adv. 2017;3(7):25–9.

62. Baumann E. Ueber einige Vinylverbindungen. Ann der Chemie und Pharm. 1872;163:308–22.

63. Shah AA, Hasan F, Hameed A, Ahmed S. Biological degradation of plastics: A comprehensive review. Biotechnol Adv. 2008;26(3):246–65.

64. Frère L, Maignien L, Chalopin M, Huvet A, Rinnert E, Morrison H, et al. Microplastic bacterial communities in the Bay of Brest: Influence of polymer type and size. Environ Pollut. 2018;242:614–25.

65. Cole M, Lindeque P, Halsband C, Galloway TS. Microplastics as contaminants in the marine environment: A review. Mar Pollut Bull. 2011;62(12):2588–97.

66. Horton AA, Walton A, Spurgeon DJ, Lahive E, Svendsen C. Microplastics in freshwater and terrestrial environments: Evaluating the current understanding to identify the knowledge gaps and future research priorities. Sci Total Environ. 2017;586:127–41.

67. Liu P, Zhan X, Wu X, Li J, Wang H, Gao S. Effect of weathering on environmental

behavior of microplastics: Properties, sorption and potential risks. Chemosphere. 2020;242.

68. Akdogan Z, Guven B. Microplastics in the environment: A critical review of current understanding and identification of future research needs. Environ Pollut. 2019;254:113011.

69. Ivleva NP, Wiesheu AC, Niessner R. Microplastic in Aquatic Ecosystems. Angew Chemie - Int Ed. 2017;56(7):1720–39.

70. Erni-Cassola G, Zadjelovic V, Gibson MI, Christie-Oleza JA. Distribution of plastic polymer types in the marine environment; A meta-analysis. J Hazard Mater. 2019;369(February):691–8.

71. Koelmans AA, Mohamed Nor NH, Hermsen E, Kooi M, Mintenig SM, De France J. Microplastics in freshwaters and drinking water: Critical review and assessment of data quality. Water Res. 2019;155:410–22.

72. Kasirajan S, Ngouajio M. Polyethylene and biodegradable mulches for agricultural applications: a review. Agron Sustain Dev. 2012;32:501–29.

73. Sintim HY, Flury M. Is Biodegradable Plastic Mulch the Solution to Agriculture's Plastic Problem? Environ Sci Technol. 2017;51(3):1068–9.

74. Ng E-L, Huerta Lwanga E, Eldridge SM, Johnston P, Hu HW, Geissen V, et al. An overview of microplastic and nanoplastic pollution in agroecosystems. Sci Total Environ. 2018;627:1377–88.

75. Astner AF, Hayes DG, Pingali SV, O'Neill HM, Littrell KC, Evans BR, et al. Effects of soil particles and convective transport on dispersion and aggregation of nanoplastics via small-angle neutron scattering (SANS) and ultra SANS (USANS). PLoS One. 2020;15(7 July):1–14.

76. Iwata T. Biodegradable and Bio-Based Polymers: Future Prospects of Eco-Friendly Plastics. Angew Chemie - Int Ed. 2015;54(11):3210–5.

77. Lott C, Eich A, Pauli N-C, Mildenberger T, Laforsch C, Petermann JS, et al. Marine Fate of Biodegradable Plastic—Substitution Potential and Ecological Impacts. In: Proceedings of the International Conference on Microplastic Pollution in the Mediterranean Sea. 2018. p. 195–7.

78. Mallardo S, De Vito V, Malinconico M, Volpe MG, Santagata G, Di Lorenzo ML. Biodegradable Poly(Butylene Succinate)-Based Composites for Food Packaging. In: Cocca M, Di Pace E, Errico ME, Gentile G, Montarsolo A, Mossotti R, editors. Proceedings of the International Conference on Microplastic Pollution in the Mediterranean Sea. Cham: Springer International Publishing; 2018. p. 199–204.

79. Plastics Europe. Plastics - the Facts 2019 [Internet]. 2019. Available from: https://www.plasticseurope.org/en/resources/market-data

80. European Bioplastics. Bioplastics - Facts and Figures. 2020.

81. Zheng Y, Yanful EK, Bassi AS. A Review of Plastic Waste Biodegradation. Crit Rev Biotechnol. 2005;25(4):243–50.

82. Green DS, Boots B, Sigwart J, Jiang S, Rocha C. Effects of conventional and biodegradable microplastics on a marine ecosystem engineer (*Arenicola marina*) and sediment nutrient cycling. Environ Pollut. 2016;208:426–34.

83. Van Der Zee M. Analytical Methods for Monitoring Biodegradation Processes of Environmentally Degradable Polymers. Handb Biodegrad Polym Isol Synth Charact Appl. 2011;263–81.

84. Das MP, Kumar S. Microbial deterioration of low density polyethylene by *Aspergillus* and *Fusarium sp*. Int J ChemTech Res. 2014;6(1):299–305.

85. Danso D, Chow J, Streita WR. Plastics: Environmental and Biotechnological Perspectives on Microbial Degradation. Appl Environ Microbiol. 2019;85(19):1–14.

86. Hesham AEL, Mawad AMM, Mostafa YM, Shoreit A. Biodegradation Ability and Catabolic Genes of Petroleum-Degrading *Sphingomonas koreensis* Strain ASU-06 Isolated from Egyptian Oily Soil. Biomed Res Int. 2014;

87. McGivney E, Cederholm L, Barth A, Hakkarainen M, Hamacher-Barth E, Ogonowski M, et al. Rapid Physicochemical Changes in Microplastic Induced by Biofilm Formation. Front Bioeng Biotechnol. 2020;8(March):1–14.

88. Dümichen E, Eisentraut P, Bannick CG, Barthel AK, Senz R, Braun U. Fast identification of microplastics in complex environmental samples by a thermal degradation method. Chemosphere. 2017;174:572–84.

89. Dümichen E, Barthel AK, Braun U, Bannick CG, Brand K, Jekel M, et al. Analysis of polyethylene microplastics in environmental samples, using a thermal decomposition method. Water Res. 2015;85:451–7.

90. Duemichen E, Braun U, Senz R, Fabian G, Sturm H. Assessment of a new method for the analysis of decomposition gases of polymers by a combining thermogravimetric solid-phase extraction and thermal desorption gas chromatography mass spectrometry. J Chromatogr A. 2014;1354:117–28.

91. Eisentraut P, Dümichen E, Ruhl AS, Jekel M, Albrecht M, Gehde M, et al. Two Birds with One Stone - Fast and Simultaneous Analysis of Microplastics: Microparticles Derived from Thermoplastics and Tire Wear. Environ Sci Technol Lett. 2018;5(10):608–13.

92. Fischer M, Scholz-Böttcher BM. Simultaneous Trace Identification and Quantification of Common Types of Microplastics in Environmental Samples by Pyrolysis-Gas Chromatography-Mass Spectrometry. Environ Sci Technol. 2017;51(9):5052–60.

93. Dehaut A, Cassone AL, Frère L, Hermabessiere L, Himber C, Rinnert E, et al. Microplastics in seafood: Benchmark protocol for their extraction and characterization. Environ Pollut. 2016;215:223–33.

94. Hendrickson E, Minor EC, Schreiner K. Microplastic Abundance and Composition in Western Lake Superior As Determined via Microscopy, Pyr-GC/MS, and FTIR. Environ Sci Technol. 2018;52(4):1787–96.

95. Zhou XX, Hao LT, Wang H, Li YJ, Liu JF. Cloud-Point Extraction Combined with Thermal Degradation for Nanoplastic Analysis Using Pyrolysis Gas Chromatography-Mass Spectrometry. Anal Chem. 2019;91(3):1785–90.

96. Fries E, Dekiff JH, Willmeyer J, Nuelle MT, Ebert M, Remy D. Identification of polymer types and additives in marine microplastic particles using pyrolysis-GC/MS and scanning electron microscopy. Environ Sci Process Impacts. 2013;15(10):1949–56.

97. Anger PM, von der Esch E, Baumann T, Elsner M, Niessner R, Ivleva NP. Raman microspectroscopy as a tool for microplastic particle analysis. TrAC - Trends Anal Chem. 2018;109:214–26.

98. Von Der Esch E, Kohles AJ, Anger PM, Hoppe R, Niessner R, Elsner M, et al. TUM-ParticleTyper: A detection and quantification tool for automated analysis of (Microplastic) particles and fibers. PLoS One. 2020;15(6 June):1–20.

99. von der Esch E, Lanzinger M, Kohles AJ, Schwaferts C, Weisser J, Hofmann T, et al. Simple Generation of Suspensible Secondary Microplastic Reference Particles via Ultrasound Treatment. Front Chem. 2020;8(169).

100. Domogalla-Urbansky J, Anger PM, Ferling H, Rager F, Wiesheu AC, Niessner R, et al. Raman microspectroscopic identification of microplastic particles in freshwater bivalves (Unio pictorum) exposed to sewage treatment plant effluents under different exposure scenarios. Environ Sci Pollut Res. 2019;26(2):2007–12.

101. Schymanski D, Goldbeck C, Humpf HU, Fürst P. Analysis of microplastics in water by micro-Raman spectroscopy: Release of plastic particles from different packaging into mineral water. Water Res. 2018;129:154–62.

102. Schwaferts C, Sogne V, Welz R, Meier F, Klein T, Niessner R, et al. Nanoplastic Analysis by Online Coupling of Raman Microscopy and Field-Flow Fractionation Enabled by Optical Tweezers. Anal Chem. 2020;92(8):5813–20.

103. Imhof HK, Laforsch C, Wiesheu AC, Schmid J, Anger PM, Niessner R, et al. Pigments and plastic in limnetic ecosystems: A qualitative and quantitative study on microparticles of different size classes. Water Res. 2016;98:64–74.

104. Oßmann BE, Sarau G, Holtmannspötter H, Pischetsrieder M, Christiansen SH, Dicke W. Small-sized microplastics and pigmented particles in bottled mineral water. Water Res. 2018;141:307–16.

105. Mintenig SM, Int-Veen I, Löder MGJ, Primpke S, Gerdts G. Identification of microplastic in effluents of waste water treatment plants using focal plane array-based micro-Fourier-transform infrared imaging. Water Res. 2017;108:365–72.

106. Cabernard L, Roscher L, Lorenz C, Gerdts G, Primpke S. Comparison of Raman and Fourier Transform Infrared Spectroscopy for the Quantification of Microplastics in the Aquatic Environment. Environ Sci Technol. 2018;52(22):13279–88.

107. Käppler A, Fischer D, Oberbeckmann S, Schernewski G, Labrenz M, Eichhorn KJ, et al. Analysis of environmental microplastics by vibrational microspectroscopy: FTIR, Raman or both? Anal Bioanal Chem. 2016;408(29):8377–91.

108. Renner G, Sauerbier P, Schmidt TC, Schram J. Robust Automatic Identification of Microplastics in Environmental Samples Using FTIR Microscopy. Anal Chem. 2019;91:9656–64.

109. Renner G, Schmidt TC, Schram J. Analytical methodologies for monitoring micro(nano)plastics: Which are fit for purpose? Curr Opin Environ Sci Heal. 2018;1:55–61.

110. Primpke S, Lorenz C, Rascher-Friesenhausen R, Gerdts G. An automated approach for microplastics analysis using focal plane array (FPA) FTIR microscopy and image analysis. Anal Methods. 2017;9(9):1499–511.

111. Primpke S, Dias PA, Gerdts G. Automated Identification and Quantification of

Microfibres and Microplastics. Anal Methods. 2019;11(16):2138–47.

112. Doern CD, Butler-Wu SM. Emerging and Future Applications of Matrix-Assisted Laser Desorption Ionization Time-of-Flight (MALDI-TOF) Mass Spectrometry in the Clinical Microbiology Laboratory: A Report of the Association for Molecular Pathology. J Mol Diagnostics. 2016;18(6):789–802.

113. Pahlow S, Meisel S, Cialla-May D, Weber K, Rösch P, Popp J. Isolation and identification of bacteria by means of Raman spectroscopy. Adv Drug Deliv Rev. 2015;89:105–20.

114. Mullis KB. The unusual origin of the polymerase chain reaction. Sci Am. 1990;262(4):56–65.

115. Mullis K, Faloona F, Scharf S, Saiki R, Horn G, Erlich H. Specific Enzymatic Amplification of DNA In Vitro: The Polymerase Chain Reaction. In: Cold Spring Harbor Symposia on Quantitative Biology. 1986. p. 17–27.

116. Anjum MF, Zankari E, Hasman H. Molecular Methods for Detection of Antimicrobial Resistance. Microbiol Spectr. 2017;5(6):33–50.

117. Mackay IM. Real-time PCR in the microbiology laboratory. Clin Microbiol Infect. 2004;10(3):190–212.

118. Franco-Duarte R, Černáková L, Kadam S, Kaushik KS, Salehi B, Bevilacqua A, et al. Advances in chemical and biological methods to identify microorganisms—from past to present. Microorganisms. 2019;7(5).

119. Walsh F, Duffy B. The Culturable Soil Antibiotic Resistome: A Community of Multi-Drug Resistant Bacteria. PLoS One. 2013;8(6).

120. World Health Organization. Guidelines for Drinking-Water Quality: fourth edition incorporating the first addendum. Geneva; 2017.

121. Sproß J, Sinz A. Monolithic media for applications in affinity chromatography. J Sep Sci. 2011;34(16–17):1958–73.

122. Walsh Z, Paull B, Macka M. Inorganic monoliths in separation science: A review. Anal Chim Acta. 2012;750:28–47.

123. Acquah C, Moy CKS, Danquah MK, Ongkudon CM. Development and characteristics of polymer monoliths for advanced LC bioscreening applications: A review. J Chromatogr B. 2016;1015–1016:121–34.

124. Bracken CL, Hendricks CW, Harding AK. Apparent bias in river water inoculum following centrifugation. J Microbiol Methods. 2006;67(2):304–9.

125. Abdel-Hamid I, Ivnitski D, Atanasov P, Wilkins E. Flow-through immunofiltration assay system for rapid detection of *E. coli* O157:H7. Biosens Bioelectron. 1999;14(3):309–16.

126. Sung YJ, Suk HJ, Sung HY, Li T, Poo H, Kim MG. Novel antibody/gold nanoparticle/magnetic nanoparticle nanocomposites for immunomagnetic separation and rapid colorimetric detection of *Staphylococcus aureus* in milk. Biosens Bioelectron. 2013;43(1):432–9.

127. Zhang Y, Riley LK, Lin M, Hu Z. Determination of low-density *Escherichia coli* and *Helicobacter pylori* suspensions in water. Water Res. 2012;46(7):2140–8.

128. Göpfert L, Klüpfel J, Heinritz C, Elsner M, Seidel M. Macroporous epoxy-based monoliths for rapid quantification of *Pseudomonas aeruginosa* by adsorption elution method optimized for qPCR. Anal Bioanal Chem. 2020;412(29):8185–95.

129. Kunze A, Pei L, Elsässer D, Niessner R, Seidel M. High performance concentration method for viruses in drinking water. J Virol Methods. 2015;222:132–7.

130. Wunderlich A, Torggler C, Elsässer D, Lück C, Niessner R, Seidel M. Rapid quantification method for *Legionella pneumophila in surface water. Anal Bioanal Chem. 2016;408(9):2203–13.*

131. Peskoller C, Niessner R, Seidel M. Development of an epoxy-based monolith used for the affinity capturing of *Eschericha coli* bacteria. J Chromatogr A. 2009;1216(18):3794–801.

132. Elsäßer D, Ho J, Niessner R, Tiehm A, Seidel M. Heterogeneous asymmetric recombinase polymerase amplification (haRPA) for rapid hygiene control of large-volume water samples. Anal Biochem. 2018;546(February):58–64.

133. Peskoller C, Niessner R, Seidel M. Cross-flow microfiltration system for rapid enrichment of bacteria in water. Anal Bioanal Chem. 2009;393(1):399–404.

134. Hall AN, Hogg SD, Phillips GO. Gradient Elution of *Salmonella typhimurium* and *Escherichia coli* Strains from a DEAE-Cellulose Column. J Appl Bacteriol. 1976;41(1):189–92.

135. Martzy R, Kolm C, Krska R, Mach RL, Farnleitner AH, Reischer GH. Challenges and perspectives in the application of isothermal DNA amplification methods for food and water analysis. Anal Bioanal Chem. 2019;411(9):1695–702.

136. Notomi T, Mori Y, Tomita N, Kanda H. Loop-mediated isothermal amplification (LAMP): principle, features, and future prospects. J Microbiol. 2015;53(1):1–5.

137. Li Y, Fan P, Zhou S, Zhang L. Loop-mediated isothermal amplification (LAMP): A novel rapid detection platform for pathogens. Microb Pathog. 2017;107:54–61.

138. Walker GT, Fraiser MS, Schram JL, Little MC, Nadeau JG, Malinowski DP. Strand displacement amplification — an isothermal, in vitro DNA amplification technique. Nucleic Acids Res. 1992;20(7):1691–6.

139. Vincent M, Xu Y, Kong H. Helicase-dependent isothermal DNA amplification. EMBO Rep. 2004;5(8):5–10.

140. An L, Tang W, Ranalli TA, Kim H-J, Wytiaz J, Kong H. Characterization of a thermostable UvrD helicase and its participation in helicase dependent amplification. J Biol Chem. 2005;280(32):28952–8.

141. Motré A, Li Y, Kong H. Enhancing helicase-dependent amplification by fusing the helicase with the DNA polymerase. Gene. 2008;420:17–22.

142. Tong Y, Lemieux B, Kong H. Multiple strategies to improve sensitivity, speed and robustness of isothermal nucleic acid amplification for rapid pathogen detection. BMC Biotechnol. 2011;11(1):50.

143. Piepenburg O, Williams CH, Stemple DL, Armes NA. DNA Detection Using Recombination Proteins. PLoS Biol. 2006;4(7):1115–21.

144. Higgins M, Ravenhall M, Ward D, Phelan J, Ibrahim A, Forrest MS, et al.

PrimedRPA: Primer design for recombinase polymerase amplification assays. Bioinformatics. 2019;35(4):682–4.

145. James A, MacDonald J. Recombinase polymerase amplification: Emergence as a critical molecular technology for rapid, low-resource diagnostics. Expert Rev Mol Diagn. 2015;15(11):1475–89.

146. Crannell ZA, Rohrman B, Richards-Kortum R. Equipment-Free Incubation of Recombinase Polymerase Amplification Reactions Using Body Heat. PLoS One. 2014;9(11):1–7.

147. Lobato IM, O'Sullivan CK. Recombinase polymerase amplification: Basics, applications and recent advances. Trends Anal Chem. 2018;98:19–35.

148. Li J, Macdonald J, Stetten F Von. Review: a comprehensive summary of a decade development of the recombinase polymerase amplification. Analyst. 2019;144(1):31–67.

149. Kunze A, Dilcher M, Abd El Wahed A, Hufert F, Niessner R, Seidel M. On-Chip Isothermal Nucleic Acid Amplification on Flow-Based Chemiluminescence Microarray Analysis Platform for the Detection of Viruses and Bacteria. Anal Chem. 2016;88(1):898–905.

150. Kober C, Niessner R, Seidel M. Quantification of viable and non-viable *Legionella* spp. by heterogeneous asymmetric recombinase polymerase amplification (haRPA) on a flow-based chemiluminescence microarray. Biosens Bioelectron. 2018;100(August 2017):49–55.

151. Sollweck K, Schwaiger G, Seidel M. A chemiluminescence-based heterogeneous asymmetric recombinase polymerase amplification assay for the molecular detection of mycotoxin producers. Analyst. 2021;

152. Kersting S, Rausch V, Bier FF, Nickisch-rosenegk M Von. A recombinase polymerase amplification assay for the diagnosis of atypical pneumonia. Anal Biochem. 2018;550:54–60.

153. Kersting S, Rausch V, Bier FF, von Nickisch-Rosenegk M. Multiplex isothermal solid-phase recombinase polymerase amplification for the specific and fast DNA-based detection of three bacterial pathogens. Microchim Acta. 2014;181:1715–23.

154. Tsaloglou M-N, Nemiroski A, Camci-Unal G, Christodouleas DC, Murray LP, Connelly JT, et al. Handheld isothermal amplification and electrochemical detection of DNA in resource-limited settings. Anal Biochem. 2018;543:116–21.

155. Santiago-Felipe S, Tortajada-Genaro LA, Puchades R, Maquieira Á. Recombinase polymerase and enzyme-linked immunosorbent assay as a DNA amplification-detection strategy for food analysis. Anal Chim Acta. 2014;811:81–7.

156. Santiago-Felipe S, Tortajada-Genaro LA, Puchades R, Maquieira Á. Parallel solid-phase isothermal amplification and detection of multiple DNA targets in microliter-sized wells of a digital versatile disc. Microchim Acta. 2016;183(3):1195–202.

157. Andresen D, Nickisch-Rosenegk M Von, Bier FF. Helicase dependent OnChip-amplification and its use in multiplex pathogen detection. Clin Chim Acta. 2009;403:244–8.

158. Zhou Q, Wang L, Chen J, Wang R, Shi Y, Li C, et al. Development and evaluation of a real-time fluorogenic loop-mediated isothermal amplification assay integrated

on a microfluidic disc chip (on-chip LAMP) for rapid and simultaneous detection of ten pathogenic bacteria in aquatic animals. J Microbiol Methods. 2014;104:26–35.

159. Fang X, Liu Y, Kong J, Jiang X. Loop-Mediated Isothermal Amplification Integrated on Microfluidic Chips for Point-of-Care Quantitative Detection of Pathogens. Anal Chem. 2010;82(7):3002–6.

160. Santiago-Felipe S, Tortajada-Genaro LA, Carrascosa J, Puchades R, Maquieira Á. Real-time loop-mediated isothermal DNA amplification in compact disc micro-reactors. Biosens Bioelectron. 2016;79:300–6.

161. Rivoarilala OL, Garin B, Andriamahery F, Collard JM. Rapid in vitro detection of CTX-M groups 1, 2, 8, 9 resistance genes by LAMP assays. PLoS One. 2018;13(7):1–15.

162. Anjum MF, Lemma F, Cork DJ, Meunier D, Murphy N, North SE, et al. Isolation and Detection of Extended Spectrum β-Lactamase (ESBL)-Producing Enterobacteriaceae from Meat using Chromogenic Agars and Isothermal Loop-Mediated Amplification (LAMP) Assays. J Food Sci. 2013;78(12).

163. Thirapanmethee K, Pothisamutyothin K, Nathisuwan S, Chomnawang MT, Wiwat C. Loop-mediated isothermal amplification assay targeting the bla CTX-M9 gene for detection of extended spectrum β-lactamase-producing *Escherichia coli* and *Klebsiella pneumoniae*. Microbiol Immunol. 2014;58:655–65.

164. Luo J, Fang X, Ye D, Li H, Chen H, Zhang S, et al. A real-time microfluidic multiplex electrochemical loop-mediated isothermal amplification chip for differentiating bacteria. Biosens Bioelectron. 2014;60(15):84–91.

165. Zhao X, Wang L, Li Y, Xu Z, Li L, He X, et al. Development and application of a loop-mediated isothermal amplification method on rapid detection of *Pseudomonas aeruginosa* strains. World J Microbiol Biotechnol. 2011;27:181–4.

166. Andresen D, von Nickisch-Rosenegk M, Bier FF. Helicase-dependent amplification : use in OnChip amplification and potential for point-of-care diagnostics. Expert Rev Mol Diagn. 2009;9(7):645–50.

167. Barreda-García S, Miranda-castro R, De-los-Santos-Álvarez N, Miranda-Ordieres AJ, Lobo-Castañón MJ. Helicase-dependent isothermal amplification : a novel tool in the development of molecular-based analytical systems for rapid pathogen detection. Anal Bioanal Chem. 2018;410:679–93.

168. Hu C, Kalsi S, Zeimpekis I, Sun K, Ashburn P, Turner C, et al. Ultra-fast electronic detection of antimicrobial resistance genes using isothermal amplification and Thin Film Transistor sensors. Biosens Bioelectron. 2017;96(May):281–7.

169. Nakano M, Kalsi S, Morgan H. Fast and sensitive isothermal DNA assay using microbead dielectrophoresis for detection of anti-microbial resistance genes. Biosens Bioelectron. 2018;117:583–9.

170. Kalsi S, Valiadi M, Tsaloglou M-N, Parry-Jones L, Jacobs A, Watson R, et al. Rapid and sensitive detection of antibiotic resistance on a programmable digital microfluidic platform. Lab Chip. 2015;15(14):3065–75.

171. Kalsi S, Sellars SL, Turner C, Sutton JM, Morgan H. A programmable digital microfluidic assay for the simultaneous detection of multiple anti-microbial resistance genes. Micromachines. 2017;8(4).

172. Valiadi M, Kalsi S, Jones IGF, Turner C, Sutton JM, Morgan H. Simple and rapid sample preparation system for the molecular detection of antibiotic resistant pathogens in human urine. Biomed Microdevices. 2016;18(1):1–10.

173. Renner LD, Zan J, Hu LI, Martinez M, Resto PJ, Siegel AC, et al. Detection of ESKAPE Bacterial Pathogens at the Point of Care Using Isothermal DNA-Based Assays in a Portable Degas-Actuated Microfluidic Diagnostic Assay Platform. Appl Environ Microbiol. 2017;83(4):1–13.

174. Renner G, Nellessen A, Schwiers A, Wenzel M, Schmidt TC, Schram J. Data preprocessing & evaluation used in the microplastics identification process: A critical review & practical guide. TrAC - Trends Anal Chem. 2019;111:229–38.

175. Primpke S, Wirth M, Lorenz C, Gerdts G. Reference database design for the automated analysis of microplastic samples based on Fourier transform infrared (FTIR) spectroscopy. Anal Bioanal Chem. 2018;410(21):5131–41.

176. Renner G, Schmidt TC, Schram J. Automated rapid & intelligent microplastics mapping by FTIR microscopy: A Python–based workflow. MethodsX. 2020;7.

177. Leroy A, Ribeiro S, Grossiord C, Alves A, Vestberg RH, Salles V, et al. FTIR microscopy contribution for comprehension of degradation mechanisms in PLA-based implantable medical devices. J Mater Sci Mater Med. 2017;28(87).

178. Löder MGJ, Imhof HK, Ladehoff M, Löschel LA, Lorenz C, Mintenig S, et al. Enzymatic Purification of Microplastics in Environmental Samples. Environ Sci Technol. 2017;51(24):14283–92.

179. Imhof HK, Schmid J, Niessner R, Ivleva NP, Laforsch C. A novel, highly efficient method for the separation and quantification of plastic particles in sediments of aquatic environments. Limnol Oceanogr Methods. 2012;10(JULY):524–37.

180. Cole M, Webb H, Lindeque PK, Fileman ES, Halsband C, Galloway TS. Isolation of microplastics in biota-rich seawater samples and marine organisms. Sci Rep. 2014;4:1–8.

181. de Souza Machado AA, Lau CW, Till J, Kloas W, Lehmann A, Becker R, et al. Impacts of Microplastics on the Soil Biophysical Environment. Environ Sci Technol. 2018;52(17):9656–65.

182. Rillig MC. Microplastic in Terrestrial Ecosystems and the Soil? Environ Sci Technol. 2012;46:6453–4.

183. Lambert S, Wagner M. Formation of microscopic particles during the degradation of different polymers. Chemosphere. 2016;161:510–7.

184. Bagheri AR, Laforsch C, Greiner A, Agarwal S. Fate of So-Called Biodegradable Polymers in Seawater and Freshwater. Glob Challenges. 2017;1(4):1700048.

185. Lendlein A, Sisson A. Handbook of Biodegradable Polymers: Isolation, Synthesis, Characterization and Applications. Wiley; 2011.

186. Yoshida S, Hiraga K, Takehana T, Taniguchi I, Yamaji H, Maeda Y, et al. A bacterium that degrades and assimilates poly(ethylene terephthalate). Science. 2016;351(6278):1196–9.

187. Negi H, Gupta S, Zaidi MGH, Goel R. Studies on biodegradation of LDPE film in the presence of potential bacterial consortia enriched soil. Biologija. 2011;57(4):141–7.

188. Orhan Y, Hrenović J, Büyükgüngör H. Biodegradation of plastic compost bags under controlled soil conditions. Acta Chim Slov. 2004;51(3):579–88.

189. Fojt J, David J, Přikryl R, Řezáčová V, Kučerík J. A critical review of the overlooked challenge of determining micro-bioplastics in soil. Sci Total Environ. 2020;745.

190. Valenza G, Nickel S, Pfeifer Y, Eller C, Krupa E, Lehner-Reindl V, et al. Extended-Spectrum-β-Lactamase-Producing *Escherichia Coli* as Intestinal Colonizers in the German Community. Antimicrob Agents Chemother. 2014;58(2):1228–30.

191. Donhauser SC, Niessner R, Seidel M. Quantification of E. coli DNA on a Flow-through Chemiluminescence Microarray Readout System after PCR Amplification. Anal Sci. 2009;25:669–74.

192. Wolter A, Niessner R, Seidel M. Preparation and Characterization of Functional Poly(ethylene glycol) Surfaces for the Use of Antibody Microarrays. Anal Chem. 2007;79(12):4529–37.

193. Gröbner S, Linke D, Schütz W, Fladerer C, Madlung J, Autenrieth IB, et al. Emergence of carbapenem-non-susceptible extended-spectrum β-lactamase-producing *Klebsiella pneumoniae* isolates at the university hospital of Tübingen, Germany. J Med Microbiol. 2009;58(7):912–22.

194. Lengger S, Otto J, Elsässer D, Schneider O, Tiehm A, Fleischer J, et al. Oligonucleotide microarray chip for the quantification of MS2, Φx174, and adenoviruses on the multiplex analysis platform MCR 3. Anal Bioanal Chem. 2014;406(14):3323–34.

195. Pier GB. *Pseudomonas aeruginosa* lipopolysaccharide: a major virulence factor, initiator of inflammation and target for effective immunity. Int J Med Microbiol. 2007;297(5):277–95.

196. Tanner RS, James SA. Rapid bactericidal effect of low pH against *Pseudomonas aeruginosa*. J Ind Microbiol. 1992;10(3–4):229–32.

197. Salehi B, Mehrabian S, Sepahi AA. The Efficacy of Cadmium Oxide Nanoparticles on *Pseudomonas aeruginosa* Bacteria. Adv Stud Biol. 2013;5(11):473–88.

198. Göpfert L, Elsner M, Seidel M. Isothermal haRPA detection of $bla_{\text{CTX-M}}$ in bacterial isolates from water samples and comparison with qPCR. Anal Methods. 2021;13:552–7.

199. Kunze A. Aufkonzentrierung und Detektion viraler und bakterieller Pathogene in Trinkwasser. 2016.

200. Rojas JA, Miles TD, Coffey MD, Martin FN, Chilvers MI. Development and Application of qPCR and RPA Genus and Species-Specific Detection of *Phytophthora sojae* and *P. sansomeana* Root Rot Pathogens of Soybean. Plant Dis. 2017;101(7):1171–81.

201. Yin D, Zhu Y, Wang K, Wang J, Zhang X, Han M, et al. Development and evaluation of a rapid recombinase polymerase amplification assay for the detection of human enterovirus 71. Arch Virol. 2018;163(9):2459–63.

202. Shahin K, Ramirez-Paredes JG, Harold G, Lopez-Jimena B, Adams A, Weidmann M. Development of a recombinase polymerase amplification assay for rapid detection of *Francisella noatunensis* subsp. *orientalis*. PLoS One. 2018;13(2):1–21.

203. Wu YD, Zhou DH, Zhang LX, Zheng W Bin, Ma JG, Wang M, et al. Recombinase polymerase amplification (RPA) combined with lateral flow (LF) strip for equipment-free detection of *Cryptosporidium* spp. oocysts in dairy cattle feces. Parasitol Res. 2016;115(9):3551–5.

204. Babu B, Ochoa-Corona FM, Paret ML. Recombinase polymerase amplification applied to plant virus detection and potential implications. Anal Biochem. 2018;546(October 2017):72–7.

205. Mena KD, Gerba CP. Risk Assessment of *Pseudomonas aeruginosa* in Water. Vol. 201, Reviews of environmental contamination and toxicology. 2009. 71–115 p.

206. Favero MS, Carson LA, Bond WW, Petersen NJ. *Pseudomonas aeruginosa*: Growth in Distilled Water from Hospitals. Science (80-). 1971;173(3999):836–8.

207. Martino TK, Hernández JM, Beldarraín T, Melo L. Identification of Bacteria in Water for Pharmaceutical Use. Rev Latinoam Microbiol. 1998;40:142–50.

208. Bohus V, Kéki Z, Márialigeti K, Baranyi K, Patek G, Schunk J, et al. Bacterial communities in an ultrapure water containing storage tank of a power plant. Acta Microbiol Immunol Hung. 2011;58(4):371–82.

209. Green PN, Bousfield IJ, Hood D. Three New *Methylobacterium* Species: *M. rhodesianum* sp. nov., *M. zatmanii* sp. nov., *M. fujisawaense* sp. npv. Int J Sytematic Bacteriol. 1988;38(1):124–7.

210. Green P, Bousfield I. Emendation of *Methylobacterium* Patt, Cole, and Hanson 1976; *Methylobacterium rhodinum* (Heumann 1962) comb. nov. corrig.; *Methylobacterium radiotolerans* (Ito and Iizuka 1971) comb. nov. corrig.; and *Methylobacterium mesophilicum* (Autin and Goodfellow 1979). Int J Syst Biol. 1983;4(33):875–7.

211. Dabboussi F, Hamze M, Elomari M, Verhille S, Baida N, Izard D, et al. *Pseudomonas libanensis*, sp. nov., a new species isolated from Lebanese spring waters. Int J Syst Bacteriol. 1999;49:1091–101.

212. Lee JS, Shin YK, Yoon JH, Takeuchi M, Pyun YR, Park YH. *Sphingomonas aquatilis* sp. nov., *Sphingomonas koreensis* sp. nov. and *Sphingomonas taejonensis* sp. nov., yellow-pigmented bacteria isolated from natural mineral water. Int J Syst Evol Microbiol. 2001;51(4):1491–8.